Physico-Biological Mechanisms of Focused Low-Intensity Pulsed Ultrasound in Musculoskeletal Regeneration

Inaugural-Dissertation
to obtain the academic degree
Doctor rerum naturalium (Dr. rer. nat.) submitted to the
Department of Biology, Chemistry and Pharmacy of
Freie Universität Berlin

by Regina Puts
from Zelenodolsk, Russia
November, 2016

I conducted my doctoral studies from 01.11.2012 until 30.10.2016 at Berlin-Brandenburg School for Regenerative Therapies at Charité Universitätsmedizin Berlin under the supervision of Prof. Dr. rer. nat. Kay Raum.

1st Reviewer	Prof. Dr. rer. nat. Kay Raum
2nd Reviewer	Prof. Dr. rer. nat. Petra Knaus
Date of Defense	21.02.2017

Acknowledgements

I would like to express my sincere gratitude to my supervisor Prof. Kay Raum, for his motivation, patience, stimulatory conversations, and faith in me. I greatly appreciate that he could always find time for me if needed, and supply me with further ideas during troubling times. I am very thankful for his deep understanding and support throughout personal difficulties that I had. I would also like to express my thanks to my adjacent supervisor Prof. Petra Knaus, who assisted me with her vast scientific knowledge in experimental designs and the field of biochemistry overall, providing constructive criticism and valuable advices on future research directions. My PhD thesis would not be possible without close work with my mentor Dr. Karen Ruschke, who always supported my ideas, helped improving experimental designs, and shared as much of her knowledge and experience as possible to make my work the most productive. I could not have imagined having better supervisors and mentors for my PhD path.

My faithful thanks also goes to our former technical assistant, Anke Kadow-Romacker, who was insightful, experimental, and psychologically helpful throughout the entire PhD program. I could always rely on her competent experience and she would jump in the middle of any experiment to help me finish it. She never let me feel down, always encouraging me with new ideas. I have missed her greatly these past two months since she started her way off in industry.

I am very grateful to all the lab members of the AG Raum, for a special friendly, caring, and fun atmosphere. I appreciate the support of Paul Rikeit from the AG Knaus group for our scientific discussions and his suggestions on improvement of experimental designs.

Finally, I would like to thank my family: my wonderful parents Alfiya and Aleksandr Puts and my amazing brother Ruslan. They never doubted me and were there for me no matter what. My special thanks goes to my husband, Ivan Minchev, who believed in me and my research, providing immense emotional support, cheering me up, and motivating me with his successful scientific career, as well as his son Marco for his kind and caring heart.

Abstract

Ultrasound is an inexpensive, portable, and real-time mode technique, which has generated increasing interest in the medical community not only for imaging purposes, but also for tissue regeneration. Low-Intensity Pulsed Ultrasound (LIPUS) has already been demonstrated to be a safe, non-invasive, non-ionizing clinical tool for bone regenerative treatment, recently showing potential for soft tissue repair as well. Although the benefits of LIPUS-induced biological effects have been explicitly demonstrated *in vitro* and in small animal models *in vivo*, a detailed understanding of the mechanism is still beyond our reach. Moreover, controversial findings in clinical trials limit the appreciation and use of this physical technique, which, in contrast to growth factors, has minimum side effects.

In this thesis a novel focused LIPUS (FLIPUS) *in-vitro* set-up has been developed and characterized. The new set-up ensured deposition of well-defined acoustic intensity at the bottom of a 24-well tissue culture plates, minimizing the introduction of unwanted physical effects. It was first demonstrated that FLIPUS enhances the osteogenic potential of rat mesenchymal stem/stromal cells (rMSCs). Furthermore, an impact on the pro-osteogenic effects of FLIPUS was found due to both variation in the stimulation intensity levels and the age of the donor rMSCs. Murine pluripotent C2C12 mesenchymal precursors also exhibited mechanoresponse upon FLIPUS exposure, which was evaluated by the activity and the expression of the mechanosensitive transcription factors and genes, respectively. The activation of the transcription factors varied in a stimulation time-dependent manner. These findings suggest that the clinical LIPUS protocol, i.e., intensity level and stimulation time, might need optimization in accordance with, e.g., the patients' age group. The fundamental mechanism of the FLIPUS-activated TEAD (transcriptional enhancer factor TEF-1) mechanosensitive transcription factor was further investigated, revealing the role of cell-geometry-regulated Yes-associated protein (YAP) in the mechanotransduction. FLIPUS was found to enhance proliferation of C2C12s, while delaying cellular myogenesis through YAP functioning. The understanding of the YAP-associated complete mechanotransductive mechanism of FLIPUS is underway.

Owing to the arbitrarily adjustable acoustic beam properties of focused ultrasound and the ability to stimulate with well-characterized and defined intensity levels, the application of FLIPUS technology is planned to be extended to small animal models *in vivo*. The volume of FLIPUS energy can be adjusted to the size of the treated tissue region, enabling comprehension of the regenerative outcomes in direct response to variations in FLIPUS parameters. Co-

application of FLIPUS with bone morphogenetic proteins (BMPs) is to be performed further in an attempt to enhance regeneration of the co-stimulated tissues with reduced concentrations of the growth factor. This approach is anticipated to decrease both the treatment costs and the risk of unwanted side effects of the growth factor application. Moreover, the imaging capability of focused ultrasound is planned to be combined with the regenerative properties of FLIPUS, leading to the development of a clinical device, which will allow for visual monitoring of the local tissue regeneration.

Zusammenfassung

Ultraschall ist eine preiswerte und portable Echtzeit-Technik, die zunehmendes Interesse in der medizinischen Forschung, nicht nur für bildgebende Zwecke, sondern auch für die Geweberegeneration stößt. Gepulster Ultraschall mit niedrigen Intensitäten (engl.: Low-Intensity Pulsed Ultrasound – LIPUS) wird bereits klinisch als ein sicheres, nicht-invasives, nicht-ionisierendes klinisches Hilfsmittel zur Knochenregeneration eingesetzt. In den letzten Jahren konnte zudem sein Potential zur Reparatur von Weichteilgeweben gezeigt werden. Obwohl die Vorteile von LIPUS-induzierten biologischen Effekten *in vitro* und in Kleintiermodellen *in vivo* explizit gezeigt wurden, ist der genaue Wirkmechanismus noch nicht vollständig verstanden. Kontroverse Ergebnisse in klinischen Studien mindern derzeit die Wertschätzung und Anwendung dieser physikalischen Technik, die im Gegensatz anderen stimulierenden Methoden, z.B. der Anwendung von Wachstumsfaktoren minimale Nebenwirkungen hat.

In dieser Dissertation wurde ein neues fokussiertes LIPUS (FLIPUS) *in-vitro*-System entwickelt und charakterisiert. Der Aufbau gewährleistet die reproduzierbare Applikation der gewünschten Ultraschallintensität am Boden von 24-Well-Gewebekulturplatten und minimiert die Übertragung von unerwünschten physikalischen Effekten. FLIPUS erhöhte die osteogene Differenzierung von mesenchymalen Stromazellen aus Ratten (rMSCs). Außerdem zeigten Veränderungen der Stimulationsintensitäten und das Alter der Zellspender einen Einfluss auf die pro-osteogenen Effekte von FLIPUS. Murine pluripotente C2C12 mesenchymale Zellen zeigten ebenfalls eine Antwort auf mechanische FLIPUS-Stimulation, die über die Aktivität bzw. Expression der mechanosensitiven Transkriptionsfaktoren bzw. -gene, ausgewertet wurde. Die Aktivierung der Transkriptionsfaktoren variierte abhängig von der Stimulationszeit. Die Ergebnisse deuten darauf hin, dass eine Optimierung der klinisch-angewandten LIPUS-Protokolle, insbesondere Intensität und Stimulationszeit, auf Faktoren wie bspw. die Altersgruppe der Patienten notwendig sind. Der grundlegende Mechanismus des durch FLIPUS aktivierten TEAD-Mechanosensitiven Transkriptionsfaktors wurde untersucht, wobei die entscheidende Rolle des zellgeometrie-regulierten Yes-assoziierten Proteins (YAP) bei der Mechanotransduktion entdeckt wurde. FLIPUS verbesserte die Proliferation von C2C12-Zellen und verzögerte die zelluläre Myogenese durch eine Erhöhung der YAP-Aktivität. Momentan wird der genaue YAP-assoziierte Mechanismus von FLIPUS erforscht.

Aufgrund regulierbarer akustischer Strahlungseigenschaften von fokussiertem Ultraschall und der Fähigkeit, mit gut charakterisierten und definierten Intensitäten zu stimulieren, lässt sich FLIPUS in der Zukunft einfach an Kleintiermodellen *in vivo* anwenden. Die Energie von FLIPUS kann exakt auf die zu reparierende Gewebsgröße eingestellt werden, so dass Variationseffekte der FLIPUS-Parameter auf das regenerative Ergebnis nachvollziehbar werden. In Zukunft soll eine gemeinsame Anwendung von FLIPUS mit bone morphogenic proteins (BMPs) erprobt werden, um zum einen die Regeneration weiter zu steigern, zum anderen die Dosis von BMPs zu verringern. Es ist anzunehmen, dass sich somit sowohl die Behandlungskosten, als auch unerwünschte Nebenwirkungen der Wachstumsfaktoren verringern lassen. Darüber kann das bildgebende Potential des fokussierten Ultraschalls mit den regenerativen Eigenschaften von FLIPUS kombiniert werden, was das eine gezielte Stimulation und Überwachung der lokalen Geweberegeneration ermöglicht.

List of Abbreviations

ALP	Alkaline Phosphatase
AP-1	Activator Protein-1
BMP	Bone Morphogenetic Protein (e.g. BMP-2, BMP-4, BMP-7)
Col	Collagen (e.g. Col-1, Col-2, Col-2α1, Col-3, Col-9, Col-10, Col-12)
COX-2	Cyclooxygenase-2
DC	Duty Cycle
ECM	Extracellular Matrix
Egr-1	Early Growth Response-1 Factor
Erk1/2	Extracellular Signal-Regulated Kinase 1 and 2
FGF	Fibroblast Growth Factor (e.g. basic FGF – bFGF)
FLIPUS	Focused Low-Intensity Pulsed Ultrasound
GPCR	G-protein Coupled Receptors
GTPase	Guanosine Triphosphatases
I_{SATA}	Spatial Average Temporal Average Intensity
JNK	Jun Kinase
LIPUS	Low-Intensity Pulsed Ultrasound
Lats1/2	Large Tumor Suppressor Kinase 1 and 2
MAPK	Mitogen Activated Protein Kinase
MSCs	Mesenchymal Stem/Stromal Cells
NFκB	Nuclear Factor ´kappa-light-chain-enhancer´ of activated B-cells
NOS	Nitric Oxide Synthase (e.g. inducible NOS – iNOS)
OCN	Osteocalcin
OPN	Osteopontin
p38	p38 Protein Kinase
PRF	Pulse Repetition Frequency
mRNA	messenger Ribonucleic Acid
Runx-2	Runt-Related Transcription Factor 2
Sp1	Specificity Protein 1
TEAD	Transcriptional Enhancer Factor
TGF-β	Transforming Growth Factor-β (e.g. TGF-β1)
VEGF	Vascular Endothelial Growth Factor
YAP	Yes-Associated Protein
ZO-1/2	Zonula Occludent-1 and -2

The abbreviations are collected from the general sections “Introduction” and “Discussion”.

Each individual Chapter might contain its own abbreviations, which are explained in the text.

List of Publications

Puts,R., Albers,J., Kadow-Romacker,A., Geißler,S., and Raum,K. Influence of Donor Age and Stimulation Intensity on Osteogenic Differentiation of Rat Mesenchymal Stromal Cells in Response to Focused Low-Intensity Pulsed Ultrasound. *Ultrasound Med. Biol.*, Sept.2016.

Puts,R., Rikeit,P., Ruschke,K., Kadow-Romacker,A., Hwang,S., Jenderka,K.V., Knaus,P., and Raum,K. Activation of Mechanosensitive Transcription Factors in Murine C2C12 Mesenchymal Precursors by Focused Low-Intensity Pulsed Ultrasound (FLIPUS). *IEEE Trans. Ultrason. Ferroelectr. Freq. Control*, July2016.

Puts,R., Ruschke,K., Ambrosi,T.H., Kadow-Romacker,A., Knaus,P., Jenderka,K.V., and Raum,K. A Focused Low-Intensity Pulsed Ultrasound (FLIPUS) System for Cell Stimulation: Physical and Biological Proof of Principle. *IEEE Trans. Ultrason. Ferroelectr. Freq. Control*, vol. 63, no. 1, pp. 91-100, Jan.2016.

Klatte-Schulz,F., Giese,G., Differ,C., Minkwitz,S., Ruschke,K., **Puts,R.**, Knaus,P., and Wildemann,B. (2016). An investigation of BMP-7 mediated alterations to BMP signalling components in human tenocyte-like cells. *Sci. Rep.*, vol. 6, p. 29703, 2016.

Padilla,F., **Puts,R.**, Vico,L., Guignandon,A., and Raum,K. (2016). Stimulation of Bone Repair with Ultrasound. *Adv. Exp. Med. Biol.*, vol. 880, pp. 385-427, 2016 (Book Chapter).

Padilla,F.*, **Puts,R.***, Vico,L., and Raum,K. (2014). Stimulation of bone repair with ultrasound: a review of the possible mechanic effects. *Ultrasonics*, vol. 54, no. 5, pp. 1125-1145, July2014. (*equal contributions).

Table of Content

Introduction

Fast-growing athletically-active aging population and performance of complex reconstructive orthopedic surgeries, associated with genetic diseases, trauma or lesion formation, are a strong motivation to advance the field of regenerative therapies. In contrast to allograft and/or autograft transplants, the tissue engineering approach, which employs combinations of scaffolds, pluripotent cells and biological factors, has acquired increasing attention, due to the possibility to eliminate the risks of donor-site morbidity, immune rejection and transmission of infectious agents (Naughton et al., 1995).

1. Ex-vivo Implants for Tissue Engineering

The utilization of Mesenchymal Stromal Cells (MSCs) originating from bone marrow represents a major cell type for regeneration of skeletal disorders (Caplan, 1991). MSCs are pluripotent cells, whose progeny differentiates into skeletal tissues, i.e., cartilage, muscle, bone, ligament, tendon, fat (Pittenger et al., 1999). In addition to the vast differentiation potential of MSCs, their immunosuppressive properties makes them ideal candidates for application in *ex-vivo* implants (Beyth et al., 2005).

The initiation of healing signaling cascades in cells is often accomplished with the help of growth factors. Amongst bioactive proteins, which instruct tissue regeneration processes, are bone morphogenetic proteins (BMPs, especially BMP-2 and BMP-7), transforming growth factor-β (TGF-β), fibroblast growth factor (FGF), vascular endothelial growth factor (VEGF). These factors supply various stimuli to the cells: mitogenic, chemotactic, morphogenic, angioigenic (Varkey et al., 2004). Despite the high potency of the growth factors, there is a range of side effects associated with them (Argintar et al., 2011; Fortier et al., 2011), averting the "gold standard" application of these proteins.

In order to functionally reconstruct the damaged site of the organ, along with MSCs and/or growth factors, often application of a scaffold is required. Scaffolds, which are meant to rebuild the original organ architecture, have to fulfill a number of requirements: from the support of crucial physiological conditions of inhabitant cells, to the securing of optimal mechanical properties, able to sustain the organ integrity (Griffith and Naughton, 2002). Thus, amongst many other functions, the scaffolds have to be biocompatible, degrade over time after implantation, but

especially importantly for musculoskeletal tissues - still able to withstand mechanical forces and stresses at the organ site (Martin et al., 2004).

In an attempt to achieve controlled and reproducible tissue engineering approaches a number of bioreactors have been developed. Perfusion bioreactors, which mimic interstitial fluid conditions, improve mass transfer within the scaffold and allow for strict supervision of temperature, gas, pressure, nutrient supply, and waste removal, as well as provide better organized cellular populations throughout the entire construct (Yeatts and Fisher, 2011). Oxygen, nutrient, and waste gradients directly affect cellular viability, which can be significantly improved as soon as cells are moved to perfusion bioreactor (Volkmer et al., 2008). Not only the viability, but also the osteogenic differentiation potential of bone precursors is enhanced, when the cells are cultured in dynamic conditions (Pisanti et al., 2012; Potier et al., 2007).

Along with biological factors, the mechanical environment experienced by cells defines their phenotypic features and directs their functional properties. The mechanical stimulations, imitating forces at the regenerated site, can be achieved with the help of bioreactors, which are presented in the next section.

2. Bioreactors with Mechanical Conditioning

In the past twenty years there is a number of bioreactors mimicking local deformations of extracellular matrix (ECM) in response to mechanical loading were developed (Fig.1). These bioreactors with mechanical conditioning hold a potential to promote regeneration of various skeletal tissues, i.e., bone, tendon, ligament, cartilage.

The study of Mauney *et al.* (Mauney et al., 2004) showed that a set-up with four point bending, subjecting human MSCs in partially demineralized bone scaffolds to both compressive and tensile forces (Fig.1a), resulted in an increase of alkaline phosphatase (ALP) and osteopontin (OPN) production, and an enhanced calcium deposition into the matrix, which implied more intensive bone formation.

Through the application of uniaxial tensile stretching (Fig1.b) on avian flexor tendon cells in collagen scaffolds in the study of Garvin et al. (Garvin et al., 2003), the expression of collagen-1 (Col-1), Col-3, Col-12, fibronectin, prolyl hydroxylase, and tenascin were upregulated, increasing the ultimate tensile strength of engineered tendons by 3 fold. Similarly, rabbit MSCs grown in previously optimized Col-1 sponges yielded the best results in the maximum force and

linear stiffness, when the constructs were mechanically stretched, imitating tensile stresses during movement of patellar tendons in rabbit (Butler et al., 2008).

Tensile-compressive and torsional loading applied in a bioreactor mimicking forces in ligament (Fig1.c) resulted in higher expression levels of Col-1, Col-3, and fibronectin in bovine MSCs grown in Col-1 gels, eventually leading to elongated cells, which bundled in the direction of loading and resembled structure of ligaments (Altman et al., 2002a).

Uniaxial compression is a prevalent force experienced by articular cartilage *in vivo*. The bovine cartilage explants subjected to a 0.1 MPa compression in a continuous mode (Fig.1d) experienced the enhanced expression of the chondrogenic marker aggrecan (Valhmu and Raia, 2002). The compression delivered to the cells in a cyclic mode was evaluated by Huang *et al.* (Huang et al., 2004), who revealed that mechanical loading at 10 % strain and 1 Hz frequency promoted chondrogenesis of rabbit MSCs. Similar results were observed when the cells were treated with the TGF-β1 growth factor. Cyclic hydrostatic pressure is another force experienced by a liquid-filled cartilage tissue, which has been supplied in bioreactor system to human MSCs aggregates (Angele et al., 2003). The pressure at a magnitude of maximum 7.58 MPa enhanced chondrogenic phenotype of the cells. Chondrocytes isolated from bovine articular cartilages and grown under shear stress conditions, mimicking movement of synovial fluid, expressed more intensively Col-2 and experienced increase of the Young modulus and the ultimate strength of the tissue (Gemmiti and Guldberg, 2006).

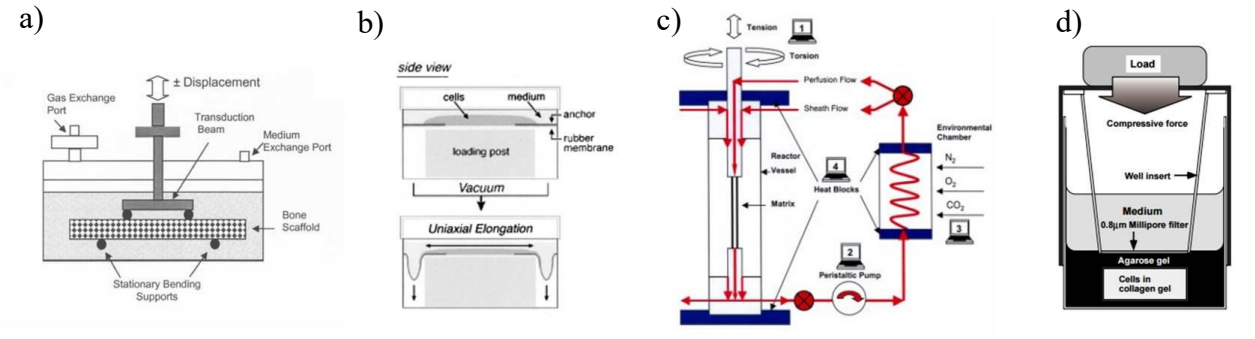

Fig.1: Bioreactors with mechanical conditioning for bone (a), tendon (b), ligament (c) and cartilage (d) tissue engineering, reproduced from (Mauney et al., 2004), (Garvin et al., 2003), (Altman et al., 2002b), (Takahashi et al., 1998), respectively.

Despite the studies, demonstrating the advances in bioreactors' development, mechanical conditioning remains a challenging topic to investigate. The designed *ex-vivo* implants, most of the time, do not fulfill the mechanical demands of the tissue. Therefore, the actual mechanical doses experienced by tissues *in vivo* need to be precisely evaluated. It is important to take into

account that the forces will modify throughout the lifetime of the organ. Moreover, a development of bioreactors, which apply a combination of forces closely resembling the mechanical means of the tissue, is in demand. Finally, the designed *in-vitro* bioreactors must be supplemented with the detailed reports, describing the physical phenomena introduced by the set-up and, very importantly, with the dose of mechanical stimuli delivered to the cells.

Amongst the bioreactors maintaining cellular viability and directing their differentiation, mechanical stimulation can be delivered to the cells also in the form of ultrasound. Ultrasound is supplied by relatively low-cost equipment and has been shown to mediate differentiation of musculoskeletal precursors into bone (Pounder and Harrison, 2008), cartilage, tendon and ligament (Khanna et al., 2009). In clinics, this technique is applied *in situ* on the damaged tissue *in vivo* and also has an advantage to be used as a mechanical conditioning tool for *ex-vivo* tissue engineering. The next section presents a detailed description of the Low-Intensity Pulsed Ultrasound (LIPUS) technique, elaborating on crucial components that need to be taken into account in order to optimize this physical approach.

3. Low-Intensity Pulsed Ultrasound

Ultrasound has a wide range of clinical applications. One of them is Low-Intensity Pulsed Ultrasound (LIPUS), - a therapeutic tissue regenerative technique utilizing intensity levels within a diagnostic range. LIPUS represents a non-invasive, non-ionizing gentle treatment currently used for regeneration of fresh fractures, delayed- and non-union bone in clinic as a device named EXOGEN. It employs a protocol consisting of 1.5 MHz acoustic wave delivered at 1 kHz pulse repetition frequency (PRF) at 20 % duty cycle (DC) (200 μs signal ON, 800 μs signal OFF) with a resultant spatial average temporal average intensity I_{SATA} of 30 mW/cm^2 (Pounder and Harrison, 2008). Recent reports emphasize the plausibility that LIPUS can be used for healing of soft tissues, naturally possessing poorer regenerative potential, i.e., tendon, cartilage, ligament, etc. (Khanna et al., 2009). Although numerous *in-vitr*o studies have attempted to explain the biological rationale behind the beneficial ultrasound mechanical stimulation, the mechanisms dictating cellular behavior deserve further investigation (Padilla et al., 2016). The irreproducibility of clinical outcomes in bone healing is highly influenced by the patients' gender, age and health history, as well as the specific fracture site and its stabilization (Watanabe et al., 2010), once again emphasizing the necessity to understand better LIPUS-induced physico-biological mechanisms and to create patient-characteristics-optimized stimulation protocols.

3.1 Basics of Ultrasound

Ultrasound represents mechanical waves (Fig.2a) traveling through a medium with frequencies above the human audible range (20 kHz) (Azhari, 2010). For longitudinal waves, the oscillation of particles occurs in the direction of the wave propagation (Fig.2b top), forming regions of compression (dense grid) and rarefaction (loose grid). In solid materials, ultrasound can also travel in shear, or transverse, mode, where the particle motion is perpendicular to the wave propagation direction (Fig.2b bottom). This phenomenon is not effectively achieved in liquids and gases (Carvalho et al., 2015).

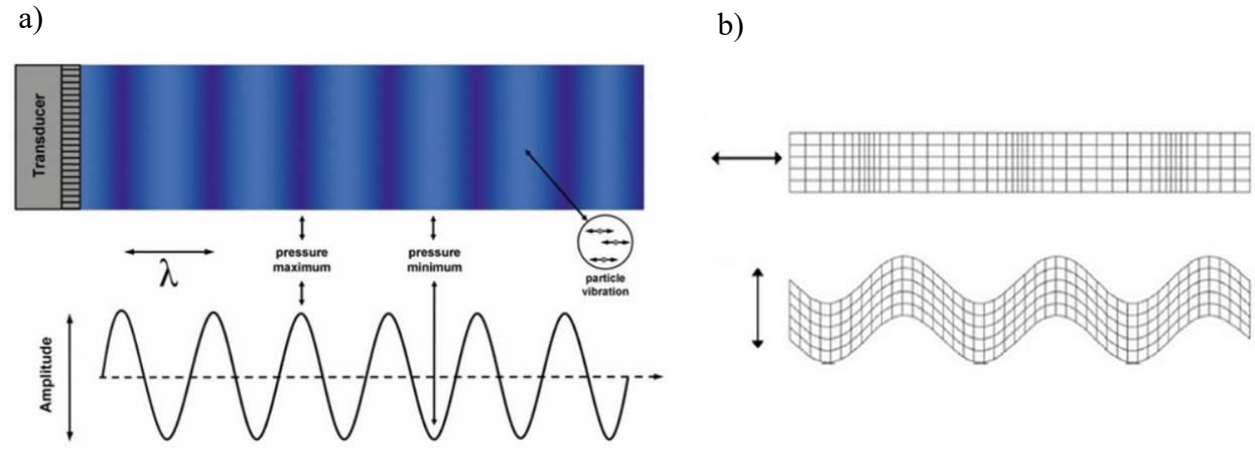

Fig.2: Propagating ultrasound wave (a), where λ is a wavelength (Hauff et al., 2008), and modes of ultrasound wave propagation (b): longitudinal (top) and shear (bottom) motion of particles (Carvalho et al., 2015).

The ultrasound waves can be generated with the help of piezoelectric crystals, which convert a supplied voltage pulse into an elastic vibration that is transmitted to the propagating medium. The frequency of the wave is indirectly proportional to the wavelength and represents the number of oscillations per given unit of time:

$$f = \frac{c}{\lambda}, \tag{1}$$

where λ (m), c (m/s), and f (Hz) are the wavelength, speed of sound, and frequency, respectively (Laugier and Haiat, 2011).

Ultrasound propagating from one medium to another will encounter a resistance, which is determined by the acoustic impedance mismatch of the two media. The acoustic impedance is directly proportional to the mass density and speed of sound in the medium (2):

$$Z = \rho \cdot c, \tag{2}$$

where Z (Pa·s/m) and ρ (kg/m^3) are the acoustic impedance and mass density, respectively (Laugier and Haiat, 2011).

The energy carried by a propagating ultrasound wave is described by an acoustic intensity, i.e., the energy transported per unit of time (s) per unit of area (cm^2), and measured in W/cm^2. The acoustic intensity of the wave is proportional to the square of acoustic pressure:

$$I = \frac{|p_{\mathrm{r}}|^2}{2 \cdot Z}, \tag{3}$$

where I (W/cm^2) and $|p_{\mathrm{r}}|$ (Pa) are the acoustic intensity and absolute acoustic peak pressure, respectively (Laugier and Haiat, 2011).

The spatial average temporal average acoustic intensity I_{SATA} is used to report the final power output parameter in most of the LIPUS studies. It is determined as the acoustic radiation force F_{rad} exhibited by a large absorber positioned perpendicular to the sound field (Padilla et al., 2014):

$$F_{\mathrm{rad}} = \frac{W}{c}, \tag{4}$$

where W (watt) is the acoustic output power. I_{SATA} averaged over the transducer surface area a (cm^2) is then found as:

$$I_{\mathrm{SATA}} = \frac{W}{a}. \tag{5}$$

For a continuous wave the acoustic pressure does not change with time, whereas for the wave delivered in a pulsed mode it depends on PRF and DC. For instance, for an ultrasound wave transmitted at 1 kHz PRF and 20 % DC, the temporal peak (TP) and temporal average (TA) intensities are related as following:

$$I_{\mathrm{TA}} = \tau_{\mathrm{on}} \cdot PRF \cdot I_{\mathrm{TP}} = 0.2 \cdot I_{TP}, \tag{6}$$

where τ_{on} (s) is the pulse duration (in this case 200 µs). The resultant local radiation pressure is dependent on PRF and proportional to the intensity averaged over the pulse duration (I_{PA}):

$$P_{rad} = \frac{1}{2} \cdot \frac{|p_r|^2}{\rho \cdot c^2} = \frac{I_{PA}}{c}. \quad (7)$$

Ultrasound is attenuated by the medium through various mechanisms. Absorption converts mechanical energy partially into heat. Reflection and refraction of ultrasound occurs when the travelling wave hits an interface having an impedance mismatch (Fig.3a). Acoustic scattering arises when the wave hits objects similar to, or smaller than, the acoustic wavelength and is reflected in different directions (Laugier and Haiat, 2011). If two strong reflectors confine the medium of the propagating ultrasound wave, the incident waves will interfere with the reflected ones, resulting in spatially immobile but temporally changing amplitude wave patterns, i.e., the standing wave effect (Azhari, 2010) (Fig.3b).

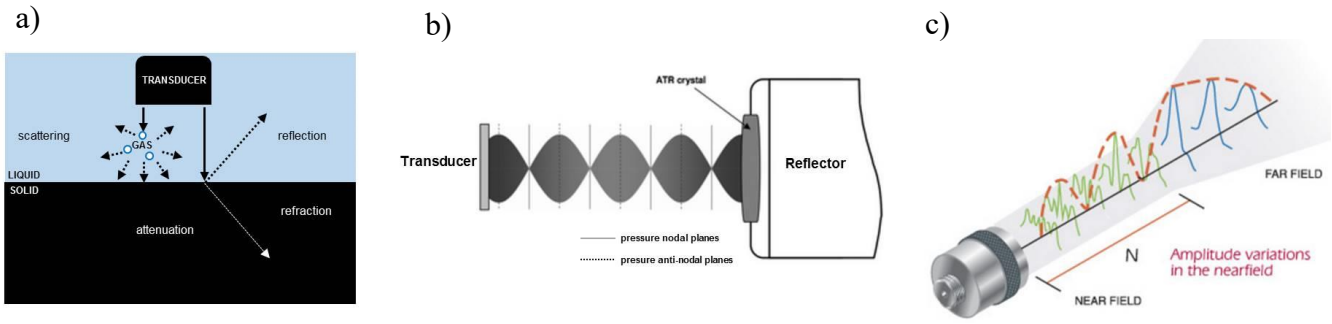

Fig.3: Interaction of ultrasound with a medium (a), standing waves effect (b) (reproduced and modified from (Wiklund et al., 2013)), and radiated fields of ultrasonic transducer (c) (courtesy of http://www.olympus-ims.com/en/ndt-tutorials/transducers/characteristics/).

The region of the propagating ultrasound wave in close proximity to the transducer is known as near-field and is characterized by high spatial variations of sound pressure (Fig.3c). The region further away from the probe, named far-field, exhibits a smooth gradual change of pressure.

3.2 Physical Effects of LIPUS *in vitro*

The understanding of regenerative biological LIPUS-regulated mechanisms is hindered by the complexity of physical phenomena simultaneously introduced by the treatment (Padilla et

al., 2014). The potential LIPUS-generated effects can be categorized into thermal and non-thermal.

Thermal effects arise from wave attenuation when it is propagated through materials, such as coupling gel, polystyrene cell culture plates. Temperature fluctuations can range from tenth of a degree to several degrees (Leskinen and Hynynen, 2012). The temperature rise could be high enough to activate metalloproteinases - thermo-sensitive enzymes - increasing reaction rate by a factor of 3 for each increase of 2ºC (Welgus et al., 1981).

Non-thermal, or mechanical, effects can be further subdivided into following groups: *oscillatory strains* at acoustic excitation frequency (1.5 MHz for conventional LIPUS EXOGEN device); *acoustic radiation force*, or oscillatory strains, at PRF (1 kHz, EXOGEN) (Sarvazyan et al., 2010); *acoustic streaming* produced by pressure gradients, generated by travelling mechanical wave and resulting in fluid movement directed away from the transducer (Zauhar et al., 2006); and *shear stresses* created by the fluid flow.

In addition to the described above mechanical effects, other physical forces can be generated depending on the design of the 2D *in-vitro* set-up, which might significantly alter the delivered mechanical dose. For instance, if the ultrasound-propagating media contains an inhomogeneity, e.g., gas, the bubbles will start oscillating, which results in *cavitation* (Baker et al., 2001). At high acoustic intensities the oscillating bubble can collapse and lead to the destruction of the matter it encounters. However, most of the described *in-vitro* set-ups employ stimulation intensities lower than 500 mW/cm^2, which is below the cavitation threshold and, therefore, are not affected by this physical effect (Harle et al., 2005). The travelling acoustic wave will be reflected at interfaces with different impedances (e.g. liquid-solid), which potentially can cause generation of *standing waves*. This can result in amplification of the delivered to the cells signal and prolongation of the duty cycle (Iwabuchi et al., 2005). Furthermore, the exposure of cells to the near-field of a planar transducer leads to a highly *heterogeneous intensity distribution* within the monolayer, which makes it unobvious what mechanical input the observed biological effect corresponds to.

Likewise, the application of the transducer's near-field is ambiguous in small animal models *in vivo*. Fig. 4 illustrates simulated sound fields of the planar probe versus the focused transducer. The high variation of intensity levels in the near-field (left) makes it challenging to stimulate the small gap region of the animal. Instead, the entire femur is subjected to stimulation with various intensity levels. On the other hand, focused transducer deposits the homogenous far-

field directly into the gap region (right), providing control over the volume of the irradiated region and the input intensity.

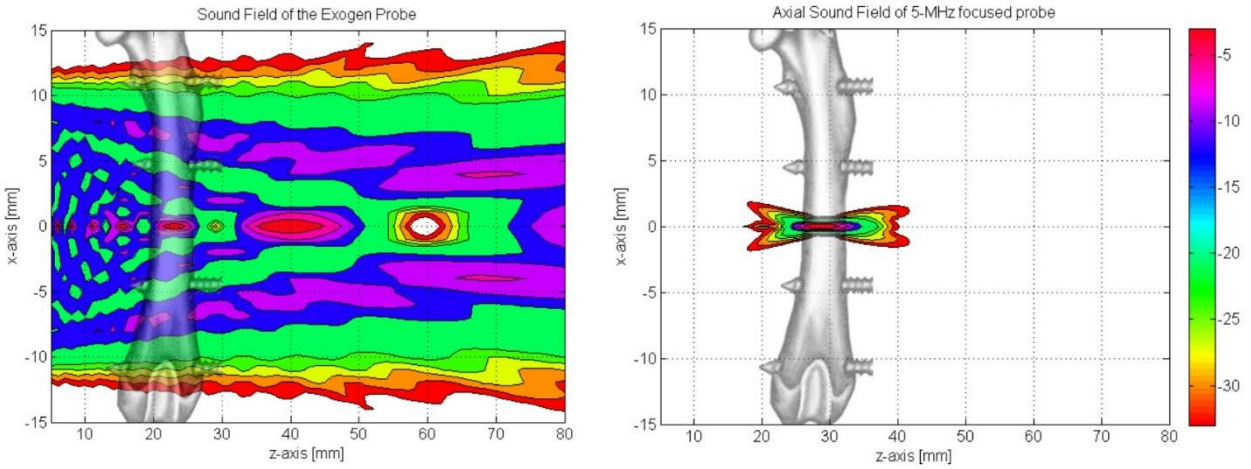

Fig.4: Simulated sound fields of planar (left) and focused (right) transducers. Figure is a courtesy of Prof. Kay Raum.

3.3 Overview of Existing LIPUS *in-vitro* Set-ups

Most of the *in-vitro* LIPUS set-ups described in the literature can be summarized in three main groups (Fig.5): (a) a transducer positioned at the bottom of the cell-culture plate through a coupling gel (Zhou et al., 2004; Unsworth et al., 2007; Takeuchi et al., 2008); (b) a transducer positioned at the top and submerged in the media of the cell-culture plate 3-4 mm away from the cells (Wang et al., 2004; Suzuki et al., 2009a; Suzuki et al., 2009b); and (c) a transducer positioned at the bottom of the temperature controlled water tank and cells positioned in the far-field of the generated field, shielded by a sound-absorbing chamber from the top (Iwabuchi et al., 2005; Bandow et al., 2007; Nakao et al., 2014).

The set-up in Fig.5a is the most popular amongst researches, however, it has a major shortcoming in its design that needs to be taken into account during data interpretation. As demonstrated in the study of Leskinen and Hynynen (Leskinen and Hynynen, 2012), during ultrasound propagation the coupling gel cannot cool fast enough, leading to up to 3°C temperature rise at the cell monolayer, when I_{SATA} of 30 mW/cm^2 is used. In this set-up the biological read-outs will be influenced by both mechanical and thermal effects. Along with temperature elevations, propagation of shear and Lamb waves can be observed at the bottom of the tissue-culture plate, transmitting the mechanical wave to the neighboring wells, where stimulation is undesired (Leskinen and Hynynen, 2012). The temperature rise can be minimized

in the set-up like in Fig.5c, where the temperature-maintained water tank is used as a coupling medium between the plate and the transducer.

Furthermore, in the gel-coupled set-ups the traveling pressure wave will be reflected at the liquid-air interface, potentially leading to standing waves (Hensel et al., 2011). The reflection of the wave at the interfaces with impedance mismatch could be also encountered in the set-up presented in Fig.5b, altering the delivered to the cells acoustic intensity.

Both set-ups in Fig.5a&b, employing planar transducers, are also prone to the introduction of a large variation in intensity levels at the cellular monolayer, due to stimulation of the cells in the near- field of the transducer. This complicates interpretation of the results, whereas the set-up in Fig.5c, subjecting the cells to the far-field of the transducer, has the advantage of introducing more homogenous signal distribution throughout the well. The use of a silicon shield absorbing the propagated wave from the top in the set-up in Fig.5c also prevents the cells from being subjected to standing waves (Iwabuchi et al., 2005).

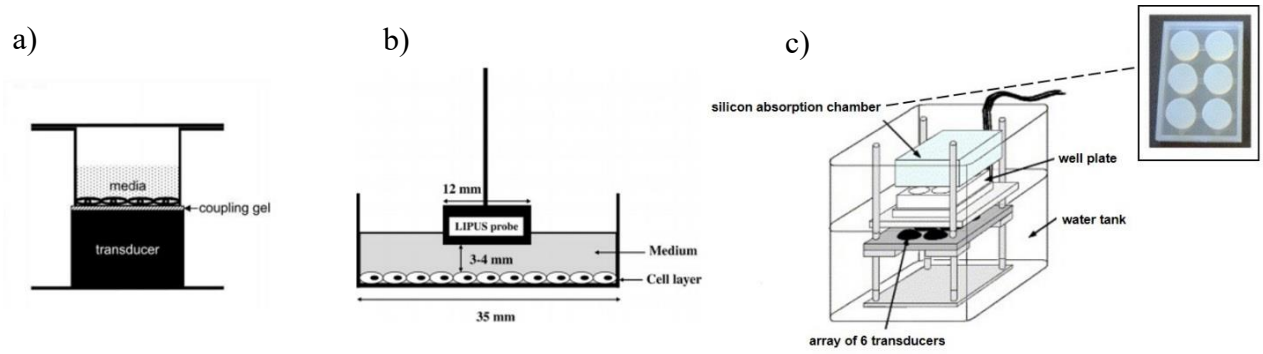

Fig.5: Most encountered in literature LIPUS *in-vitro* set-ups. (a-c) are used and modified from (Sena et al., 2005), (Ikeda et al., 2006), (Iwabuchi et al., 2005), respectively.

3.4 Summary of LIPUS-Induced Biological Effects in Bone Fracture Healing

Fig.6 is an overview of possible biological mechanisms triggered by the LIPUS stimulation. The data was gathered from the *in-vitro* reports and represented in detail below in the order of the overlapping stages of fracture healing (stages 1-4).

The expression of mechanosensitive gene c-fos was upregulated in rat MSCs, primary rat osteoblasts and murine ST2 stromal cell line as early as 20 min following the LIPUS exposure (Naruse et al., 2003; Naruse et al., 2000; Warden et al., 2001; Sena et al., 2005). Several hours later the increased expression of c-jun, c-myc and Erg-1 has been demonstrated in rat MSCs treated with LIPUS (Sena et al., 2005) (Fig.6, st.1). *c-jun, c-fos, c-myc and Erg-1 are*

transcriptional factors regulating both proliferation and osteogenesis of bone-lining cells (Bozec et al., 2010; Thiel and Cibelli, 2002; Kirstein and Baglioni, 1988).

Bone healing process starts with a hematoma formation, which secludes the defect and initiates innate inflammatory response, attracting macrophages, monocytes, dendritic cells, etc. LIPUS enhanced the mRNA accumulation of monocyte chemoattractant protein-1 (CCL2) and macrophage-inflammatory protein-1 (CCL4) in murine pre-osteoblasts, supposedly boosting the body inflammatory response (Bandow et al., 2007) (Fig.6, st.1-4). *The formed hematoma also triggers attraction of cellular precursors intending to repair the fracture site.* The enhanced migration of osteogenic precursors in response to LIPUS has been shown by several studies (Jang et al., 2014; Kumagai et al., 2012; Man et al., 2012) (Fig.6, st.1).

The formation of new blood vessels is initiated early enough to assure proper functioning of the newly forming bone. An increase in secretion of inteleukin-8 (IL-8), VEGF and bFGF by osteoblasts of different origin was observed after LIPUS stimulation (Wang et al., 2004; Doan et al., 1999; Bandow et al., 2007) (Fig.6, st.1&2). *These cytokines serve as pro-mitogenic and chemotactic factors for endothelial cells, supporting process of angiogenesis* (Koch et al., 1992; Radomsky et al., 1998; Ferrara et al., 2003). *Inducible nitric oxide synthase (iNOS) and cyclooxygenase-2 (COX-2), catalyzing synthesis of nitric oxide (NO) free radical gas and prostaglandin E2 (PGE2), respectively, positively influence fracture regeneration* (Liedert et al., 2006). Both of the enzymes were found to be up-regulated after LIPUS introduction in a number of studies (Reher et al., 2002; Wang et al., 2004; Tang et al., 2006) (Fig.6, st.1).

As a next step, the mechanically unstable fracture site gets gradually filled with chondrocytes and soft callus tissue is formed. The LIPUS treatment had also an impact on cellular chondrogenesis. Proliferation of chondrocytes, isolated form different species, was enhanced by the LIPUS stimulation (Takeuchi et al., 2008; Kobayashi et al., 2009) (Fig.6, st.3&4). The mechanical treatment with ultrasound increased the expression of chondrogenic markers, i.e., Sox-9 pro-chondrogenic transcription factor, proteoglycans, Col-2, Col-9 and Col-10, TGF-β and its receptor (TGF-β R1), in MSCs and chondrocytes (Lee et al., 2006; Schumann et al., 2006; Mukai et al., 2005) (Fig.6, st.3&4).

In order to gain functional stability, the soft callus is eventually replaced by a hard bony tissue, which is built by osteoblasts, depositing minerals into the matrix. The mitosis of bone precursors and maturating osteoblasts greatened after the LIPUS exposure, implying an increase in bone formation after the mechanical stimulation (Reher et al., 1998; Hasegawa et al., 2009; Hayton et al., 2005; Doan et al., 1999) (Fig.6, st.2&3). Along with the bone formation, bone

maturation was enhanced when LIPUS was supplied to the cells. This was quantified by expression of osteogenic markers, i.e., runt-related transcription factor 2 (Runx2) and osterix (Osx), Msx2 and Dlx5 homeobox proteins, OPN, osteocalcin (OCN), bone sialoprotein (BSP), Col-1, ALP, and BMPs and their receptors, in various osteoblasts-like cells (Gleizal et al., 2006; Suzuki et al., 2009a; Suzuki et al., 2009b; Maddi et al., 2006; Unsworth et al., 2007; Sant'Anna et al., 2005; Ikeda et al., 2006) (Fig.6, st.2&3).

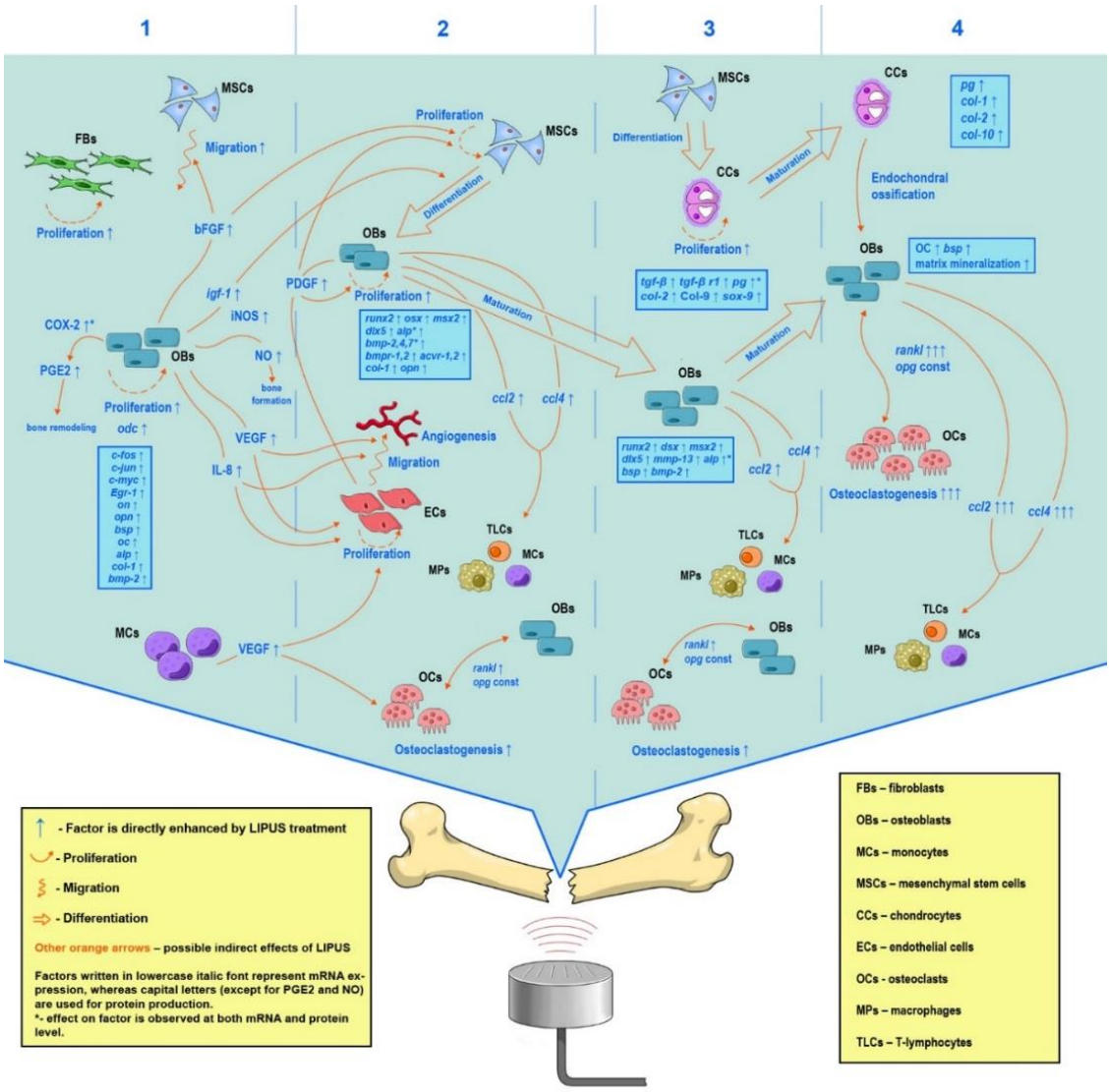

Fig.6: Possible biological mechanisms regulating bone fracture regeneration by LIPUS, summarized from *in-vitro* reports: each compartment is a separate healing stage in the course of endochondral ossification (Padilla et al., 2014).

Chondrocytes rebuilding the bone defect eventually undergo hypertrophy and cede to osteoblasts, which guide the process of bone restoration. By cooperative functioning of

osteoblasts and osteoclasts the formed woven bone gets slowly remodeled into a lamellar bone. In murine osteoblasts LIPUS increased the mRNA accumulation of NFκB ligand (RANKL), which enhances osteoclastic activity, whereas the amounts of osteoclasts inhibiting osteoprotegerin (OPG) remained unchanged throughout 4 weeks of the exposure (Bandow et al., 2007) (Fig.6, st.2-4). The expression of RANKL was the most pronounced during week 3, which corresponds to the formation of mature lamellar bone in mice (Fig.6, st.4).

3.5 LIPUS and Conflicting *in-vitro* Reports

Despite the enormous evidence of LIPUS advantageous effects described in the previous section, there is a number of studies presenting data sets which contradict one another. The disagreement in the reported biological outcomes could be attributed to variation of species, cell-site specificity and the maturation state of the cells. However, it is important as well to take into account the design of the LIPUS set-up and the stimulation parameters used in each study.

In the study by Tsai *et al.* (Tsai et al., 1992), stimulation with 1.5 MHz frequency at 200 μs pulses and I_{SATA} = 0.5 W/cm^2 significantly improved healing of rabbit fibulae, whereas Reher *et al.* (Reher et al., 1997), using 3 MHz frequency at 2 ms pulses and the same intensity, observed no effect on murine calvaria bone synthesis. The discrepancies in the results could be due to differences in species and bone types. However, they could also be frequency- and PRF-dependent. The changes in PRF leading to variation of biological response to LIPUS has been shown previously by Marvel *et al.* (Marvel et al., 2010).

Proliferation of human hematoma-derived osteoprogenitors was not affected by LIPUS, when parameters introduced by EXOGEN were used (Hasegawa et al., 2009). On the other hand, human MSCs isolated from amniotic membrane were more viable when stimulated with continuous ultrasound (97 % DC) at 350 mW/cm^2 (Shah et al., 2013). These differences could be explained by the delivery mode: pulsed vs continuous. However, one should note that ultrasound at 97 % DC was introduced through a gel-coupling, which most likely led to an increase in temperature at the cell monolayer. From my personal experience, rat MSCs stimulated with LIPUS at I_{SATA} = 44.5 mW/cm^2, corresponding to mean pressure of 85 kPa, had no pro-mitogenic effect on the cells when cultured in normal conditions. Nevertheless, the benefits of the ultrasound treatment were observed when the cells were moved to starving condition.

Contradictory effects of LIPUS on proliferation of human osteosarcoma SaOS2 cell-line have been reported. Hayton *et al.* (Hayton et al., 2005), using the set-up from the top (Fig.5b), observed significant increase in cell numbers on day three of the stimulation. Sawai *et al.* (Sawai

et al., 2012), using the same set of parameters, but the set-up with transducer submerged in a water tank (Fig.5c), observed no changes in cellular proliferation within three days of LIPUS treatment. The variation in cellular outcomes could be explained by the inequality of stimulation times: 20 min in the study by Sawai *et al.* vs 40 min twice a day reported by Hayton *et al.* However, it is also important to keep in mind the possibility that in the set-up from the top, the signal was amplified by reflective interfaces.

Similarly to the last two studies, contradicting effects on osteogenic differentiation of MC3T3-E1 pre-osteoblasts have been shown by Bandow *et al*. (Bandow et al., 2007) and Unsworth *et al.* (Unsworth et al., 2007). The former team observed no changes in cellular osteogenic differentiation and used the set-up with the water tank (Fig.5c), stimulating the cells in the far-field of the transducer. The latter group coupled LIPUS through gel from the bottom (Fig.5a), demonstrating that ALP expression and matrix mineralization in the cells are enhanced upon the mechanical stimulation. Both groups used the same set of LIPUS stimulation parameters and the temporal evaluation of biological responses overlap with each other. Therefore, the inconsistencies in the reported results most likely solely arise from the set-up designs. The gel-coupled set-up is prone to temperature rise and standing waves, whereas the water tank set-up most likely has constant temperature and lower intensity levels, due to positioning of the plate away from the transducer, although no distance between the probe and the plate was specified. Further reports have shown disagreeing LIPUS effects on the osteogenic differentiation of cells of bone origin (Naruse et al., 2000; Warden et al., 2001) and both inhibition and enhancement of osteoclastic activity upon ultrasound exposure have been demonstrated (Hayton et al., 2005; Bandow et al., 2007; Maddi et al., 2006; Sun et al., 2001).

Therefore, in order to gain deep understanding in LIPUS-induced regenerative mechanisms, it is crucial to design *in-vitro* set-ups minimizing the introduction of signal-amplifying physical effects and temperature elevations and enabling control over the delivered mechanical dose. ***Application of focused transducers is one of the possible ways to restrict mechanical effects for mechanistic studies of LIPUS-induced biological responses in vitro and in vivo. This approach was utilized and developed in this thesis.***

The next section is dedicated to a summary of biochemical mechanisms, which are generated in response to diverse mechanical stimuli.

4. Biochemistry of Mechanotransduction

Mechanical stimuli are as important as biological factors for cellular homeostasis during the embryonic development and maintenance of adult tissues. Mechanically stimulated adherent cells sense deformations of the ECM and respond to the experienced forces, adjusting the tissue functionality (Mammoto et al., 2012). Mechanotransduction starts with the cellular receptors sensing the signal and transmitting it intracellularly. The signal is then propagated by signaling pathways, eventually affecting the function of the mechanoresponsive transcription factors and regulating the expression of various genes. The mechanisms of mechanotransduction are summarized in Fig.7.

4.1 Mechanosensitive receptors

Integrins

Integrins are the most characterized mechanosensitive receptors, which represent heterodimeric transmembrane proteins connecting the ECM, made of elastin, collagen, proteoglycans, and glycosaminoglycans, to the cytoskeleton through linker proteins, i.e., vinculin, talin, α-actinin, filamin, paxillin (Humphrey et al., 2014).

Integrins are known to be activated by hydrostatic and osmotic pressure, shear and tensile stresses leading to formation of focal adhesion complexes (Katsumi et al., 2004). The mechanical forces promote binding between talin and vinculin, which in turn binds actin and reinforces the integrin-cytoskeleton link (Humphrey et al., 2014). This accomplished through conformational changes in the integrin structure (Chen et al., 2012). The mechanical stresses sensed by integrins are transmitted to actin filaments and non-muscle myosin reaching all the way to the nuclear lamina and chromatin (Le et al., 2016). The mechanisms of mechanotransduction through the activation of integrins by LIPUS has been numerously demonstrated in the cells of the musculoskeletal system (Whitney et al., 2012; Tang et al., 2006; Yang et al., 2005)

Syndecans

Syndecans are also transmembrane proteins providing a link between the ECM and cytoskeleton. The core protein structure of syndecans is modified by glycosaminoglycan chains, most of which are heparin sulfates (Couchman, 2003). One of the members of the receptors' family is ubiquitous throughout tissues, syndecan-4, which provides cellular adhesion and

spreading via clustering at focal adhesion complexes (Bellin et al., 2009). Syndecans-4 are linked intracellularly to the cytoskeleton through paxillin, syndesmos and hic-5 (Denhez et al., 2002).

There has been a cooperative functioning of integrins and syndecans established (Bass et al., 2007), which most likely occurs through a functioning of protein kinase Cα (PKCα). Syndecan-4, possessing binding site for PKCα, recruits the kinase to the focal adhesions and induces cellular motility. Similarly, integrin β1 interacts with PKCα and promotes cellular migration, suggesting a synergistic functioning of these two receptors at signaling of the kinase (Morgan et al., 2007). Cooperative functioning of syndecan-4 and integrin in fibroblasts is also crucial to facilitate successful wound healing (Echtermeyer et al., 2001) and ablation of syndecan-4 prevents cells from formation of the focal adhesions. The treatment of fibroblasts with LIPUS restores the cell ability to adhere and spread and compensates for the loss of syndecan-4 (Mahoney et al., 2009).

Cadherins

Cadherins are calcium-dependent adhesion proteins forming homophilic bonding with the cadherins of neighboring cells, maintaining cell-cell junction contacts (Kemler, 1993), and building structures, which resemble focal adhesions (Maruthamuthu et al., 2011). Cadherins transduce intercellular tension into intracellular processes through an indirect binding to the cytoskeleton: the cytodomain of cadherins interacts with β-catenin, which in turn binds to α-catenin (Leckband et al., 2011). During the application of tensile stress, cellular α-catenin releases a site, which is specific for the vinculin-actomyosin binding, and allows transmission of the mechanical force. Zonula occludent-1 (ZO-1), eplin and vezatin are also possible partners achieving the binding between actin and α-catenin (Leckband et al., 2011).

Stretch-Activated Ion Channels

Application of a mechanical force increases tension within the lipid bilayer, increasing the probability of an opening of the transmembrane ion channels. This triggers flux of cations, i.e., Ca^{2+}, Na^{+}, K^{+}, across the membrane, activating intracellular signaling pathways, such as protein kinase C (PKC), calmodulin-dependent kinase, and Ras (Iqbal and Zaidi, 2005; Liedert et al., 2006).

Substrate stiffness can directly affect the flux of Ca^{2+} and softening of the matrix reduces the frequency and magnitude of the cation oscillations (Kim et al., 2009). Intracellular changes in Ca^{2+} concentrations were shown to regulate differentiation of human MSCs (Sun et al., 2007),

whereas epithelial-like Na^+ and Ca^{2+} channels were found to control the responsiveness of osteocytes to mechanical stimulation (Mikuni-Takagaki, 1999). LIPUS has been shown to increase the intracellular Ca^{2+} concertation, inducing enhanced differentiation of chondrocytes (Parvizi et al., 2002).

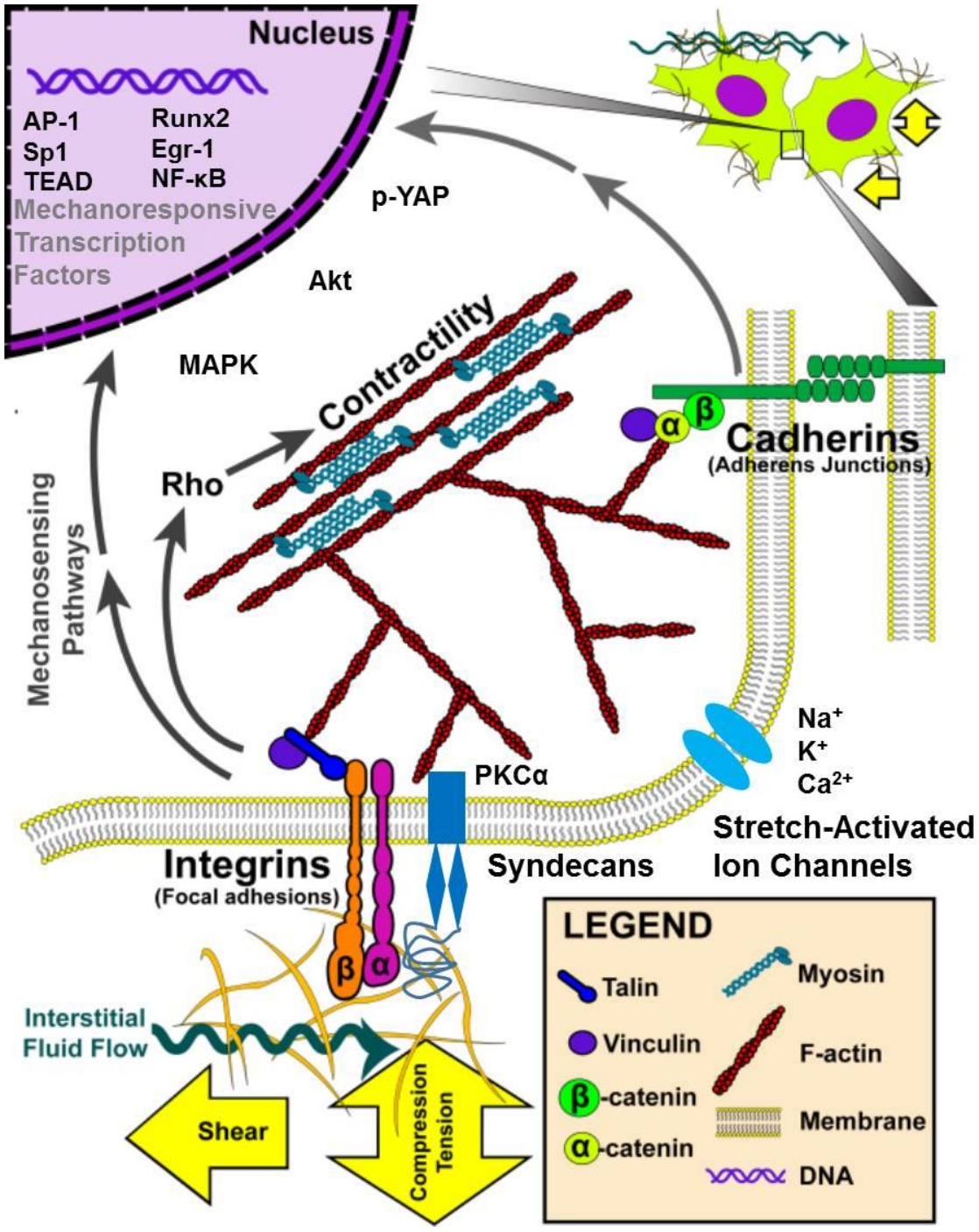

Fig.7: Mechanisms of mechanotransduction. Figure is used and modified from (Freedman et al., 2015).

Other Receptors

Angiotensin II type 1 (AT1) receptor regulates cardiac hypertrophy by mechanical loading (Zou et al., 2004). The receptor is encountered in osteoblasts and its expression elevates with cellular maturation. The transmission of the mechanical stimulus generated by LIPUS in differentiating pre-osteoblasts has been shown to be mediated through activation of AT1 receptor and enhanced phosphorylation of extracellular signal-regulated kinase (Erk) (Bandow et al., 2007).

The co-application of BMP-2 and cyclic mechanical loading enhances phosphorylation of downstream Smad1/5/8 transcription factors and upregulates expression of DNA-binding inhibitor Id-1 – the direct BMP-2 target gene (Kopf et al., 2012), suggesting a role of BMP receptors in mechanotransduction. Shear stress regulates activity of integrins and BMP receptor type IA, resulting in cell cycle arrest of human MG63 sarcoma cells (Chang et al., 2008). Co-localization of BMP receptors I and II with integrins has been previously demonstrated to be responsible for BMP-2-mediated differentiation of human osteoblasts (Lai and Cheng, 2005). The combined treatment with LIPUS and BMP-2 (Sant'Anna et al., 2005), or BMP-7 (Lee et al., 2013), resulted in synergistically enhanced osteogenic differentiation of osteoprogenitors in comparison to the treatment with the growth factor alone.

4.2 Intracellular Mechanotransduction Pathways

The summary of mechanotransduction pathways is presented in Fig.7.

Mitogen-Activated Protein Kinases

Mitogen-Activated Protein Kinases (MAPK) are protein serine-threonine kinases, which are activated in response to mitogens and diverse stress stimuli, i.e., ultraviolet exposure, heat, mechanical force and regulate proliferation, apoptosis, differentiation and chemotaxis of mammalian cells (Chen et al., 2001). The three most characterized members of the MAPK are extracellular signal-regulated kinase 1 and 2 (Erk1/2), p38 kinase, and Jun kinase (JNK). Activation of the kinases occurs through a consequent phosphorylation, which transmits the signal further to the regulatory proteins in the cell (Yang et al., 2003).

Integrins appear to be important players in activation of MAPK in response to mechanical stimuli (MacKenna et al., 1998; Hanke et al., 2010). The mechanical stretching of cells, seeded on anti-syndecan-4 antibody coated surfaces, also results in activation of Erk, similarly to integrin signaling (Bellin et al., 2009). The actin depolymerizing agents, latrunculin-B and cytochalasin-D, abolish syndecan-4 mediated Erk phosphorylation. Cyclic compression

and shear stress applied on cartilage activates Erk1/2 and p38 kinases (Fitzgerald et al., 2008). Rat MSCs subjected to cyclic loading express more intensively chondrogenic markers, i.e., aggrecan, Col-2α1, Sox-9, and the expression is regulated by activation of p38 kinase (Li et al., 2009). Hydrostatic pressure applied on MSCs promotes their osteogenic differentiation through activation of Erk1/2 but not p38 (Liu et al., 2009). Stimulation of cells with LIPUS promoted phenotypic features of osteoblasts, chondrocytes, tenocytes, etc., through activation of all three MAPK (Ikeda et al., 2006; Angle et al., 2011; Chao et al., 2011; Ren et al., 2013; Whitney et al., 2012; Nakao et al., 2014).

Akt Signaling

Along with MAPK, integrins can also activate the protein kinase B (Akt) pathway. Mechanically stretched human epidermal keratinocytes receive a pro-proliferative and an anti-apoptotic signal through activation of Akt kinase (Yano et al., 2006). Shear stress activates Akt, stimulating NOS and small resistance arteries dilation (Loufrani et al., 2008). Activation of Akt in response to LIPUS enhances proliferation of chondrocytes (Takeuchi et al., 2008) and osteogenic differentiation of osteoblasts (Tang et al., 2006).

Small Guanosine Triphosphatases

Another type of sensor-proteins, transmitting the mechanical signal intracellularly, are small Rho guanosine triphosphatases (GTPases), i.e., Rho, CDC42, and Rac. They are key regulators of the cytoskeletal dynamic, which affect various cellular functions: cytokinesis, endocytosis, and migration (Pertz, 2010). Rho GTPases are active in GTP- and inactive in GDP-bound form. Due to this chemical switch mode, they function transient and local: Rho stimulates actomyosin fiber formation, Rac promotes lamellipodia, and CDC42 induces filopodia and activates Rac (Hall, 1998).

The mechanical stress applied on smooth muscle cells results in a very fast (less than 300 ms) increase in Rac activation (Poh et al., 2009). Shear force induces osteogenic phenotype in murine MSCs, through the activation of RhoA (Arnsdorf et al., 2009), whereas chondrogenic and adipogenic differentiations of the cells are inhibited by mechanical stimulation. Both Rac and CDC42 are activated by shear stress in osteoblasts, regulating bone formation through β-catenin signaling (Wan et al., 2013). Activation of Rac1 (Roper et al., 2012) and RhoA GTPases (Zhou et al., 2004) was also observed in response to LIPUS stimulus.

Yes-Associated Protein Signaling

Yes-Associated Protein (YAP) represents an important mediator of Hippo signaling pathway, which controls organ size and tissue patterning. YAP was first discovered bound to the SH3 domain of non-receptor tyrosine kinase Yes1 (Sudol, 1994). The regulatory domains of YAP are summarized in Fig.8. Two isoforms, produced by alternative splicing, contain either one conserved WW domain (in chicken) or two WW domains (in human and mouse). The WW-domain is responsible for interaction with proteins containing PPXY motifs (Yagi et al., 1999). The C-terminal of YAP, i.e., transcriptional activation domain (TAD), is responsible for the transcriptional co-activator function of the protein (Vassilev et al., 2001). The C-terminal of the protein is also responsible for interaction with PDZ-domain containing proteins, e.g., ZO-1/2 (Ye and Zhang, 2013). The N-terminal of YAP is responsible for binding to the family of transcriptional enhancer factors (TEADs), which regulate cellular survival and proliferation (Ota and Sasaki, 2008). In human, phosphorylation of YAP on Ser127 (mouse Ser112) results in its cytoplasmic retention by 14-3-3 proteins, whereas phosphorylation of Ser397 (mouse Ser381) leads to degradation of YAP, inhibiting its nuclear activity (Varelas, 2014).

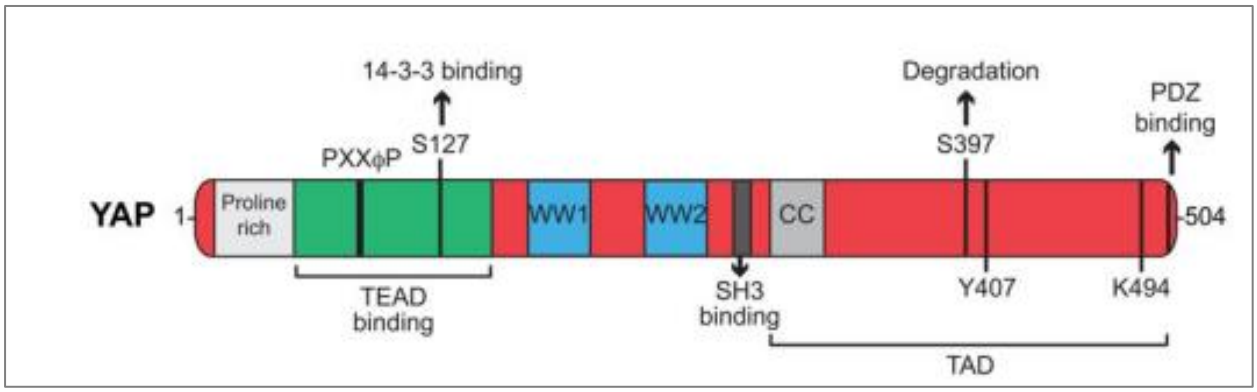

Fig.8: Important regulatory domains of human YAP1 (Varelas, 2014).

The YAP protein has no DNA binding activity and promotes transcription through its binding partners, i.e., TEAD, Runx2, Smad1 transcription factors, etc. (Piccolo et al., 2014). The fate of YAP can be regulated by extracellular biological factors through functioning of, e.g., G-protein coupled receptors GPCRs, leukemia inhibitory factor receptors (LIFRs), and E-cadherins, which either inhibit or activate Hippo pathway (Low et al., 2014). The core mammalian Hippo cascade consists of Mammalian Sterile20-like kinase 1 and 2 (Mst1/2), which interact with a scaffold protein Salvador1 (Sav1) and activates large tumor suppressor kinase 1 and 2 (Lats1/2) regulated by a Mob1 protein, and YAP. As a result of the activated Hippo pathway, YAP is

phosphorylated by Lats1/2 on Ser127 and retained in the cytoplasm, inhibiting cellular growth (Huang et al., 2005; Hao et al., 2008; Song et al., 2010; Lai et al., 2005; Pantalacci et al., 2003) (Fig.9).

Activation of YAP is not solely dependent on extracellular biological stimuli, cell-cell contacts were also found to regulate functioning of the protein (Fig.9). Apically localized crumbs complex (CRB) can bind YAP and detain it in the cytoplasm at tight junctions (Varelas et al., 2010). Angiomotin proteins (AMOTs) can also inhibit YAP activity either by direct sequestration in the cytoplasm or through activation of Hippo pathway (Piccolo et al., 2014). Inhibition of YAP could also occur at adherent junctions through the linker protein α-catenin (Schlegelmilch et al., 2011).

Functioning of YAP gained even more interest when mechanosensitive properties of the protein were discovered (Dupont et al., 2011). Cells constrained to small adhesive areas or grown on soft extracellular matrix has YAP localized in the cytoplasm and undergo growth arrest and apoptosis. On the other hand, large adhesive areas and stiff substrate promote translocation of YAP to the nucleus and cellular proliferation is enhanced (Fig.10). Similarly, growth of MSCs on the ECM with the increasing stiffness, enhances osteogenic potential of the cells through functioning of YAP (Piccolo et al., 2014).

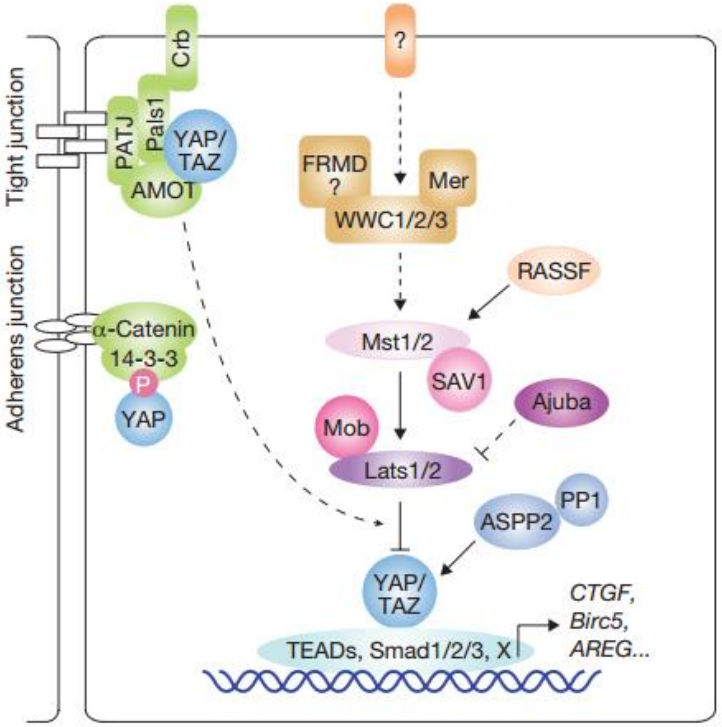

Fig.9: Mammalian Hippo Cascade (Zhao et al., 2011).

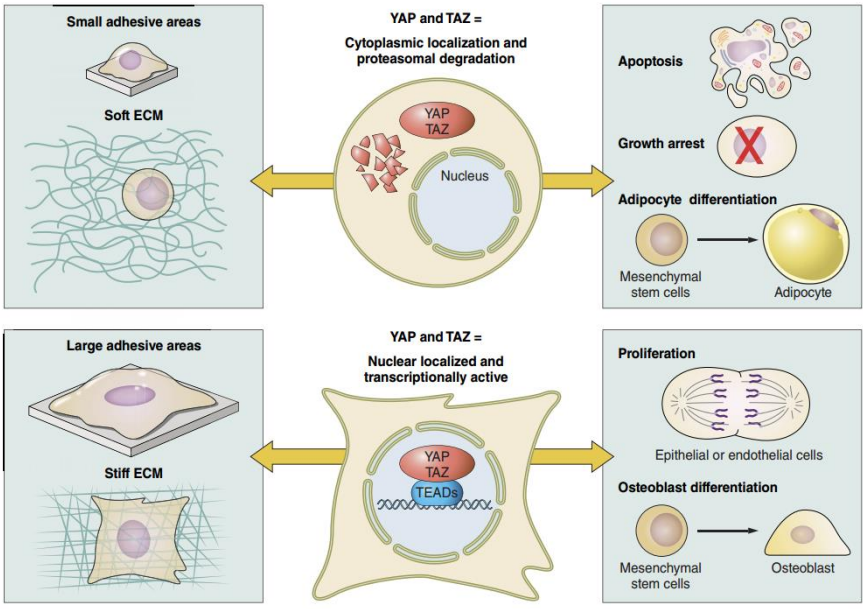

Fig.10: Regulation of cellular fate by YAP in response to cellular geometry (Piccolo et al., 2014).

Despite the intensive efforts the mechanism of YAP mechanotransduction is not fully understood and the upstream from YAP participants are yet to be determined. ***The involvement of YAP in the mechanism in response to LIPUS mechanical stimulation has not been previously demonstrated and is investigated in this thesis.***

Other Pathways

Cyclic mechanical stretching inhibits adipogenic differentiation of C2C12 mesenchymal precursors through activation of Wnt cascade (Akimoto et al., 2005). Similar mechanical application in mineralizing osteoblasts inhibits Wnt/β-catenin signaling (Jansen et al., 2010), which was activated when the short-term stimulation was introduced. TGF-β signaling can be directly affected by integrins or indirectly with help of GPCRs (Margadant and Sonnenberg, 2010). Matrix elasticity regulates the balance between matrix-bound and released TGF-β ligands, affecting signaling of the growth factors (Dingal et al., 2014). Stimulation of chondrocytes with LIPUS significantly induces expression of TGF-β1 and mimics the effects of cell-treatment with the recombinant TGF-β1 growth factor (Mukai et al., 2005). LIPUS exposure on rat osteosarcoma cells activates Smad1 transcription factor and enhances mRNA expression of BMP receptors I and II, as well as BMP-2, BMP-4, and BMP-7 protein production (Suzuki et al., 2009a), which suggests the involvement of canonical BMP-pathway in mechanotransduction.

4.3 Mechanosensitive Transcription Factors

A number of transcription factors has been found to be regulated by mechanical stimuli (Fig.7). Activator protein-1 (AP-1) transcription factor represents a heterodimer of c-fos and c-jun proteins (Karin et al., 1997). The AP-1 binding sites are encountered in promoters of cyclic adenosine monophosphate (AMP) response elements (CRE) and shear stress response elements (SSRE) found in promoters of mechanosensitive genes, i.e., c-fos and insulin growth factor-1 (IGF-1) (Liedert et al., 2006). Fluid shear force induces expression of COX-2 and mutation of the AP-1 binding sites ablates expression of the protein (Ogasawara et al., 2001). AP-1 also binds to promoters of iNOS, Col-1, and OPN genes (Nomura and Takano-Yamamoto, 2000). The phosphorylation of Erk1/2 and JNK kinases in response to mechanical stimulus activates AP-1 and upregulates expression of Col-1 in human periodontal ligament cells (hPDLCs) (Kook et al., 2009).

Application of tensile forces in fibroblasts induces the expression of filamin-A, regulating actin reorganization in the mechanism mediated by integrins, p38 and specificity protein 1 (Sp1) mechanosensitive transcription factor (D'Addario et al., 2002). Cyclic stretching of human MSCs, stably transfected with AP-1 and Sp1 responsive luciferase reporters, results in enhanced activity of the transcription factors and upregulates the expression of the mechanosensitive genes (Seefried et al., 2010).

TEAD family of transcription factors lack transcriptional function without co-activator proteins. Amongst TEAD partners are MAX nuclear phosphoprotein, TONDU and YAP. TEADs are the most encountered partners of the mechanosensitive YAP co-activator protein, interacting with it through its Ser65 and driving cellular proliferation (Vassilev et al., 2001). The described target genes of the TEAD-YAP complex are Survivin (Birc5) – inhibitor of apoptosis, CyclinD and E – cell cycle regulators, connective tissue growth factor (CTGF) – pro-mitogenic protein (Zhao et al., 2011).

Nuclear factor ´kappa-light-chain-enhancer´ of activated B-cells (NFκB) is a transcription factor activated by shear force (Nomura and Takano-Yamamoto, 2000). It can bind to the SSRE and induce expression of platelet-derived growth factor-β (PDGF-β) in endothelial cells in response to fluid flow (Khachigian et al., 1995). Along with NFκB, early growth response-1 factor (Egr-1) binds to the SSRE and maintains homeostasis of blood vessels (Gimbrone, Jr. et al., 2000). The functioning of NFκB is mediated by activity of integrins and p38 (Mammoto et al., 2012). Runx2 transcription factor is essential for skeletal mechanotransduction. Mechanically

activated Erk1/2 phosphorylates and activates Runx2, which in turn promotes cellular osteogenesis (Papachristou et al., 2009).

The functioning of three transcription factors AP-1, Sp1 and TEAD after mechanical stimulation with LIPUS was investigated in this thesis.

To summarize, the biochemistry of mechanotransduction consists of numerous mutually interacting components. Therefore, the investigation of regenerative mechanisms after mechanical stimulation with such complex physical phenomena as LIPUS requires development of *in-vitro* set-ups with well-controlled acoustic parameters. One of these set-ups was designed, optimized, and described in this thesis.

The Aim Statement

It can be concluded from the complexity of mechanotransduction phenomena and the conflicting biological effects in response to LIPUS discussed in the Introduction, a variation of stimulation set-ups and a limited control over the mechanical input can lead to misinterpretation of *in-vitro* results and their inadequate translation into *in-vivo* setting. Therefore, the aim of my thesis was to characterize a focused LIPUS (FLIPUS) set-up, enabling standardized introduction of "acoustic dose" with limited exposure to unwanted physical artifacts. The quantified FLIPUS acoustic intensities were then used for osteogenic stimulation of rat Mesenchymal Stromal Cells to reveal the age- and intensity-dependent differences in cellular responses. The FLIPUS technique was also applied to investigate the mechanical transcriptional activity in murine C2C12 mesenchymal precursors, with an emphasis on the role of evolutionary conserved yes-associated protein (YAP) in mechanotransduction mechanism in response to ultrasound.

The Results at a Glance

Throughout this work I utilized the FLIPUS set-up to evaluate the cellular responses of skeletal-muscular tissue precursors to a well-defined acoustic intensity. Investigation of fundamental cellular mechanisms was carried out, attempting to explain the pro-regenerative properties of LIPUS. These results are described in four chapters.

The first chapter of this thesis is dedicated to the detailed characterization of the FLIPUS *in-vitro* set-up. The set-up consists of an array of four focused transducers submerged in a temperature-controlled water tank positioned at the bottom of a 24-well-plate carrying cell monolayers and enabling cell stimulation in the homogenous far-field of the transducer. The intensity measurements within the well indicated a smooth decrease of the signal moving from the center to the periphery. The set-up avoids temperature elevations, standing wave effects, and near-field interferences. The output intensity can be varied up to 60 mW/cm^2 and is introduced simultaneously to four wells at a time, allowing for efficient analyses in quadruplicate. The set-up was used to stimulate rat Mesenchymal Stromal Cells (rMSCs) and revealed more enhanced osteogenic differentiation of the cells, measured by quantification of gene expression of bone markers.

Chapter 2 of this thesis demonstrated that with age osteogenic differentiation potential of rMSCs declined, whereas adipogenesis became more pronounced. This influenced the responsiveness of cells to acoustic intensity by FLIPUS mechanical stimulation: rMSCs from young donors experienced more enhanced osteogenic phenotype when 11.7 mW/cm^2 intensity was supplied, whereas cells from aged donors rather benefited from 44.5 mW/cm^2. These results suggested further the need for optimization of existing clinical stimulation protocols, with age being one of the factors significantly contributing to the bone regenerative outcome.

Due to the poor regenerative potential of soft musculoskeletal tissues and growing indication of benefits acquired from LIPUS treatment, the fundamental biological processes were evaluated in murine C2C12 mesenchymal precursors, isolated form muscle crash trauma and possessing myogenic, adipogenic and osteogenic differentiation potentials. In Chapter 3 of the thesis the mechanoresponsiveness of C2C12s was evaluated through activation of mechanosensitive transcription factors AP-1, Sp1 and TEAD at FLIPUS acoustic intensity of 44.5 W/cm^2. Interestingly, the activation profile of the factors differed depending on FLIPUS stimulation time, with 5 min being suitable for all three of them. The expression of several target

genes of the transcription factors, i.e., c-fos, c-jun, Cyr61, was increased soon after the stimulation, enhancing cellular viability.

The mechanism of TEAD-mediated mechanotransduction in C2C12s by FLIPUS was further investigated, uncovering the mechanosensitive functioning of Yes-associated protein (YAP). These findings are summarized in Chapter 4. Exposure to ultrasound led to YAP activation and resulted in enhanced proliferation of C2C12s. Knocking down YAP abolished the mitogenic effect of FLIPUS. The expression of the pro-myogenic transcription factor MyoD was reduced, suggesting that myogenic differentiation was delayed by the ultrasound. Further investigation into the functioning of the evolutionary conserved protein YAP in response to FLIPUS is in progress. The detailed description of the performed work is represented in the separate chapters below.

Chapter 1: A NOVEL FOCUSED LOW-INTENSITY PULSED ULTRASOUND (FLIPUS) SYSTEM FOR CELL STIMULATION

Reprinted with permission from: Puts, R., Ruschke, K., Ambrosi, T.H., Kadow-Romacker, A., Knaus, P., Jenderka, K.V., and Raum, K. A Focused Low-Intensity Pulsed Ultrasound (FLIPUS) System for Cell Stimulation: Physical and Biological Proof of Principle," *IEEE Trans. Ultrason. Ferroelectr. Freq. Control*, vol. 63, no. 1, pp. 91-100, Jan.2016.
http://dx.doi.org/10.1109/TUFFC.2015.2498042

ABSTRACT

Quantitative Ultrasound (QUS) is a promising technique for bone tissue evaluation. Highly focused transducers used for QUS also have a capability to be applied for tissue-regenerative purposes and can provide spatially limited deposition of acoustic energy. We describe a focused LIPUS (FLIPUS) system, which has been developed for the stimulation of cell monolayers in the defocused far-field of the transducer through the bottom of the well plate. Tissue culture well plates, carrying the cells, were incubated in a special chamber, immersed in a temperature controlled water tank. A stimulation frequency of 3.6 MHz provided an optimal sound transmission through the polystyrene well plate. The ultrasound was pulsed for 20 min daily at 100 Hz repetition frequency with 27.8 % duty cycle. The calibrated output intensity corresponded to I_{SATA} = 44.5 ± 7.1 mW/cm^2, which is comparable to the most frequently reported nominal output levels in LIPUS studies. No temperature change by the ultrasound exposure was observed in the well plate. The system was used to stimulate rat mesenchymal stem cells (rMSCs). The applied intensity had no apoptotic effect and enhanced the expression of osteogenic markers, i.e. osteopontin (OPN), collagen 1 (Col-1), the osteoblast-specific transcription factor – Runx-2, and E11 protein, an early osteocyte marker, in stimulated cells on day 5. The proposed FLIPUS set-up opens new perspectives for the evaluation of the mechanistic effects of LIPUS.

Key words: quantitative ultrasound, low-intensity pulsed ultrasound, bone, tissue regeneration, mechanosensation.

INTRODUCTION

Ultrasound is referred to acoustic waves with frequencies above the audible limit of human hearing. While ultrasound with low spatial and temporal-average intensities (<100 mW/cm²) is used diagnostically, e.g., for real-time imaging and elastography of soft tissues [1], significantly higher intensities (>100 mW/cm²) are utilized for therapeutic purposes [2]. A wide range of applications and the low cost of ultrasound devices make them an attractive target to complement existing equipment in clinical and research facilities.

Intermediate intensity levels have been successfully introduced for the purpose of tissue regeneration, e.g., for the stimulation of bone fracture healing with low-intensity pulsed ultrasound (LIPUS) [3]. Although the latter was categorized as a "therapeutic" technique, intensity levels used in LIPUS-treatments are within diagnostic range, typically below 100 mW/cm^2. LIPUS is now well-accepted as a non-invasive and non-ionizing therapy approach for fresh fractures, delayed- and non-union bone, which shows promising healing effects in soft tissues (reviewed in [4]). However, certain inconsistencies are associated with reported *in-vitro* data and the physico-biological mechanisms leading to stimulatory effects are only partially understood.

The majority of the *in-vitro* LIPUS studies have been conducted with planar transducers, generating a 1.5 MHz wave with spatial average temporal average intensity (I_{SATA}) of 30 mW/cm^2, delivered in a pulsed manner at 1 kHz pulse repetition frequency (PRF) with 20 % duty cycle (DC) [3]. The exposure of cells *in vitro* with LIPUS generates a plethora of physical phenomena that can potentially induce stimulatory biological effects. While pressure levels applied with LIPUS systems are well below inertial cavitation thresholds [2], the wave propagation causes oscillations with local cyclic compression and expansion of the encountered matter at the frequency of the traveling wave (typically between 500 kHz and 5 MHz). Moreover, the absorption of acoustic energy generates an acoustic radiation force in the wave propagation direction. Therefore, pulsed excitation induces cyclic loading-like effects on cells at the rate of the PRF (typically between 100 Hz and 1 kHz) [3]. Finally, in fluids and porous materials the acoustic radiation force triggers bulk movement of the fluid phase, also known as acoustic streaming at quasi-static velocities, causing mass transfer, redistribution of nutrients, waste, and signaling molecules, as well as applying shear-forces on cellular membranes [2].

Unlike for other mechanical treatments of cells, e.g., stretching of cells seeded in elastic culture plates [5;6], application of fluid flow with controlled flow rates in bio-reactors [7], and/or

the generation of shear-forces [7-11], the quantification of mechanical stimuli introduced by LIPUS-exposure is not straightforward. In addition to the plethora of physical effects simultaneously introduced by pulsed ultrasound, it is important to take into account unwanted artifacts. Both, the introduced effects and artifacts are not easy to quantify and are therefore often not addressed in the reported LIPUS-studies, which limits the comparability between studies and the successful translation of *in-vitro* findings to *in-vivo* applications.

The most common LIPUS-stimulation set-ups consist of planar transducers directly gel-coupled to the bottom of a tissue culture well plate [12-14]. These set-ups are prone to temperature elevations caused by transducer heating [15]. Moreover, the intensity distribution in the near-field of the transducer is very inhomogeneous and multiple reflections at plastic-fluid and fluid-air interfaces result in standing waves, prolonging the pulse duration [16] and modulating the intensity levels experienced by the cells [17]. These set-ups are also prone to the generation of different wave modes propagating through the plastic material to neighboring wells, which can potentially affect the outcome in multi-well plate stimulation set-ups [15]. Similar effects have been observed [17], if the cells are stimulated from the top by a transducer immersed in the culture medium [18-20]. The aforementioned artifacts can be reduced or eliminated by immersion set-ups, i.e., by the use of a coupling material between transducer and a well, which allows the stimulation of the cells in the far-field and avoids heat transfer to the well [17]. Moreover, low reflective interfaces or absorbing materials can be used to avoid the generation of standing waves in the well [16]. The need for improved *in-vitro* set-ups has led to the development of various new configurations, which provide exposure of the cells with well-controlled acoustic parameters [16;21-23].

Quantitative Ultrasound (QUS) can be used for the evaluation of bone properties, and it has shown promising results in the assessment of bone fracture healing [24]. Moreover, the application of focused ultrasound transducers in transverse-transmission mode has imaging capabilities [25]. In a previous study we have shown that the evaluation of local changes of sound velocity and attenuation enabled the differentiation of early healing stages in a rat osteotomy model [26]. In this study we describe a LIPUS stimulation set-up, which utilizes focused transducers (herein called focused LIPUS or FLIPUS), enabling deposition of controlled intensity levels to the given region and ensuring reproducible cellular outcomes *in vitro*. The cells in the set-up were positioned 13.3 mm behind the focal point in the diverging field of the transducer. Here we report that I_{SATA} of 44.5 ± 7.1 mW/cm^2, introduced by our FLIPUS set-up, enhanced gene expression of osteogenic markers on day 5 in rat mesenchymal stem cells (rMSCs).

MATERIALS AND METHODS

A. *FLIPUS Set-Up*

A schematic drawing of our custom FLIPUS device is shown in Fig. 1. It consists of *xy*-axis and *z*-axis scanning stages (M-ILS 100CC, Newport-Spectra-Physics GmbH, Darmstadt, Germany), which allow precise positioning (accuracy: 1 µm) of the transducer array and the incubation chamber, respectively, using a motion control system (Model XPS, Newport, Spectra-Physics GmbH, Darmstadt, Germany). The array of five identical focused transducers (center frequency: 5 MHz; diameter: 19 mm; epoxy lens with focus distance at 22.8 mm; epoxy backing; STT Richter, Mühlanger, Germany) is placed below the incubation chamber in a temperature-controlled water tank (Memmert GmbH & Co. KG, Schwabach, Germany) with the sound fields directed upwards. The water tank is filled with sterilized, de-ionized, degassed water and maintained at 37°C. Water was degassed using a vacuum pump at 200 mbar (Van der Heijden Labortechnick GmbH, Dörentrup, Germany). To support the degassing procedure the bottle with water was placed in an ultrasonic cleaner (Elmasonic S30H, 220–240 V, Singen), working in degas mode.

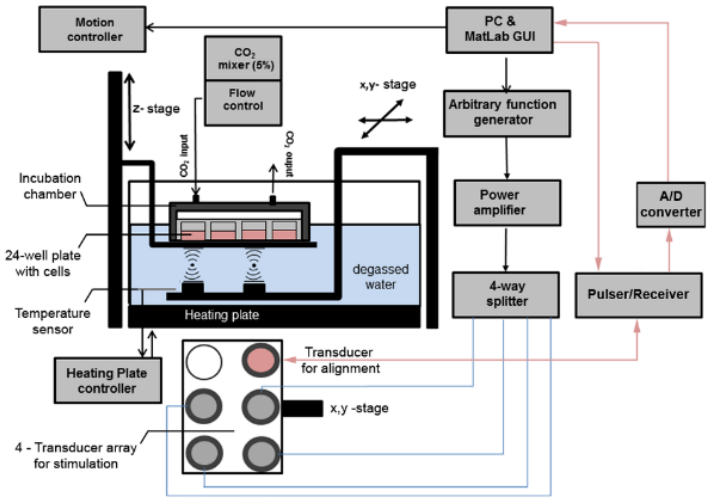

Fig. 1: Schematic representation of stimulation set-up used for *in-vitro* FLIPUS experiments.

All transducers were adjusted in the array such that the focal plane was in the same *z*-distance. The distance between the transducer center points was equal to twice the distance between individual well center points of 24-well plates (Becton, Dickinson and Company, Franklin Lakes, NJ, USA), i.e., 38.6 mm. The plates were made of polystyrene (bottom thickness:

1.27 mm; speed of sound: 2400 m/s [17]). Four transducers were used for stimulation and one was used to control the alignment between transducer array and bottom of the well plate. A burst signal (frequency: 3.6 MHz; peak-to-peak voltage: 500 mV_{pp}; PRF: 100 Hz; duty cycle: 27.8 %, i.e., 2.78 ms "on" and 7.22 ms "off") was generated by an arbitrary waveform generator (33522A, Agilent Technologies, Santa Clara, CA, USA). The signal was amplified by 50 dB by a power amplifier (325LA, Electronics & Innovation, Rochester, NY, USA) and divided using a power splitter (D5855, Werlatone, Inc. Patterson, NY, USA) to excite four stimulation transducers simultaneously. The corresponding acoustic output parameters are described in detail in the next section. A dual pulser/receiver (DPR500, Imaginant, Pittsford, NY, USA) was connected to the fifth transducer to measure the time-of-flight (*ToF*) of the well plate bottom reflection. The received signals were digitized at 100 MS/s using a 10-bit data analogue-to-digital (A/D) converter system (Agilent U1062A-002 DC152, Keysight, Inc., Santa Rosa, CA, USA). The accuracy of the *ToF* estimation was approximately ± 0.1 µs, which corresponds to an accuracy of the distance estimation of ± 75 µm.

Twenty-four well plates were placed into a custom-made sealed, autoclavable incubation chamber (Medizinisch-Technische Labore, Charité-Universitätsmedizin Berlin, Berlin, Germany). An automatic CO_2-mixer (FC-5, Life Cell Instrument, Seoul, Korea) was connected to an air inlet of the incubation chamber, which ensured an incubator-like environment with 5 % CO_2, 95 % air supply, controlled temperature and humidity at a flow rate of 70 ml/min in the chamber. The chamber was magnetically fixed to a holder that was connected to the z-stage. The chamber has an open window on the bottom side to provide i) direct coupling of sound from the transducer through the water to the well plate bottom and ii) efficient thermal coupling between water tank and well plate. The well plate bottom was in direct contact with water throughout the stimulation time. Air bubbles created during the insertion of the well plate into the chamber were removed from the bottom of the well plate prior to the stimulation. The well plate was set to a height of 13.3 mm above the focus point of the transducer. Parallel alignment at the above mentioned distance ensured by scanning the transducer array over a large well plate area and visualization of the pulse-echo time of flight using the fifth transducer. The alignment accuracy was within 0.08 mm. This configuration ensured a reproducible positioning of the stimulated cells in the diverging field of the transducers with a cross-sectional stimulation area of approximately 0.81 cm^2 per well. All hardware components, positioning and the stimulation settings (e.g. duration, intensity) were controlled via a custom graphical user interface and automated protocols developed with MATLAB 2009a (The MathWorks, Natick, MA, USA).

B. Numerical Sound Propagation Simulations

Numerical sound propagation simulations were conducted using the finite-difference time-domain (FDTD) simulation package SimSonic [27] (see Supplementary Materials A1). The model includes a complete description of the elastic properties, mass density, and acoustic absorption. The physical dimensions of the lens-focusing emitting transducer and the well plate were identical with the experimental setup. The fluid in the stimulation chamber and in the well was assumed to be water (i.e., the bulk modulus, shear modulus, and density are 2.25 GPa, zero and 1000 kg/m^3, respectively). The polystyrene well plate chamber was modeled with bulk modulus, shear modulus, and density of 5.8 GPa, 1.32 GPa and 1050 kg/m^3, respectively. Attenuation values for water and polystyrene were set to 0.002 dB/mm and 0.35 dB/mm, respectively. The simulation box was surrounded by perfectly matched layers to avoid spurious reflections. The simulations were conducted with burst pulses of variable frequency (3.0 – 5.0 MHz) and burst length. A virtual receiver array was placed directly above the well plate bottom. A preliminary convergence study indicated that a spatial increment of 16 µm provided stable simulation results. In addition to signals recorded by the receiver array, snapshots of the displacement velocity distribution were recorded in the entire simulation field at 1-µs intervals. For comparison, simulations were also conducted for a free field (i.e., without the well plate, data not shown) and for an unfocused configuration.

C. Acoustic Output Power Measurements

The acoustic output power P of each transducer was determined by an ultrasonic power balance according to IEC standard IEC 61161 [28] with a polyurethane rubber target (HAM A, Precision Acoustics, Dorchester, UK) connected to a balance. The experiments were conducted in a water bath at an average temperature of 19.5°C, with the corresponding speed of sound of c_0 = 1479 m/s [29]. The transducer was excited in continuous mode to increase the sensitivity of the measurement. The transmission of long burst signals through the well plate bottom is affected by sound velocity and thickness of the well plate material, frequency, and angle of incidence [15]. Therefore, the acoustic radiation force F_{rad} was measured with and without a well plate phantom (side-walls were cut off). Well plate phantom and the absorber were placed 13.3 mm and 25 mm above the focal plane, respectively. F_{rad} is related to the total acoustic output power P [28]:

$$F_{\mathrm{rad}} = \frac{P}{c_0}\frac{\left(1+\cos\gamma\right)}{2}, \qquad (1)$$

where γ is the half-opening angle of the transducer. The measured power values were corrected for the burst mode using the correction factor $k_{\text{burst}} = 0.278$ and the spatial average temporal average intensities (I_{SATA}) were obtained by normalization to the cross-sectional (-6 dB) beam area *a*:

$$I_{\text{SATA}} = \frac{P \cdot k_{\text{burst}}}{a} . \quad (2)$$

The measurement uncertainty for the output power measurements were ± 5 %.

D. Intensity Distribution above the Well Plate Bottom

The acoustic waves transmitted through the cell-free well plate was measured using an acoustic intensity measurement system (AIMS ver. 4.2.37, NTR Systems Inc., Seattle, WA, USA) equipped with a lipstick hydrophone (Onda HGL-0400, active diameter: 400 µm; Onda Corp. Sunnyvale, CA, USA), which has a nominal measurement uncertainty of ± 10 %. The transducers were excited using the set-up described the previous section, except that only 10 cycles were used for the burst excitation. The short burst length was chosen to avoid reflections between the hydrophone and the plate. The waveforms were recorded with an oscilloscope (MSO6034A, Keysight, Inc., Santa Rosa, CA, USA). A polystyrene well plate was placed 13.3 mm above the focus position and the hydrophone was scanned at distance of 5 mm above the bottom of the plate. The peak compressional acoustic pressure distribution $p_+(x,y)$ was analyzed.

The temperature was measured by placing a thermocouple (LR316, JUMO GmbH & Co. KG, Fulda, Germany) approximately 1 mm above the well bottom, through a specially made aperture in the plate cover.

E. Cell Cultivation

Rat mesenchymal stem cells (rMSCs), derived from bone marrow, isolated from 8-weeks old Sprague Dawley rats (GIBCO, Life Technologies, Darmstadt, Germany), were expanded until passage 5 and a confluence of 80 % in expansion media (Dulbecco Modified Eagle's Medium (DMEM), 10 % fetal calf serum (FCS), 1 % Penicillin/Streptomycin (Biochrom AG, Berlin, Germany), 2 mM GlutaMax™ (GIBCO, Life Technologies, Darmstadt, Germany) under standard cultivation conditions (37°C, 5 % CO_2, 95 % humidity). For osteogenic differentiation, cells were cultivated with osteogenic medium (ALPHA-Medium, 1 % Penicillin/Streptomycin (Biochrom AG, Berlin, Germany), 10 % PANEXIN NTA® (PAN Biotech GmbH, Aidenbach, Germany),

containing biochemical supplements: 200 µM L-ascorbic acid 2-phosphate, 0.1 µM dexamethasone (Sigma Aldrich, St. Louis, MO, USA) and 7 mM β-glycerophosphate (Calbiochem, Merck KGaA, Darmstadt, Germany). PANEXIN was used instead of FCS to ensure that the investigated biological effects in rMSCs were not biased by various growth factors, which are naturally present in FCS.

F. Apoptosis

To confirm the cell viability after FLIPUS exposure, cell apoptosis tests were performed. rMSCs were seeded in a 24-well plate in 1 ml of expansion media at a density of 10^4 cells per well. Twenty-four hours later, cells were stimulated for 20 minutes with FLIPUS, followed by 2 more days of stimulation. Negative control cells were treated identically, but without exposure to FLIPUS. On day three "APO Percentage^{TM}" apoptosis assay (Biocolor Ltd, County Antrim, UK) was performed according to the manufacturer's protocol. The released dye was quantified by photometric absorption measurements (microplate reader BIORAD, Model 680, Bio-Rad Laboratories GmbH, München, Germany) at a wavelength of 550 nm. Hydrogen peroxide, 1M H_2O_2 (Sigma Aldrich, St. Louis, MO, USA), was used to induce apoptosis in positive control.

G. Analysis of Transport Effect

Between the individual stimulations, the well plate had to be transported from and to the tissue culture incubator. To exclude impacts on cells, which are related to plate transport from incubator to FLIPUS-stimulation unit, two sets of experiments were performed. Cell activity and the expression of osteogenic markers were assessed by WST-8 assay and quantitative real-time polymerase chain reaction (qRT-PCR), respectively. In particular, alkaline phosphatase (ALP), osteopontin (OPN), collagen-1 (Col-1), Run-related transcription factor-2 (Runx-2) and osteocalcin (OC) were quantified from the isolated mRNA. rMSCs in passage 5 were seeded in 1 ml expansion medium at a density of $2*10^4$ cells. While the cells seeded for the activity assay remained in expansion media at all times, the cells used for the qRT-PCR analyses were cultured in osteogenic medium prior to the first transport. The media were changed on days 3 and 5. Over a period of seven days, one plate was kept in the cell culture incubator, while the second plate was placed in the stimulation unit for two hours per day without receiving FLIPUS stimulation. On day 7, after the cells were out of the stimulation unit, the WST-8 measurements and the cell lysis for qRT-PCR were performed.

H. Osteogenic Differentiation of rMSCs in Response to FLIPUS

rMSCs in passage 5 were seeded in 24 well plates with a density of 10^4 per well. Twenty-four hours later, medium was replaced with the osteogenic medium. In each plate, 3 wells were stimulated by FLIPUS and 3 wells served as unstimulated controls. The experiment was repeated 3 times. The cells were stimulated for 20 minutes with the aforementioned parameters for 5 consecutive days and the expression of ALP, OPN, Col-1, Runx-2, OC, transmembrane glycoprotein E11 and dentin matrix acidic phosphoprotein-1 (DMP-1) osteogenic markers was determined on day 5 by qRT-PCR.

I. RNA Isolation and Quantitative Real-Time Polymerase Chain Reaction (qRT-PCR)

At the selected day cells were lysed and further processed with the NucleoSpin RNA II kit (Machery-Nagel GmbH & Co.KG, Düren, Germany). For quantification purposes cDNA (complementary DNA) was synthesized with qScript™ cDNA superMix (Quanta BioSciences Inc., Gaithersburg, MD, USA). The amplification and quantification of targets were performed using PerfeCTa® SYBR® Green SuperMix (Quanta BioSciences Inc., Gaithersburg, MD, USA). Osteogenic primers, spanning an exon/intron boundary, were designed by Primer-BLAST (National Center for Biotechnology Information (NCBI), Bethesda, MD, USA) and synthesized by TIB MOLBIOL (Berlin, Germany). The following primers were used in the experiments: ALP forward- 5`-tttcacgtttggtggctaca-3`; reverse-5`-agacgttctcccgttcacc-`, OPN forward- 5`-ggtgatagcttggcttacgg -3`; reverse-5`-gcaactgggatgaccttgat -3`, OC forward- 5`-agctcaaccccaattgtgac -3`; reverse-5`-agctgtgccgtccatacttt -3`, Col-1 forward- 5`-gctgcatacacaatggccta -3`; reverse-5`- atgacttctgcgtctggtga -3`, Runx-2 forward- 5`-gccgggaatgatgagaacta -3`; reverse-5`- gaggcggtcagagaacaaac-3`, E11 forward-5`-cgaccacgatcacaaagaac-3`; reverse-5`-tggctaacaagacgccaat -3`, DMP-1 forward- 5`-caagggagagcaggagtcag-3`; reverse-5`- tcaatgtttttggggtggtt -3`. Glyceraldehyde 3-phosphate dehydrogenase (GAPDH) house-keeping gene was used as an expression control, with the following primer sequences forward- 5`-gtcggtgtgaacggatttg-3`; reverse-5`-ggaagatggtgatgggttt -3`.

J. WST-8 Assay

Cell activity was evaluated using the WST-8 colorimetric assay (PromoCell GmbH, Heidelberg, Germany) according to the manufacturer's protocol. The kit uses the water soluble Tetrazol salt WST-8, which is reduced by dehydrogenases in presence of the electron carrier 1-

methoxyphenazine methosulfate, resulting in orange-colored WST-8 formazan. The amount of formazan produced is directly proportional to the number of living cells. The absorptions at a wavelength of 450 nm and a reference wavelength of 595 nm were measured with a microplate reader (Model 680, Bio-Rad Laboratories GmbH, Munich, Germany).

K. Statistics

One-way ANOVA followed by post-hoc multi-comparison Tukey-Kramer tests were used to compare differences in the readout parameters between the stimulation groups using the MATLAB statistics toolbox (The MathWorks, Natick, MA, USA). All the data are represented as means and standard deviations. Differences were regarded significant if the p-value was smaller than 0.05.

RESULTS

A. Ultrasound Transmission Through the Bottom of a Well Plate

The transmitted acoustic power was measured with and without the plate in the sound field in the frequency range from 3 to 5 MHz at intervals of 0.1 MHz (Fig. 2). Pronounced transmission losses can be seen at 3.0, 4.5 and 5.0 MHz. A similar behavior was confirmed by the numerical simulations (see Fig. A1 of Supplementary Materials). Therefore, a stimulation frequency of 3.6 MHz was chosen for all further experiments.

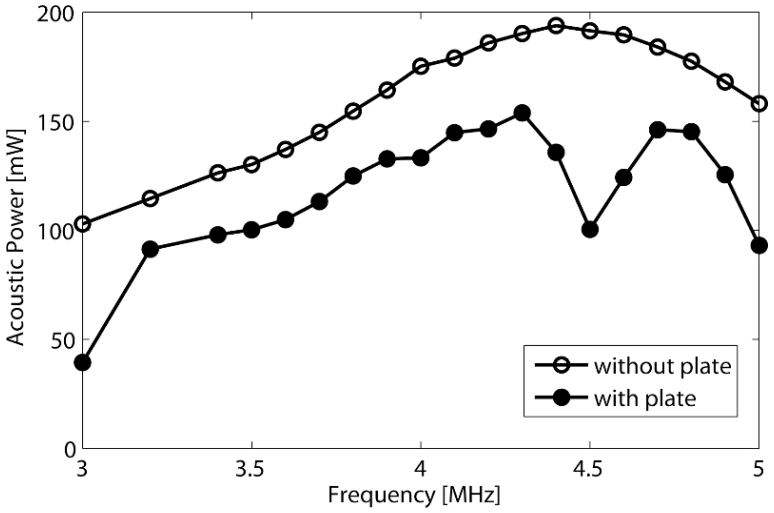

Fig. 2: Total transmitted acoustic power without and with a polystyrene plate, placed in the sound field at a distance of 13.3 mm above the focal plane. The absorbing target was placed

at a distance of 25 mm upwards from the focal plane. Multiple reflections in the plate cause destructive interference of the transmitted waves for distinct frequencies.

B. Determination of the Cross-Sectional Beam Area at the Well Plate Bottom

A representative burst signal measured with the hydrophone in the center of the acoustic beam is shown in Fig. 3. The maximum negative peak pressure amplitudes for all transducers varied between 110 kPa and 140 kPa. In addition to the fundamental frequency at 3.6 MHz, a harmonic component at 7.2 MHz could be observed in the central part of the beam. However, the harmonic component was approximately 21 dB smaller than the fundamental peak amplitude. The temporal peak intensity distribution derived from the measured positive peak pressure amplitudes are shown in Fig. 4. A smooth decrease from the central part of the well towards the periphery can be seen. The -6-dB cross-sectional area was between 0.77 and 0.85 cm². All measured parameters are summarized in Table 1. At the well edges, the intensity was approximately -12 dB lower compared to the maximum level in the center. In the adjacent wells, no signals could be detected with the hydrophone.

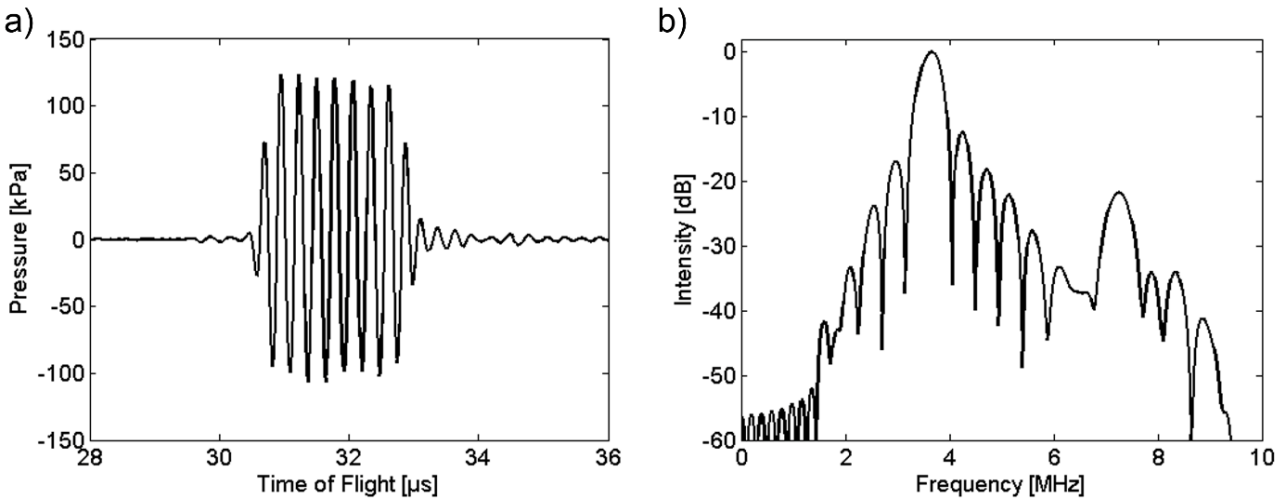

Fig. 3: A representative burst signal, measured by hydrophone at V_{pp} = 500 mV: (a) the maximum negative peak pressure amplitude and (b) fundamental (3.6 MHz) and harmonic (7.2 MHz) components of the burst.

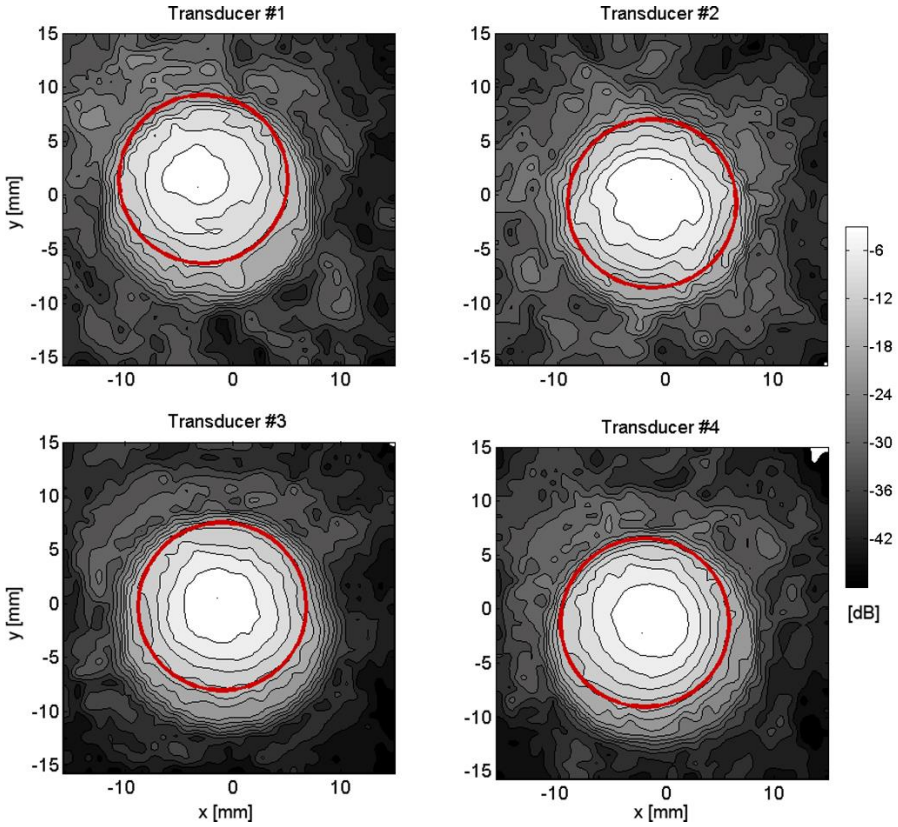

Fig. 4: Temporal peak intensity distribution for the individual stimulation transducers. Each contour line represents a decrease of 3 dB relative to the peak intensity. The cross-sectional area (1.9 cm²) of a single well is indicated by the red circles. The hydrophone was scanned at a distance of 5 mm above the well plate. Measurement parameters were: f = 3.6 MHz, burst length: 10 cycles, signal generator excitation voltage: V_{pp} = 500 mV.

Table I Cross-sectional area (-6 dB) a, mean peak pressure p_+, mechanical index MI, spatial average temporal peak intensity I_{SATP} and spatially and temporally averaged intensity I_{SATA} for the stimulation set-up (wells positioned 13.3 mm above the focus) and the following measurement parameters: f = 3.6 MHz, burst length: 10,000 cycles (2.78 ms), PRF = 100 Hz, signal generator excitation voltage: V_{pp} = 500 mV. SD designates standard deviation.

	a [cm²]	p_+ [kPa]	MI	I_{SATP} [mW/cm²]	I_{SATA} [mW/cm²]
T1	0.77	83 ± 14	0.066	231.0	49.2
T2	0.81	82 ± 15	0.058	224.3	36.2
T3	0.80	98 ± 18	0.074	323.5	51.4
T4	0.85	93 ± 17	0.070	288.6	41.2
Average	**0.81 ± 0.03**	**89 ± 16**	**0.067 ± 0.007**	**266.8 ± 47.5**	**44.5 ± 7.1**

C. Intensity Calibration

The intensity levels of the four stimulation transducers for various signal generator excitation voltages are shown in Fig. 5. The variation of I_{SATA} between the four transducers for excitation voltages above 300 mV was 16.1 % (Fig. 5). The measured temperature was 37.0 ± 0.1°C. No measurable temperature difference could be observed during the ultrasound exposure (using the stimulation parameters).

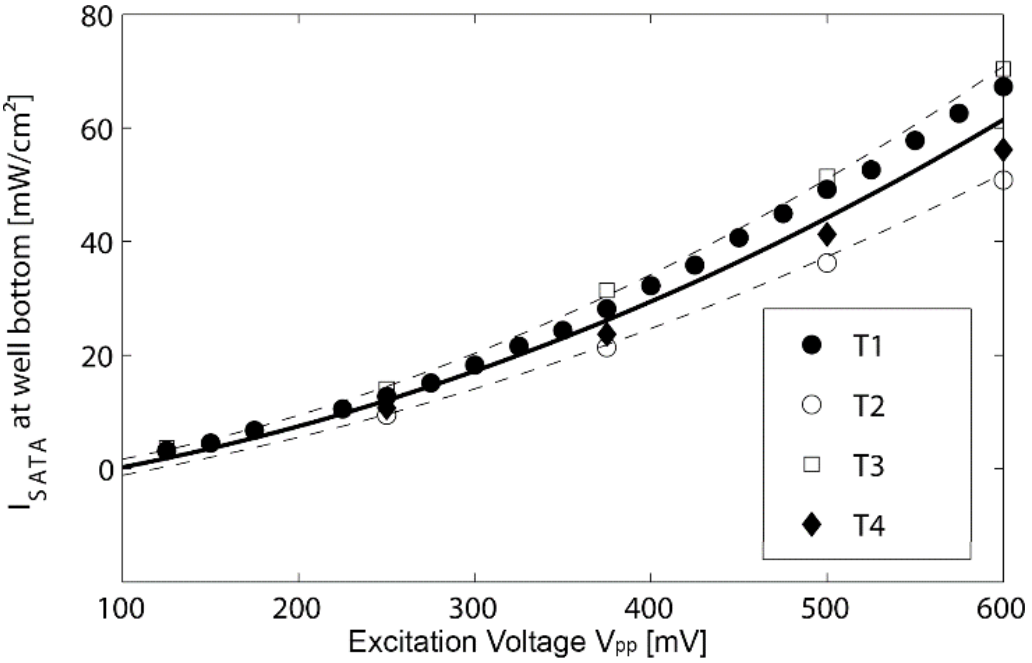

Fig. 5: Spatial average temporal average (I_{SATA}) intensities for variable signal generator excitation (peak-to-peak) voltages. The intensity values were derived from the measured acoustic output power levels using Eq. (2) at 3.6 MHz continuous wave (*cw*) excitation and a polystyrene plate placed between transducer and absorbing target (T1 to T4 are transducers 1 to 4). For transducer #1 the measurements have been conducted at closer excitation voltage increments than for the other transducers. The straight and dashed lines indicate the approximated means and standard deviations of all transducers.

D. Apoptosis

The extinction values of the photometric measurements showed no differences between stimulated and non-stimulated controls. In contrast, the values of the positive control, treated with 1M H_2O_2, were significantly higher ($F = 330$; $p < 0.01$) (Fig. 6a). Light microscope images showing apoptotic rMSCs, retaining the red dye (Fig. 6b) and vital cells with normal morphology for both, non-stimulated and stimulated cells (Figs. 6c-d).

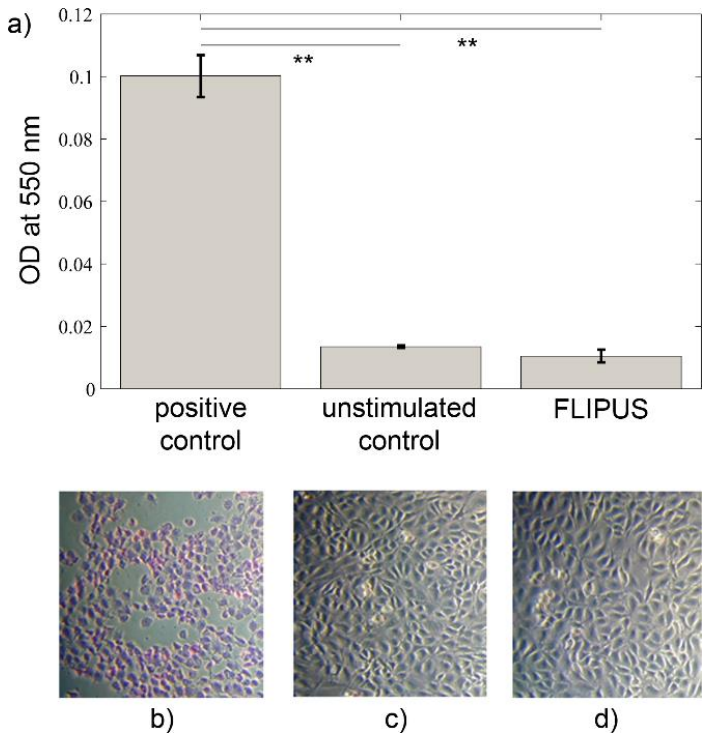

Fig. 6: FLIPUS does not induce apoptosis in rMSCs on day 3 of daily treatment: (a) plot with optical density (OD) values (mean and standard deviation) of positive controls (cells treated with 1 M H_2O_2), negative controls (cells that did not receive FLIPUS stimulation) and FLIPUS-stimulated cells. High OD values designate high apoptotic rate. Light microscopy images (10-fold magnification) of positive control (b), negative control (c) and FLIPUS-stimulated cells (d). **p<0.01.

E. Analysis of Plate Transport Effects

The absorption values of colorimetric cell-activity WST-8 assay showed no differences in cell activity between the plates positioned in the incubator and transported to the FLIPUS-stimulation unit every day for 2 hours within 7 days (Fig. A2 in Supplementary Materials), confirming no effect of the transport to the cell-stimulation unit. Similarly, no differences between groups were observed for the mRNA expressions of ALP, Col-1, OC, OPN, and Runx-2.

F. Enhanced Osteogenic Differentiation of rMSCs in Response to FLIPUS

The results of the mRNA expression analysis are summarized in Table 2 (and more detailed in Fig. A3 and Table A3 of Supplementary Materials). Except for DMP-1, ALP and OC, all analyzed osteogenic differentiation markers were significantly up-regulated in the FLIPUS group compared to the unstimulated control group on day 5 of daily stimulation.

Table II Relative change in mRNA expression in rMSC, cultured in osteogenic medium, on day 5 of daily FLIPUS stimulation, compared to unstimulated control on the same day. The stimulation parameters were following: f = 3.6 MHz, burst length: 10.000 cycles (2.78 ms), PRF = 100 Hz, signal generator excitation voltage: V_{pp} = 500 mV, expressed as mean value ± standard deviation. F and p values indicate the strength and significance obtained from the ANOVA test, respectively. N.S. designates no statistically significant change in gene expression between unstimulated and FLIPUS-stimulated groups.

	Relative Change ± SD	F	p
OPN	2.12 ± 0.72	19.5	0.0006
Col-1	1.53 ± 0.29	27.2	0.0001
Runx-2	1.70 ± 0.76	9.1	0.009
E11	1.36 ± 0.35	10.8	0.005
ALP	1.56 ± 0.95	2.8	N.S.
DMP-1	1.54 ± 0.77	3.5	N.S.
OC	1.92 ± 2.03	1.7	N.S.

DISCUSSION

The mechanical cell environment plays an important role in the determination of cellular fate. Both mechanical and biological factors tightly control the transcriptional activity of the cell, directing it into proliferation, migration, apoptosis or differentiation. LIPUS has been successfully introduced in the clinical management of delayed- and non-unions of bone. However, mechanistic interactions leading to the observed stimulatory effects of the cells behavior in response to this complex mechanical impulse are not completely clear [2]. Recent reports emphasize the need for the development of *in-vitro* cell-stimulation set-ups that allow better control of applied intensity levels [15;17;30].

A large number of published LIPUS *in-vitro* studies expose the cells to unwanted physical phenomena (reviewed in [2]). Another limiting factor of the unfocused transducers, used for *in-vitro* and small animal *in-vivo* studies, is the dimension of the generated sound field. While the commonly used transducer and sound field dimensions are suited for *in-vivo* applications in human bone fractures, they are usually too large for the application in cell culture dishes and in bones of small animals, leading to acoustic exposure of volumes much larger than the cell dish or repair volume of interest. This limitation can be overcome by the use of focused transducers,

which we utilize in our set-up. In this study, we have stimulated the cells in the diverging, defocused field of the transducers, which allowed well controlled adjustment of the cross-sectional beam area and intensity level to the dimension of the well plate. Acoustic transmission, intensity distribution and temperature rise have been characterized directly above the well plate bottom, i.e., in the same region, in which the cells are located for the stimulation experiments. The stimulation in the diverging field avoids the generation of standing waves. Moreover, the immersion of the transducer array in the water tank at a large distance to the well plate provides efficient transducer cooling and prevents temperature elevations in the wells by transducer or acoustic heating. The latter is in agreement with a study of Zhang *et al.* [21], in which murine MC3T3-E1 osteoblasts, grown in a monolayer, were stimulated using a high intensity focused ultrasound system from the top through the culture medium. The exposure of the cells with much higher negative pressure amplitudes (up to 9.18 MPa), longer burst durations (300 ms), and intensity level (4.8 W/cm²), but similar duty factors (0.15) caused less than 0.2 degrees increase in temperature.

The use of focused ultrasound set-up has also been described in *in-vivo* experiments. Jung *et al.* [31] showed that regeneration of rat calvarial bone could be enhanced by FLIPUS using an intensity of I_{SPPA} = 1 W/cm^2. This set-up, employing low frequencies (440-700 kHz), which was also used for brain stimulation in rabbits [32], supports our hypothesis that the proposed FLIPUS system may by successfully translated to future *in-vivo* research.

The application of FLIPUS is not only limited to regenerative therapy approaches. For example, in the study of Noda *et al.* [33], FLIPUS was applied to enhance the efficacy of ampicillin in the treatment of acute otitis in mice. A scanning array stimulation system, similar to the set-up, proposed in our study, but employing planar transducers, have been developed by Subramanian *et al.* [23]. In this system 6 unfocused transducers were coupled to the well-plate chamber via a fluid-filled tank at a distance of 23 mm between transducer surface and well plate bottom. Experiments with frequencies between 1 and 8 MHz, mean pressure amplitudes up to 60 kPa, long burst durations (51 s, repetition rate not specified) and up to 10 min of exposure did not introduce inertial or non-inertial cavitation, or a measurable temperature increase. The cell stimulation experiments were conducted with 5.0 MHz, an average pressure of 14 kPa, which was applied six times a day for 51 s, leading to enhanced expression of chondrogenic markers on day 10 and supported cell viability at later time points.

The ability to control exposure conditions of FLIPUS is of great importance in order to unravel the underlying cellular mechanisms leading to enhanced tissue regeneration. The great

variety of different stimulation conditions, which have been reported to induce stimulatory cellular effects emphasize the need of standardization of the acoustic exposure, in order to improve the reliability of the interpreted data in response to ultrasound. The dependence of the ultrasound transmission on the well plate material and plate thickness underlines the importance of a proper calibration of the stimulation system including the well plate. Strong decreases in the delivered intensity could be observed at 3.0, 4.5 and 5.0 MHz in our experimental set-up. This phenomenon needs to be taken into account, if different materials or plate thicknesses are used as a surface for cultured cells.

The peak pressure amplitude is another parameter which is important to be established for *in-vitro* determination of biological mechanism. With increasing amplitudes nonlinear sound propagation leads to the transformation of acoustic energy from the fundamental into harmonic frequencies, which decreases the delivered energy at the fundamental frequency and potentially increases the risk for a temperature rise due to the higher attenuation at higher frequencies. In our experimental set-up, a signal generator excitation voltage of 500 mV_{pp} resulted in very weak harmonic components, as evaluated by hydrophone measurements (Fig.3).

Therefore, the frequency, signal generator excitation voltage and burst length of our FLIPUS set-up were calibrated to be 3.6 MHz, 500 mV_{pp}, and 2.78 ms at 100 Hz PRF, respectively, which corresponded to an intensity $I_{SATA} = 44.5 \pm 7.1$ mW/cm^2 delivered to the cells. Although previous studies revealed an appreciable impact of the pulse repetition frequency only for very low PRF values (up to 5 Hz) [34], future studies should address the question, if different pulse sequences with the same I_{SATA} level, e.g., shorter burst lengths with higher PRF values or different peak pressure amplitudes with adjusted burst lengths or PRF values have different biological responses.

Mesenchymal Stem Cells (MSCs) were used to assess the stimulatory effect of the FLIPUS system. MSCs are multipotent cells, possessing the ability to surpass immune surveillance, and holding a great promise for skeletal regenerative therapies [35;36]. In our study the selected FLIPUS parameters had no apoptotic effect on rMSCs and led to enhanced osteogenic differentiation of the cells on day 5 of treatment.

The proposed FLIPUS set-up represents a reliable tool for *in-vitro* investigations of 2D and 3D cell cultures. However, our system has certain limitations. Although the intensity distribution generated with our system is more homogenous compared to the near-field of unfocused transducers, an even more flat distribution within the wells could be achieved by a more sophisticated transducer design, e.g., by apodization of the central part of the beam.

Moreover, our system required the transport of the well plates between incubator and FLIPUS system for the stimulations. Although we did not observe significant effects of the transport on cell activity and osteogenic gene expression, we cannot exclude a potential stimulatory impact on the cells. Ideally, the FLIPUS stimulation experiments should be performed in the tissue culture incubator. Moreover, the excitation with long bursts at a low repetition frequency may induce a vibration of the well plate. The amount of vibration and the potential stimulatory effect on cells need to be investigated in future studies.

The use of FLIPUS may have a beneficial impact not only on bone healing, but also for soft tissue regeneration. The favorable effect of LIPUS for the regeneration of various tissues has already been demonstrated, e.g., for ligaments [37], tendons [38], bone-tendon junctions [39], intervertebral disc [16;40;41], and articular cartilage [42]. However, the mechanisms and optimized conditions are yet to be explored. We believe that FLIPUS will foster the *in-vitro* investigation and *in-vivo* application, as the size of the stimulated area can be easily adjusted (down to less than 1 mm cross-sectional diameter in the focal plane) and the applied intensity can be controlled by the prevention of standing waves, near-field interference and transducer heating. The very same transducers have already been used for imaging purposes in transverse transmission mode in an *in-vitro* rat osteotomy bone healing study [26]. These concepts could be combined in future studies, i.e., a first transmission measurement using short broadband pulses visualizes the region of interest, e.g., a bone callus. Then, the stimulation beam focus can be precisely positioned to deposit the acoustic energy only in the osteotomy gap region.

SUPPLEMENTARY MATERIAL

A1. Numerical Simulation of Sound Propagation

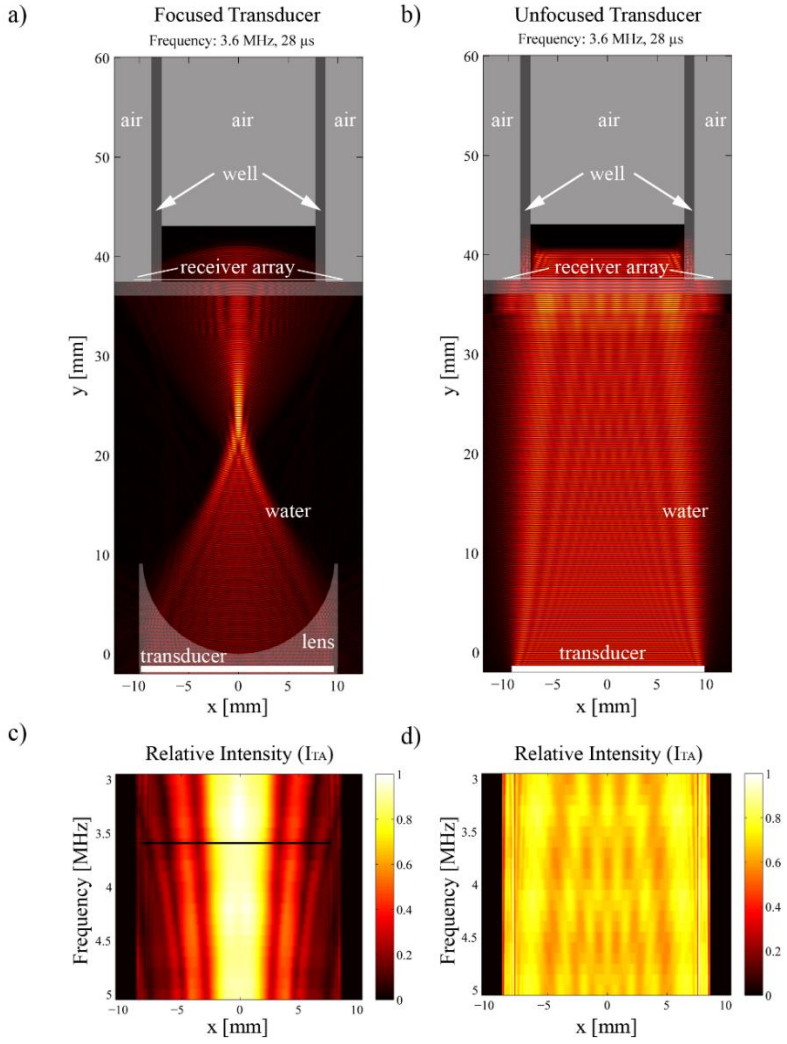

Fig. A1 Sound propagation at 3.6 MHz using focused (FLIPUS) configuration (a) in comparison to unfocused (LIPUS) setup (b). The focused beam provides a smooth transmission of a slightly curved wave front into the well chamber. The waves, reflected at the upper liquid-air interface, do not result in the generation of standing waves, which is the case for the unfocused setup (see complementary videos). Moreover, much less acoustic energy is coupled into the side walls of the well. The distribution of the temporal average intensity, detected by a virtual receiver array directly above the well plate bottom (c-d), shows much less variation with respect to the excitation frequency for the focused beam in comparison with the unfocused beam. For the focused beam the transmission maxima at the beam axis occur at 3.3, 4.2 and 4.9 MHz. At 3.6 MHz (indicated by the black line in (c)) the intensity profile is flatter, providing a more even distribution within the well.

A2. Analysis of Transport Effects

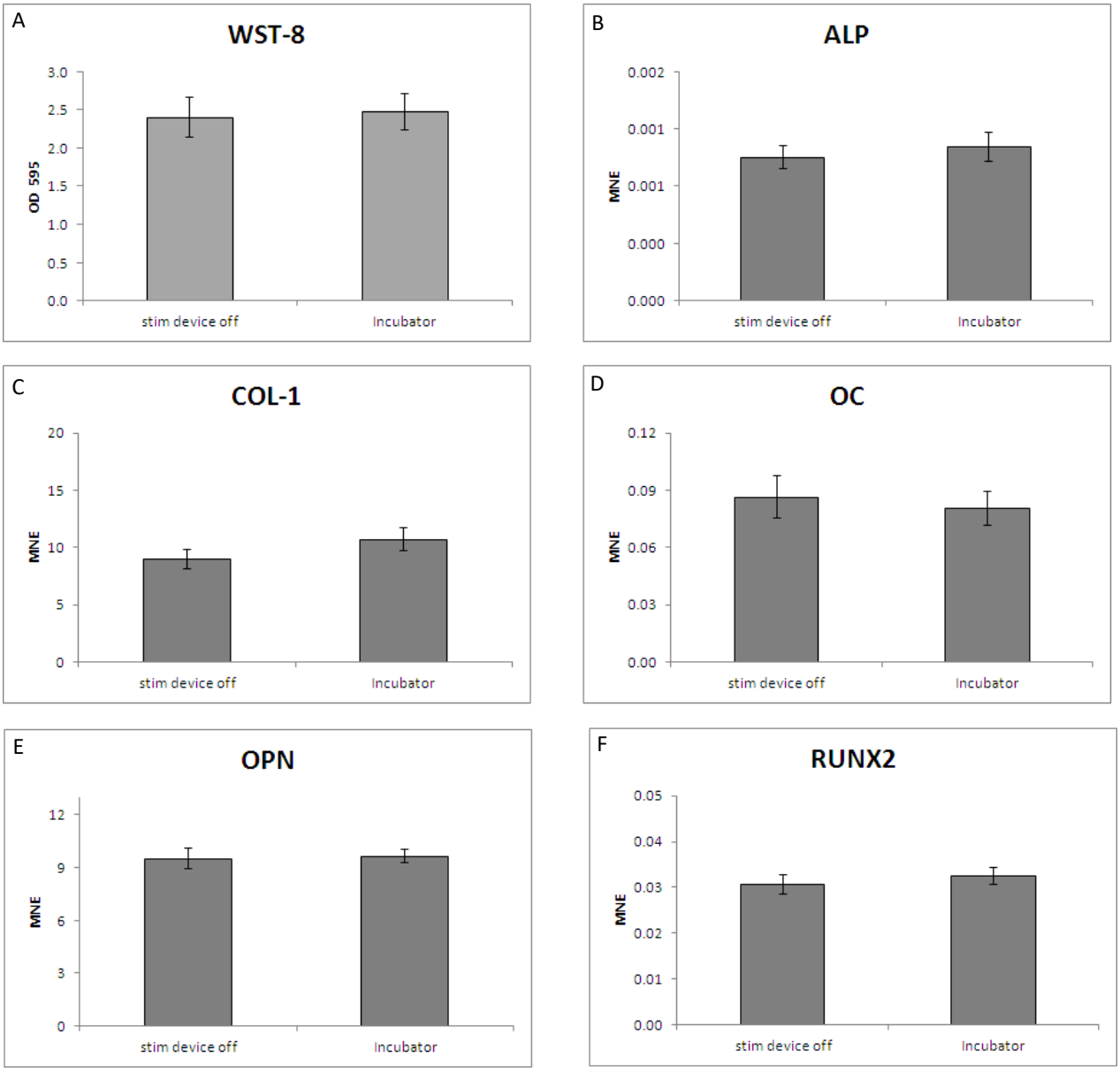

Fig. A2 Effect of plate transport on (A) cell viability WST-8 on day 7 and (B-F) expression of osteogenic markers on day 7, quantified by RT-PCR. All data are presented as mean ± standard error of mean of four independent experiments. No significant differences were found between the groups.

The absorption values of colorimetric viability assay (WST-8) measurements showed no differences in cell activity between the plates positioned in the incubator and transported to the FLIPUS-stimulation unit (Fig. A2-A). The same results were observed for ALP, Col-1, OC, OPN and RUNX-2 mRNA expressions (Figs. A2-B-F).

A3. Enhanced Osteogenic Differentiation of rMSCs in Response to FLIPUS

The gene expression of OPN, RUNX-2, COL-1, and E11 was significantly higher ($p<0.05$) in FLIPUS treated cells at an intensity of $I_{SATA} = 44.5 \pm 7.1$ mW/cm² compared to unstimulated cells (Fig. A3). The gene expression values of FLIPUS stimulated cells on day 5 are normalized to the values, obtained from unstimulated negative control cells on the same day.

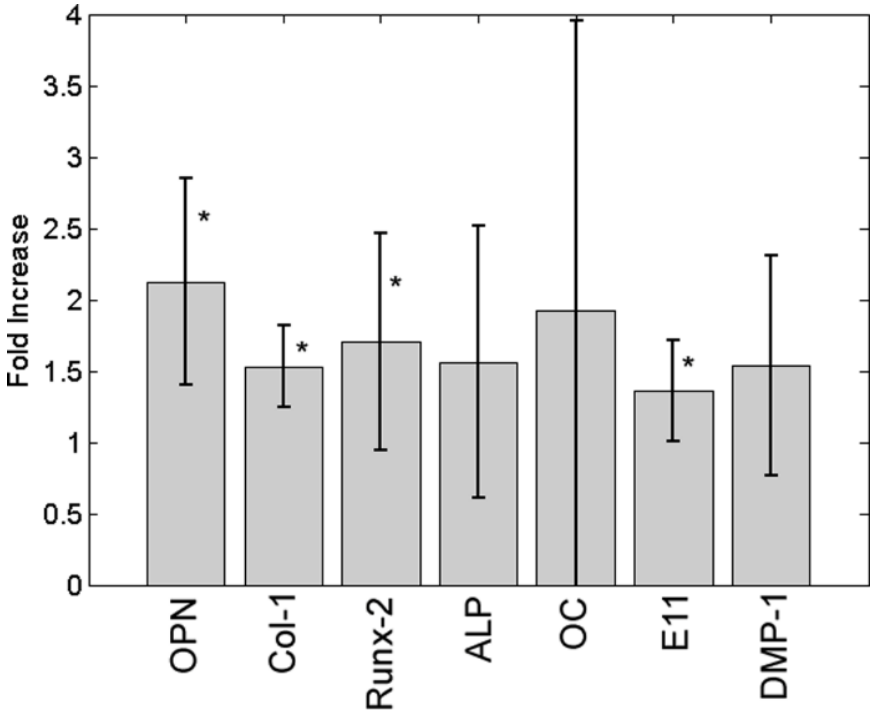

Fig. A3 Effect of FLIPUS on relative mRNA expression of osteogenic markers on day 5 of daily stimulation in rMSCs. All data are presented as mean value ± standard deviation of three independent experiments, asterisk denotes significant difference of groups compared to controls.

Table A3. Osteogenic gene expression in rMSCs on day 5 of daily 20-min-long FLIPUS stimulation. NC designates unstimulated negative control and FLIPUS ON designates ultrasound stimulated cells. All values represented as a mean value of normalized expressions ± standard deviation.

Gene	NC	FLIPUS ON
OPN	6.6 ± 3.4	12.6 ± 4.6
Col-1	10.6 ± 1.7	16.0 ± 3.3
Runx-2	0.023 ± 0.007	0.039 ± 0.019
ALP	0.00023 ± 0.00016	0.00029 ± 0.00019
E11	0.033 ± 0.007	0.040 ± 0.009
DMP-1	0.035 ± 0.008	0.052 ± 0.027
OC	0.0082 ± 0.0045	0.013 ± 0.013

REFERENCES

[1] Parker, K. J., Doyley, M. M., and Rubens, D. J., "Imaging the elastic properties of tissue: the 20 year perspective," *Phys. Med. Biol.*, vol. 56, no. 1, pp. 1-29, 2011.

[2] Padilla, F., Puts, R., Vico, L., and Raum, K., "Stimulation of bone repair with ultrasound: a review of the possible mechanic effects," *Ultrasonics*, vol. 54, no. 5, pp. 1125-1145, 2014.

[3] Pounder, N. M. and Harrison, A. J., "Low intensity pulsed ultrasound for fracture healing: a review of the clinical evidence and the associated biological mechanism of action," *Ultrasonics*, vol. 48, no. 4, pp. 330-338, 2008.

[4] Khanna, A., Nelmes, R. T., Gougoulias, N., Maffulli, N., and Gray, J., "The effects of LIPUS on soft-tissue healing: a review of literature," *Br. Med. Bull.*, vol. 89 pp. 169-182, 2009.

[5] Mikuni-Takagaki, Y., Suzuki, Y., Kawase, T., and Saito, S., "Distinct responses of different populations of bone cells to mechanical stress," *Endocrinology*, vol. 137, no. 5, pp. 2028-2035, 1996.

[6] Tang, L. L., Xian, C. Y., and Wang, Y. L., "The MGF expression of osteoblasts in response to mechanical overload," *Arch. Oral Biol.*, vol. 51, no. 12, pp. 1080-1085, 2006.

[7] Li, D., Tang, T., Lu, J., and Dai, K., "Effects of flow shear stress and mass transport on the construction of a large-scale tissue-engineered bone in a perfusion bioreactor," *Tissue Eng. Part A*, vol. 15, no. 10, pp. 2773-2783, 2009.

[8] Arnsdorf, E. J., Tummala, P., Kwon, R. Y., and Jacobs, C. R., "Mechanically induced osteogenic differentiation-the role of RhoA, ROCKII and cytoskeletal dynamics," J. Cell Sci., vol. 122, no. 4, pp. 546-553, 2009.

[9] Scaglione, S., Wendt, D., Miggino, S., Papadimitropoulos, A., Fato, M., Quarto, R., and Martin, I., "Effects of fluid flow and calcium phosphate coating on human bone marrow stromal cells cultured in a defined 2D model system," *J. Biomed. Mater. Res. A*, vol. 86, no. 2, pp. 411-419, 2008.

[10] Pavalko, F. M., Chen, N. X., Turner, C. H., Burr, D. B., Atkinson, S., Hsieh, Y. F., Qiu, J., and Duncan, R. L., "Fluid shear-induced mechanical signaling in MC3T3-E1 osteoblasts requires cytoskeleton-integrin interactions," *Am. J. Physiol*, vol. 275, no. 6, pp. 1591-1601, 1998.

[11] Yuan, L., Sakamoto, N., Song, G., and Sato, M., "Migration of human mesenchymal stem cells under low shear stress mediated by mitogen-activated protein kinase signaling," *Stem Cells Dev.*, vol. 21, no. 13, pp. 2520-2530, 2012.

[12] Unsworth, J., Kaneez, S., Harris, S., Ridgway, J., Fenwick, S., Chenery, D., and Harrison, A., "Pulsed low intensity ultrasound enhances mineralisation in preosteoblast cells," *Ultrasound Med.Biol.*, vol. 33, no. 9, pp. 1468-1474, 2007.

[13] Sena, K., Leven, R. M., Mazhar, K., Sumner, D. R., and Virdi, A. S., "Early gene response to low-intensity pulsed ultrasound in rat osteoblastic cells," *Ultrasound Med. Biol.*, vol. 31, no. 5, pp. 703-708, 2005.

[14] Takeuchi, R., Ryo, A., Komitsu, N., Mikuni-Takagaki, Y., Fukui, A., Takagi, Y., Shiraishi, T., Morishita, S., Yamazaki, Y., Kumagai, K., Aoki, I., and Saito, T., "Low-intensity pulsed ultrasound activates the phosphatidylinositol 3 kinase/Akt pathway and stimulates the growth of chondrocytes in three-dimensional cultures: a basic science study," *Arthritis Res. Ther.*, vol. 10, no. 4, pp. 77, 2008.

[15] Leskinen, J. J. and Hynynen, K., "Study of factors affecting the magnitude and nature of ultrasound exposure with in vitro set-ups," *Ultrasound Med. Biol.*, vol. 38, no. 5, pp. 777-794, 2012.

[16] Iwabuchi, S., Ito, M., Hata, J., Chikanishi, T., Azuma, Y., and Haro, H., "In vitro evaluation of low-intensity pulsed ultrasound in herniated disc resorption," *Biomaterials*, vol. 26, no. 34, pp. 7104-7114, 2005.

[17] Hensel, K., Mienkina, M. P., and Schmitz, G., "Analysis of ultrasound fields in cell culture wells for in vitro ultrasound therapy experiments," *Ultrasound Med. Biol.*, vol. 37, no. 12, pp. 2105-2115, 2011.

[18] Suzuki, A., Takayama, T., Suzuki, N., Sato, M., Fukuda, T., and Ito, K., "Daily low-intensity pulsed ultrasound-mediated osteogenic differentiation in rat osteoblasts," *Acta Biochim. Biophys. Sin. (Shanghai)*, vol. 41, no. 2, pp. 108-115, 2009.

[19] Ikeda, K., Takayama, T., Suzuki, N., Shimada, K., Otsuka, K., and Ito, K., "Effects of low-intensity pulsed ultrasound on the differentiation of C2C12 cells," *Life Sci.*, vol. 79, no. 20, pp. 1936-1943, 2006.

[20] Wang, F. S., Kuo, Y. R., Wang, C. J., Yang, K. D., Chang, P. R., Huang, Y. T., Huang, H. C., Sun, Y. C., Yang, Y. J., and Chen, Y. J., "Nitric oxide mediates ultrasound-induced hypoxia-inducible factor-1alpha activation and vascular endothelial growth factor-A expression in human osteoblasts," *Bone*, vol. 35, no. 1, pp. 114-123, 2004.

[21] Zhang, S., Cheng, J., and Qin, Y. X., "Mechanobiological modulation of cytoskeleton and calcium influx in osteoblastic cells by short-term focused acoustic radiation force," *PLoS One.*, vol. 7, no. 6, pp. e38343, 2012.

[22] Bandow, K., Nishikawa, Y., Ohnishi, T., Kakimoto, K., Soejima, K., Iwabuchi, S., Kuroe, K., and Matsuguchi, T., "Low-intensity pulsed ultrasound (LIPUS) induces RANKL, MCP-1, and MIP-1beta expression in osteoblasts through the angiotensin II type 1 receptor," *J. Cell Physiol.*, vol. 211, no. 2, pp. 392-398, 2007.

[23] Subramanian, A., Turner, J. A., Budhiraja, G., Guha, T. S., Whitney, N. P., and Nudurupati, S. S., "Ultrasonic bioreactor as a platform for studying cellular response," *Tissue Eng. Part C. Methods*, vol. 19, no. 3, pp. 244-255, 2013.

[24] Chachan, S., Tudu, B., and Sahu, B., "Ultrasound Monitoring of Fracture Healing: Is This the End of Radiography in Fracture Follow-ups?," *J. Orthop. Trauma*, vol. 29, no. 3, pp. e133-e138, 2015.

[25] Barkmann, R., Dencks, S., Laugier, P., Padilla, F., Brixen, K., Ryg, J., Seekamp, A., Mahlke, L., Bremer, A., Heller, M., and Gluer, C. C., "Femur ultrasound (FemUS)--first clinical results on hip fracture discrimination and estimation of femoral BMD," *Osteoporos. Int.*, vol. 21, no. 6, pp. 969-976, 2010.

[26] Rohrbach, D., Preininger, B., Hesse, B., Gerigk, H., Perka, C., and Raum, K., "The early phases of bone healing can be differentiated in a rat osteotomy model by focused transverse-transmission ultrasound," *Ultrasound Med. Biol.*, vol. 39, no. 9, pp. 1642-1653, 2013.

[27] Bossy, E., Talmant, M., and Laugier, P., "Effect of bone cortical thickness on velocity measurements using ultrasonic axial transmission: a 2D simulation study," *J. Acoust. Soc. Am.*, vol. 112, no. 1, pp. 297-307, 2002.

[28] *International Electrotechnical Commission (IEC): IEC 61161: Ultrasonics - Power measurements - Radiation force balances and performance requirements.*, 3rd ed. Geneva: 2013.

[29] Del Grosso, V. A. and Mader, C. W., "Speed of sound in pure water," *J. Acoust. Soc. Am.*, vol. 52 pp. 1442-1446, 1972.

[30] Leskinen, J. J., Olkku, A., Mahonen, A., and Hynynen, K., "Nonuniform temperature rise in in vitro osteoblast ultrasound exposures with associated bioeffect," *IEEE Trans. Biomed. Eng.*, vol. 61, no. 3, pp. 920-927, 2014.

[31] Jung, Y. J., Kim, R., Ham, H. J., Park, S. I., Lee, M. Y., Kim, J., Hwang, J., Park, M. S., Yoo, S. S., Maeng, L. S., Chang, W., and Chung, Y. A., "Focused low-intensity pulsed ultrasound enhances bone regeneration in rat calvarial bone defect through enhancement of cell proliferation," *Ultrasound Med. Biol.*, vol. 41, no. 4, pp. 999-1007, 2015.

[32] Yoo, S. S., Bystritsky, A., Lee, J. H., Zhang, Y., Fischer, K., Min, B. K., McDannold, N. J., Pascual-Leone, A., and Jolesz, F. A., "Focused ultrasound modulates region-specific brain activity," *Neuroimage*, vol. 56, no. 3, pp. 1267-1275, 2011.

[33] Noda, K., Hirano, T., Noda, K., Kodama, S., Ichimiya, I., and Suzuki, M., "Effect of low-intensity focused ultrasound on the middle ear in a mouse model of acute otitis media," *Ultrasound Med. Biol.*, vol. 39, no. 3, pp. 413-423, 2013.

[34] Buldakov, M. A., Hassan, M. A., Zhao, Q. L., Feril, L. B., Jr., Kudo, N., Kondo, T., Litvyakov, N. V., Bolshakov, M. A., Rostov, V. V., Cherdyntseva, N. V., and Riesz, P., "Influence of changing pulse repetition frequency on chemical and biological effects induced by low-intensity ultrasound in vitro," *Ultrason. Sonochem.*, vol. 16, no. 3, pp. 392-397, 2009.

[35] Bruder, S. P., Fink, D. J., and Caplan, A. I., "Mesenchymal stem cells in bone development, bone repair, and skeletal regeneration therapy," *J. Cell Biochem.*, vol. 56, no. 3, pp. 283-294, 1994.

[36] Aggarwal, S. and Pittenger, M. F., "Human mesenchymal stem cells modulate allogeneic immune cell responses," *Blood*, vol. 105, no. 4, pp. 1815-1822, 2005.

[37] Takakura, Y., Matsui, N., Yoshiya, S., Fujioka, H., Muratsu, H., Tsunoda, M., and Kurosaka, M., "Low-intensity pulsed ultrasound enhances early healing of medial collateral ligament injuries in rats," *J. Ultrasound Med*, vol. 21, no. 3, pp. 283-288, 2002.

[38] Fu, S. C., Shum, W. T., Hung, L. K., Wong, M. W., Qin, L., and Chan, K. M., "Low-intensity pulsed ultrasound on tendon healing: a study of the effect of treatment duration and treatment initiation," *Am .J. Sports Med.*, vol. 36, no. 9, pp. 1742-1749, 2008.

[39] Lu, H., Qin, L., Cheung, W., Lee, K., Wong, W., and Leung, K., "Low-intensity pulsed ultrasound accelerated bone-tendon junction healing through regulation of vascular endothelial growth factor expression and cartilage formation," *Ultrasound Med. Biol.*, vol. 34, no. 8, pp. 1248-1260, 2008.

[40] Chen, M. H., Sun, J. S., Liao, S. Y., Tai, P. A., Li, T. C., and Chen, M. H., "Low-intensity pulsed ultrasound stimulates matrix metabolism of human annulus fibrosus cells mediated by transforming growth factor beta1 and extracellular signal-regulated kinase pathway," *Connect. Tissue Res.*, pp. 1-9, 2015.

[41] Iwashina, T., Mochida, J., Miyazaki, T., Watanabe, T., Iwabuchi, S., Ando, K., Hotta, T., and Sakai, D., "Low-intensity pulsed ultrasound stimulates cell proliferation and proteoglycan production in rabbit intervertebral disc cells cultured in alginate," *Biomaterials*, vol. 27, no. 3, pp. 354-361, 2006.

[42] Naito, K., Watari, T., Muta, T., Furuhata, A., Iwase, H., Igarashi, M., Kurosawa, H., Nagaoka, I., and Kaneko, K., "Low-intensity pulsed ultrasound (LIPUS) increases the articular cartilage type II collagen in a rat osteoarthritis model," *J. Orthop. Res.*, vol. 28, 2010.

Chapter 2: INFLUENCE OF DONOR AGE AND STIMULATION INTENSITY ON OSTEOGENESIS OF RAT MSCs IN RESPONSE TO FLIPUS

Reprinted with permission from: Puts, R., Albers, J., Kadow-Romacker, A., Geißler, S., and Raum, K. Influence of Donor Age and Stimulation Intensity on Osteogenic Differentiation of Rat Mesenchymal Stromal Cells in Response to Focused Low-Intensity Pulsed Ultrasound, *Ultrasound Med. Biol.*, vol. 42, no. 12, pp. 2965-2974, Dec.2016.
http://dx.doi.org/10.1016/j.ultrasmedbio.2016.08.012

ABSTRACT

A focused low-intensity pulsed ultrasound (FLIPUS) set-up was used to investigate the effects of stimulation period, acoustic intensity and donor age on the osteogenic differentiation potential of rat mesenchymal stromal cells (rMSCs). rMSCs from 3-month and 12-month old female Sprague Drawly rats were isolated from the bone marrow and stimulated 20 min per day with either 11.7 or 44.5 mW/cm^2 (I_{SATA}) for 7 or 14 days. Osteogenic differentiation markers, i.e., Runt-related transcription factor 2 (RUNX2), osteocalcin (OCN), and degree of matrix calcification were analyzed. On day 7 of stimulation, OCN gene expression was enhanced 1.9-fold in cells from young rats, when stimulated with low intensity. The low intensity also led to a 40 % decrease in RUNX2 expression on day 7 in aged cells, whereas high intensity enhanced expression of RUNX2 on day 14. FLIPUS treatment with low intensity resulted in 15 % increase in extracellular matrix mineralization in young, but not in old rMSCs. These differences suggest the necessity of a donor-age related optimization of stimulation parameters.

Key words: Aging, Low-intensity pulsed ultrasound, acoustic intensity, Mesenchymal stromal cells, Regeneration

INTRODUCTION

The skeleton has a considerable repair competence and a complex interplay of various cellular, humoral and mechanical factors enable the scarless repair of bone injuries, restoring pre-fracture properties under optimal conditions [1]. However, bone is not resistant to the aging process and its regeneration potential progressively declines with increasing age [2;3]. Although age-related skeletal impairments are rarely fatal, they compromise quality of life and diminish the ability of social participation. Thus, there is a clear medical demand for optimizing existing therapeutic options and/or development of new approaches for bone regeneration, in particular for elderly patients [4].

At the cellular level, age-related changes in skeletal health can be attributed to a large extend to declines in both, number and function of mesenchymal stromal cells (MSCs) in the bone marrow [5-7]. MSCs are highly proliferative multipotent progenitor cells and have the ability to differentiate into various mesoderm-type cells such as osteoblasts, chondrocytes, adipocytes [8], and hematopoiesis-supportive stromal cells [9]. Hence, they are thought to be the major progenitor cells for intramembranous and endochondral bone formation [10]. Besides their differentiation capacity, MSCs support tissue regeneration by the modulation of immune and injury responses via the secretion of various proteinases and growth factors [11-15]. The functional behavior of MSCs does not only depend on biochemical factors, but is also strongly influenced by mechanical forces in their microenvironment. Mechanical stress in form of compression, stretching, vibration, shear force or traction on extracellular matrix (ECM) regulate signaling mechanotransduction pathways, affecting proliferation, differentiation, migration of MSCs and other bone-forming cells [16-19]. However, MSCs from aged donors often have a distorted cellular homeostasis [20], leading to dire consequences: the resulting increased intracellular stress does not only compromise their general proliferation [21] and differentiation potential [5;22-25], but also impairs their ability to sense and adapt to mechanical stimuli.

Low-intensity pulsed ultrasound (LIPUS) is a widely used technique for regeneration of fresh fractures, delayed-, non-union bone and other osseous defects [26;27]. Recent *in-vivo* and *in-vitro* studies confirmed that LIPUS could trigger signaling events involved in bone healing [28-31] and stimulate migration [32], proliferation, and differentiation [33-37] of cells with osteogenic properties. However, both experimental and clinical results remain contentious, limiting the understanding of LIPUS effects on tissue regeneration [38]. Most of the *in-vitro* set-ups established for the investigation of LIPUS stimulated bone-healing mechanisms utilize planar

transducers, exposing cells to risks of uncontrolled heat transfer, standing waves generation, and near-field signal variations [36]. These unwanted effects may lead to inadequate translations of *in-vitro* findings to *in-vivo* applications. In our previous work, we have developed a Focused Low-Intensity Pulsed Ultrasound (FLIPUS) *in-vitro* set-up, which prevents or minimizes the LIPUS-associated artifacts described above and allows for standardized investigation of the physico-biological regenerative mechanisms induced by LIPUS in adherent cell [39]. Recently, we have shown that proliferation of bone-forming cells was enhanced when they were cultured in media containing reduced serum supply and were stimulated by FLIPUS [40]. Moreover, increased expression of osteogenic markers in response to I_{SATA} = 44.5 mW/cm2 was observed in rat MSCs [39].

Although LIPUS has been successfully used in clinics, there are still a number of studies doubting its healing potential [41-43] and compromising the clinical acceptance of LIPUS. These differences could be attributed to generalization of the treatment protocol, consisting of I_{SATA} = 30 mW/cm^2, delivered at 1 kHz pulse repetition frequency with 20 % duty cycle for 20 minutes, which could be in need of further optimization, depending on fracture type, its fixation or patients' properties, such as sex and age [44].

To address the later parameter, we used our recently developed focused LIPUS (FLIPUS) *in-vitro* set-up to study age-related differences in the osteogenic differentiation potential of female rMSCs upon stimulation with two different acoustic intensities 20 min a day for 7 or 14 consecutive days.

MATERIALS AND METHODS

A. FLIPUS Cell Stimulation Conditions

The stimulation of cells was carried out with a custom-built FLIPUS system (Fig. 1), which has been described in detail in [39]. This system permits to stimulate adherent cell cultures with FLIPUS under sterile conditions (at 37°C, 95 % air and 5 % CO_2 supply). Briefly, the system consists of an array of 4 focused transducers (center frequency: 5-MHz; diameter: 19 mm; epoxy lens with geometrical focus *R* at 22.8 mm; epoxy backing; STT Richter, Mühlanger, Germany), which are placed below the well-plate chamber.

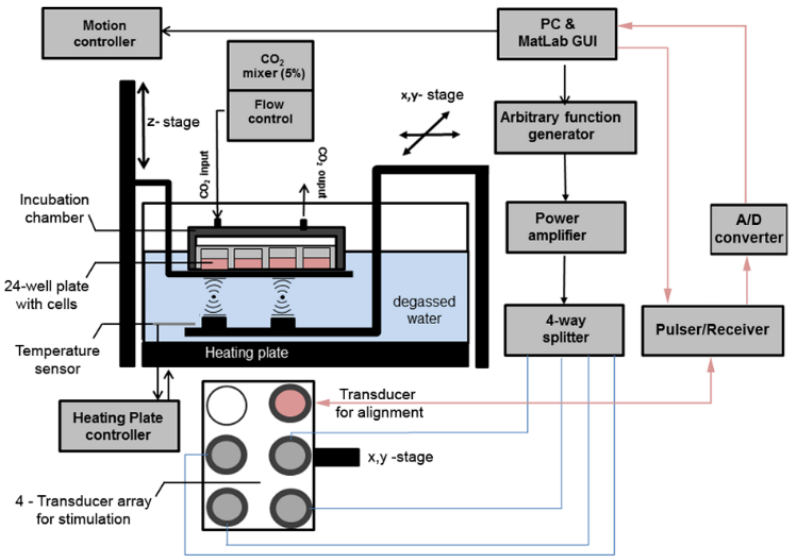

Fig. 1: FLIPUS *in-vitro* cell-stimulation set-up [39].

The system is controlled by means of a high-precision scanning stage and delivers acoustic sound waves in a temperature controlled water tank simultaneously into four wells. The well plate was placed at a distance of 13.3 mm above the focus point of the transducer, i.e., the cells were stimulated in the diverging far-field of the transducers. With this configuration, the -6-dB cross-sectional stimulation area of approximately 0.81 cm^2 of each transducer ensured a smooth and homogenous intensity distribution within the stimulated wells. It should be noted that by variation of well-transducer array distance and signal amplitude of the signal generator, the cross-sectional stimulation area can be adjusted, either to the diameter of the well or to local stimulations. The diverging wave front prevents the development of standing waves between well bottom and the upper liquid-air interface inside the well. For the described configuration, the transmission characteristics through the well-plate have been analyzed and optimized previously by means of lipstick hydrophone measurements directly above the well-plate bottom and by numerical sound propagation simulations [39]. Briefly, no measurable intensity levels have been detected in wells adjacent to the stimulated ones. Significant decreases of the transmitted intensity levels were observed at 3.0, 4.5 and 5 MHz due to reverberations inside the well plate bottom. In contrast, 3.6 MHz provided the most optimal transmission, i.e., the most homogenous intensity distribution within the well. The simulations revealed that standing waves and reverberations were much smaller for the focused beam compared to configurations using a planar transducer. The system has been calibrated for spatial average temporal average intensities

(I_{SATA}) up to 60 mW/cm², which the range typically applied in LIPUS studies [39]. FLIPUS was applied daily for 20 minutes at 3.6 MHz frequency, 100 Hz pulse repetition frequency (PRF), 27.8 % duty cycle (DC), corresponding to 2.78 ms "on" and 7.22 ms "off" signal. Two sets of spatial average temporal average intensities (I_{SATA}), I_{SATA1} = 11.7 mW/cm^2 (low) and I_{SATA2} = 44.5 mW/cm^2 (high), were used.

B. Cell Culture

Rat Mesenchymal Stromal Cells (rMSCs) were extracted from bone marrow of 3-month-old (N = 9, hereinafter called "young") and 12-month-old (N = 8, hereinafter called "aged") female Sprague Drawly (SD) rats, following the protocol established in [13]. rMCSs were expanded in Dulbecco Modified Minimal Essential low glucose Medium (DMEM) (Biochrom AG, Berlin, Germany), supplemented with 10 % fetal calf serum (FCS) (Biochrom AG, Berlin, Germany), 2 mM Glutamax (Gibco®, Life technologies, Darmstadt, Germany) and 1 % Penicillin/Streptomycin (Biochrom AG, Berlin, Germany). Culture medium was substituted twice a week and cells were harvested after reaching 70-80 % confluence using trypsin. All experiments involving the use of cells from animals were in compliance with the German Animal Welfare Act (TierSchG §4) and were approved by State Office of Health and Social Affairs Berlin (Landesamt für Gesundheit und Soziales, Reg. No.T 137/13).

C. Characterization of rMSCs

After isolation and expansion, the osteogenic and adipogenic differentiation potentials of the rMSCs were tested with help of the STEMPRO® MSC differentiation kit (Gibco®, Life technologies, Darmstadt, Germany). Primary rMSCs (passage 3) were seeded in 24-well plates at density of 10^4 cells per well in expansion medium. Twenty-four hours later, the media was changed to expansion media, containing either adipogenic or osteogenic supplements provided by the kit. On day 7, Oil Red O staining was performed according to the original protocol [45]. The matrix was destained with 100 % 2-propanol (Sigma Aldrich, St. Louis, Missouri, USA) and optical density (OD) was measured at 490 nm using a spectrophotometer (Bio-Rad Laboratories GmbH, München, Germany). On day 14, the cells, cultured in osteogenic media, were stained with Alizarin Red S dye (see procedure below). Moreover, expression of osteogenic markers Runt-related transcription factor 2 (RUNX2) and Osteocalcin (OCN) was quantified as described in the next section. Negative control groups were cultured in basal media without differentiation supplements.

D. Osteogenic Differentiation of rMSCs in Response to FLIPUS

All young and aged rMSCs (passage 3) were seeded in quadruplicate in expansion media. Twenty-four hours later, the osteogenic differentiation of primary rMSCs was initiated by exchange of expansion medium to an α-minimal essential medium (α-MEM) (Biochrom AG, Berlin, Germany), containing 2 mM Glutamax (Gibco®, Life technologies, Darmstadt, Germany), 1 % Penicillin/Streptomycin (Biochrom AG, Berlin, Germany), 0.5 mM ascorbic acid (Sigma Aldrich, St. Louis, Missouri, USA), 10 mM β-glycerol-phosphate (Sigma Aldrich, St.Louis, Missouri, USA), 100 nM dexamethasone (Sigma Aldrich, St. Louis, Missouri, USA) and 10 % PANEXIN-NTA® (PAN-Biotech GmbH, Aidenbach, Germany). PANEXIN-NTA® is a pure grade chemically defined serum substitute, composed of essential cell nutrients but lacking any growth factors. Thus, it serves as a replacement for commonly used FCS and avoids cross-reactions by unknown concentrations of natural growth factors. FLIPUS was applied every day for 20 min at two different intensities described above. On days 7 or 14 of stimulation, the cells were lysed for messenger RNA (mRNA) isolation, which was performed by means of the RNA-II Isolation kit (MACHEREY-NAGEL GmbH & Co. KG, Düren, Germany). The cDNA was synthesized with Qscript cDNA-Mix (Quanta BioSciences, Inc., Gaithersburg, MD USA). RUNX2 and OCN gene expression were assessed by quantitative real-time polymerase chain reaction (qRT-PCR). On day 7 and 14 of FLIPUS stimulation Alizarin Red S staining (see procedure below) of calcified matrix was performed. The unstimulated controls were treated identically to the procedure described, except that no FLIPUS signal was introduced to the cells.

E. qRT-PCR

SYBR® GREEN Supermix (Quanta BioSciences, Inc., Gaithersburg, MD USA) was used to quantify the selected osteogenic markers. The following primers were used: OCN forward 5`-agctcaaccccaattgtgac- 3`; reverse 5`-agctgtgccgtccatacttt- 3`; RUNX2 forward 5`-gccgggaatgatgagaacta- 3`; reverse 5`-gaggcggtcagagaacaaac- 3`. Glyceraldehyde-3-phosphate dehydrogenase (GAPDH) house-keeping gene was used as a constitutive expression control, with the following primer sequences: forward 5`-gtcggtgtgaacggatttg- 3`; reverse 5`-ggaagatggtgatgggttt- 3` (TIB Molbiol, Berlin, Germany). The qRT-PCR was performed on a Mastercycler® ep realplex RT-PCR system (Eppendorf, Hamburg, Germany). The primers were checked with no-reverse-transcription control, to reassure lack of genomic DNA.

F. Quantification of Matrix Calcification

To determine the degree of matrix mineralization Alizarin Red S staining was performed. The cells were first fixed with 4 % paraformaldehyde (Sigma Aldrich, St. Louis, Missouri, USA) for 10 minutes and stained for 10 minutes with 0.5 % Alizarin Red S solution (Sigma Aldrich, St. Louis, Missouri, USA) at pH 4. The excessive dye was removed by washing three times with double-distilled water. The matrix-bound Alizarin Red S dye was then released by 10 % cetylpyridinium chloride (Sigma Aldrich, St. Louis, Missouri, USA) for 10 minutes. The OD was measured at 570 nm using a spectrophotometer (Bio-Rad Laboratories GmbH, München, Germany).

G. Statistics

Normal distribution of data was confirmed by means of the Lilliefors test. To compare differences in the readout parameters with respect to donor age, stimulation time and intensity, multivariate ANOVA followed by post-hoc multi-comparison Tukey-Kramer tests were performed. All statistical analyses were conducted using the statistic toolbox of MATLAB® (The MathWorks GmbH, Ismaning, Germany). F-statistics and *p*-values were reported for all tests. *p*-values smaller than 0.05 were considered to be statistically significant. Each biological trial was performed in quadruplicate.

RESULTS

A. Characterization of Freshly Isolated rMSCs

First, we characterized the adipogenic and osteogenic differentiation capacity of rMSCs from aged and young donors. Adipogenic differentiation was visualized and quantified using Oil Red O staining. As shown in Fig. 2 a-b, aged rMSCs exhibited a significantly higher formation of lipid vacuoles compared to young MSCs ($F = 5.9$, $p = 0.02$). Osteogenic differentiation was quantified by matrix mineralization using Alizarin Red S (Fig. 2 c-d). In contrast to the adipogenic differentiation, we found no significant difference in matrix mineralization between rMSCs from aged and young animals. However, quantification of OCN ($F = 6.8$, $p = 0.01$) and RUNX2 ($F = 10.5$, $p = 0.002$) gene expressions revealed significantly higher values for young cells in comparison to the aged ones (Fig. 3 a-b).

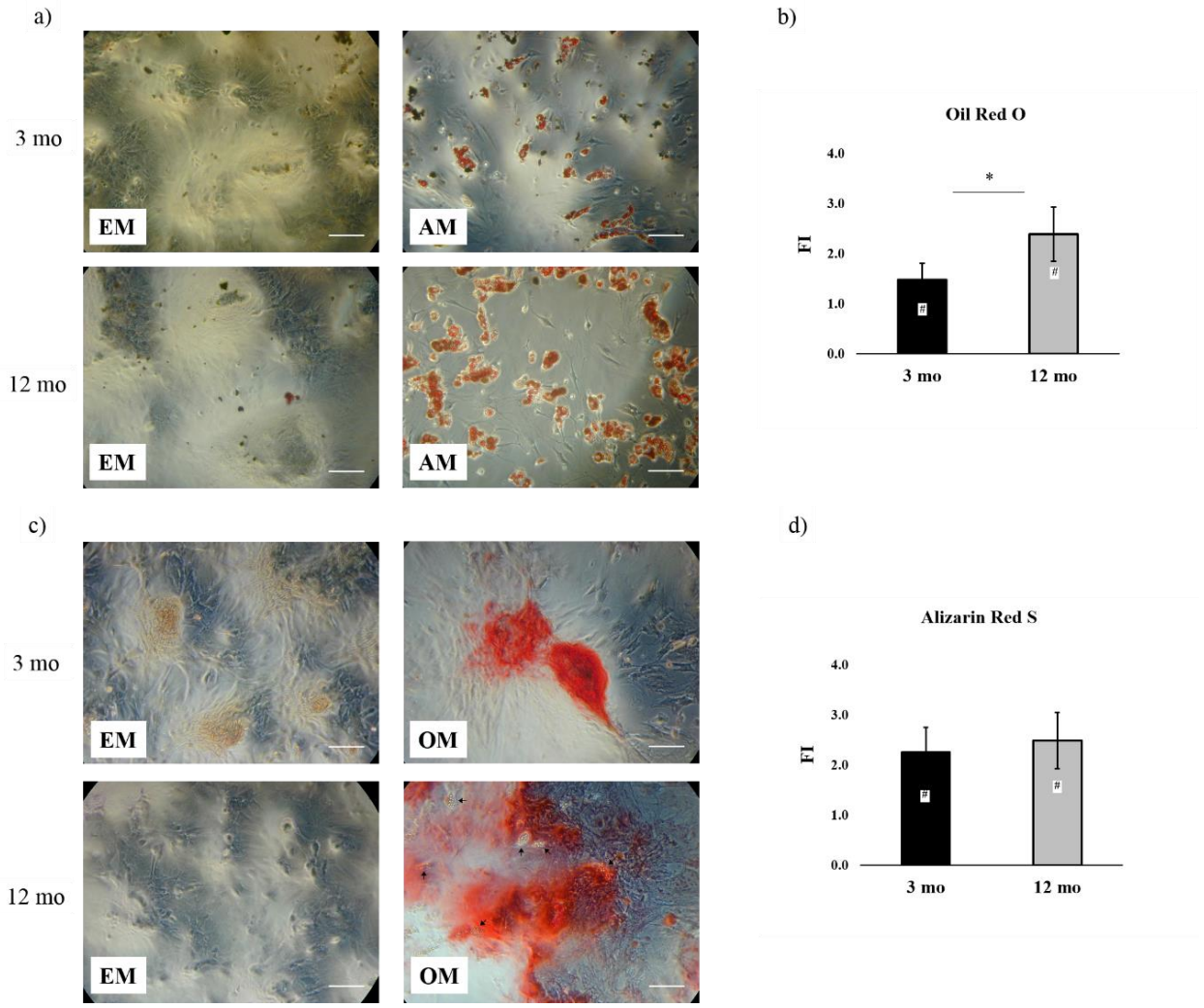

Fig. 2: Multilineage differentiation potential of 3-month-old (3 mo) and 12-month-old (12 mo) rMSCs: (a) Representative Oil Red O stained images and (b) quantification of stainings on day 7. (c) Representative Alizarin Red S stained images and (d) quantification of stainings on day 14. EM, AM, and OM indicate expansion medium, adipogenic medium, and osteogenic medium, respectively. Black arrows in (c) indicate lipid droplets. Scale bars size is 100 µm. The quantified values represent fold induction (FI) of optical density (OD) measurements normalized to undifferentiated control groups and are expressed as mean ± standard error (SE). * and # denote significant differences ($p < 0.05$) between age groups and between differentiated and undifferentiated controls, respectively.

Interestingly, in the cultures of aged rMSCs, which were differentiated into the osteogenic lineage, lipid droplets were observed together with calcium deposition, which was not the case for young cells (Fig. 2c, black arrows).

B. FLIPUS Effects on Osteogenic Differentiation of rMSCs are both Intensity- and Age-Dependent

To investigate the impact of mechanical stimulation on the progenitor phenotype of aged and young rMSCs, we compared their osteogenic differentiation capacity upon stimulation with high and low FLIPUS acoustic intensities. The results are presented as changes in mean normalized expression values of FLIPUS-stimulated cells in comparison to unstimulated control groups (OFF).

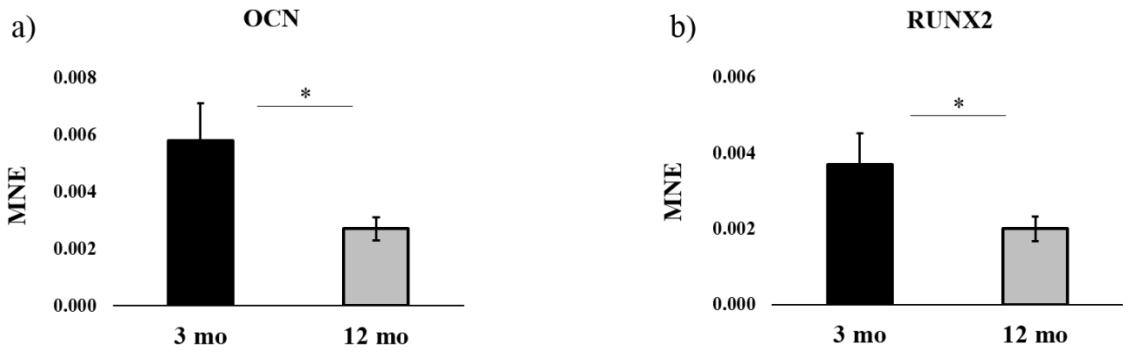

Fig. 3: Mean normalized expression (MNE) values of (a) OCN and (b) RUNX2 on day 14. The bars and whiskers represent mean ± standard error (SE) values. The asterisk denotes significant differences ($p < 0.05$).

OCN

Osteocalcin expression was significantly affected by age ($F = 5.5$, $p = 0.02$), stimulation intensity ($F = 4.3$, $p = 0.01$) and by the combination of both parameters ($F = 3.6$, $p = 0.03$). On day 7, the low FLIPUS intensity led to an 1.9-fold increase of OCN expression in rMSCs from young donors in comparison to unstimulated cells and cells stimulated with high intensity ($F = 9.4$, $p < 0.001$). The increase was also higher compared to aged cells stimulated with low intensity ($F = 7.4$, $p = 0.01$). However, these differences diminished after 14 days of stimulation (Fig.4 a).

RUNX2

RUNX2 expression was affected by intensity level ($F = 5.6$, $p = 0.004$) and stimulation period in correlation with age ($F = 8.7$, $p = 0.004$) (Fig.4 b). In aged cells the expression of RUNX2 was significantly down-regulated at day 7 in response to 11.7 mW/cm^2 acoustic intensity compared to unstimulated cells ($F = 4.5$, $p = 0.02$). This decrease was also significant in

comparison to young cells stimulated at the same acoustic intensity (F= 9.9, p = 0.0041) (Fig.4 b).

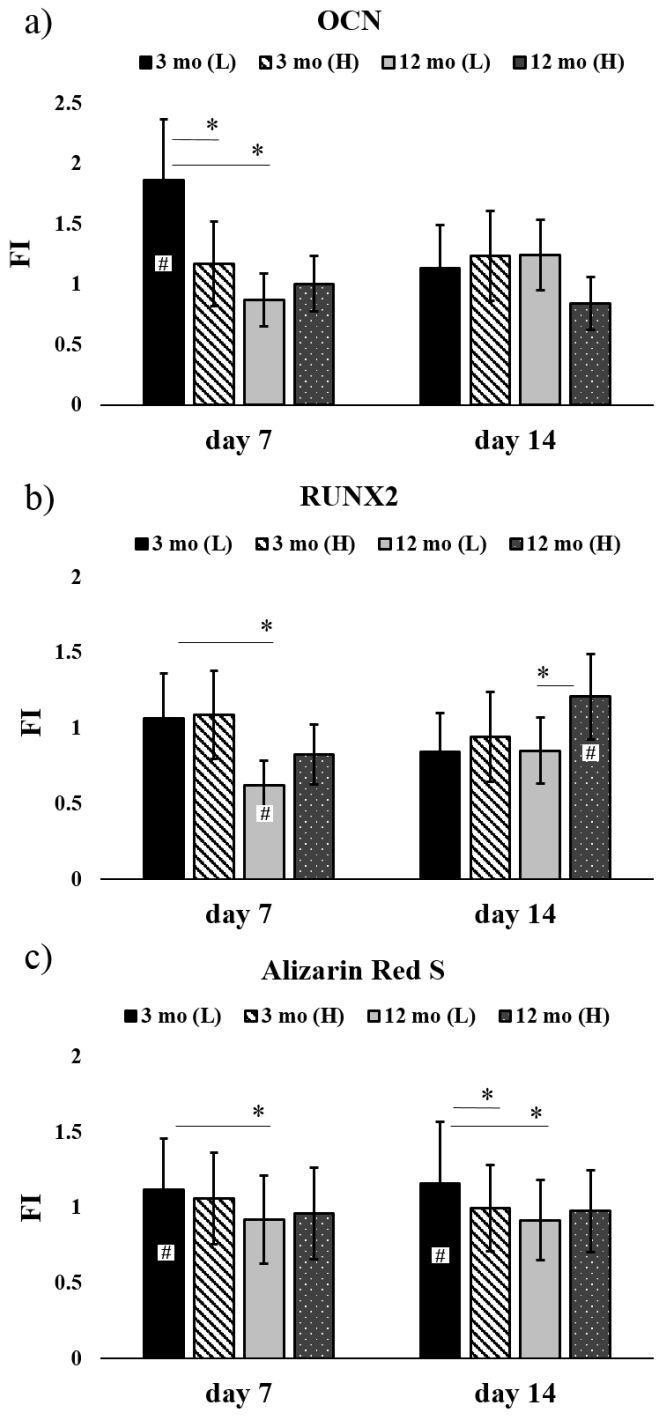

Fig. 4: Expressions of (a) OCN, (b) RUNX2 and (c) matrix calcification on days 7 and 14 in 3-month-old (3 mo) and 12-month-old (12 mo) rMSCs, stimulated for 20 minutes daily with either 11.7 mW/cm^2 (L) or 44.5 mW/cm^2 (H) FLIPUS acoustic intensities. Bar charts display fold induction (FI) of MNE values (a) and (b) and OD values (c) normalized to unstimulated control groups (OFF). Each bar represents mean ± standard error (SE). # and

*** denote significant differences ($p \leq 0.05$) compared to OFF and stimulated groups, respectively.**

After 14 days of FLIPUS-treatment, RUNX2 expression was 1.2-fold enhanced in aged cells as opposed to negative control and cells stimulated with low intensity ($F = 6.1$, $p = 0.004$) (Fig.4 b). Young MSCs showed no changes in RUNX2 expression in response to FLIPUS stimulation.

ECM Calcification

The quantified Alizarin Red S staining showed dependencies of the calcification degree with respect to age ($F = 20.0$, $p < 0.001$) and to stimulation intensity in correlation with age ($F = 17.7$, $p < 0.001$). The mineralization of ECM on day 7 was most pronounced in young cells stimulated with 11.7 mW/cm^2 intensity compared to unstimulated control ($F = 7.1$, $p = 0.002$) and rMSCs from aged donors stimulated with the same intensity ($F = 16.1$, $p < 0.001$) (Fig.4 c).

On day 14 more enhanced calcification was seen in young cells stimulated with 11.7 mW/cm^2 in contrast to unstimulated young cells or those stimulated with high intensity ($F = 14.6$, $p < 0.001$), as well as in comparison to aged cells stimulated with low intensity ($F = 18.8$, $p < 0.001$). High FLIPUS intensity did not influence calcium deposition in matrix of cells from young donors and FLIPUS had no overall effect on matrix mineralization in aged cells (Fig.4 c).

No significant differences were observed in OCN, RUNX2 gene expressions and in matrix mineralization between day 7 and 14 in response to FLIPUS treatment in rMSCs from young and aged donors.

DISCUSSION

In this study, we have used a novel focused LIPUS system to analyze the osteogenic differentiation potential of female rMSCs, isolated from 3-month- and 12-month-old rats, with respect to donor age and applied stimulation intensity.

The evaluation of differentiation potential of isolated rMSCs revealed that the cells from aged rats (12 months) had more intensive Oil Red O staining, in comparison to the cells from young rats (3 months), implying that with age rMSCs favor maturation into the adipogenic lineage. Moreover, aged rMSC, which had been differentiated into the osteogenic lineage, deposited lipid droplets in addition to calcium in the extracellular matrix. This finding is in

agreement with previous studies, in which MSCs extracted from aging donors have been shown to possess a lower osteogenic differentiation potential compared to cells from young donors [5;46]. Already in 1971 Meunier *et al*. [47] observed that with age human bone marrow increases in adipose tissue content, while the trabecular bone volume decreases. These results support the hypothesis that the differentiation potential of bone marrow MSCs is shifted towards the adipogenic lineage with increasing age. The mechanism of a gradual replacement of cells with multilineage differentiation potential by cells with an adipogenic destination could also account for the increased risk for the occurrence of osteoporosis with age. Our data show that expressions of osteogenic markers RUNX2 and OCN were down-regulated in aged rMSCs, although the Alizarin Red S staining did not indicate any significant change in ECM mineralization. The lack of ECM mineralization variations between young and aged groups may be attributed to the relatively early time points for this analysis, as the recommended incubation time is 21 days. Therefore, the mineralization assay only confirmed that all cells cultured in the osteogenic differentiation medium initiated ECM synthesis including mineralization within the evaluated time. RUNX2 is an essential transcription factor for the cells of osteogenic lineage, regulating expression of OCN [48], amongst many other bone-associated genes [49]. Our results are in agreement with Moerman *et al*. [50], who showed that murine MSCs from aged donors had lower expressions of osteogenic genes, i.e., RUNX2, Dlx5, OCN, and type I collagen, while the adipogenic potential of aged cells was enhanced. This reduction of osteogenic potential with age could be a consequence of a so-called adipogenic switch, which has been suggested to be triggered through inhibition of canonical Wnt signaling in cells [51]. The observed changes in gene expressions of RUNX2 and OCN could be partially influenced by the selected reference gene GAPDH, whose expression decreases in muscles of aged rats, as shown in study of Lowe *et al*. [52]. However, Touchberry *et al.* [53] found that expression of GAPDH does not vary in young and aged human muscles and it represents the most reliable reference gene amongst other tested genes.

In the current study, the osteogenic profile of rMSCs isolated from young and aged species and stimulated with one of the two acoustic intensities revealed distinct differences in cellular responses. Our data shows that daily stimulation with low FLIPUS intensity (11.7 mW/cm^2) led to an increased expression of OCN gene on day 7 in young rMSCs, while neither of the two intensities affected the expression of RUNX2. It is important to emphasize that in our study FCS, which is commonly used to support cellular activities was replaced by PANEXIN-NTA® in order to avoid stimulatory effects of growth factors contained in serum.

Therefore, the observed effects can be solely attributed to mechanical stimulation generated by FLIPUS. The higher acoustic intensity of 44.5 mW/cm^2 did not increase the expressions of the genes of interest on day 7 in young rMSCs compared to unstimulated controls. Furthermore, OCN expression with higher intensity was significantly lower in comparison to 11.7 mW/cm^2 in young cells. Chen *et al*. [54] previously showed that human MSCs subjected to 3 % stretching on flexible-bottomed plates expressed alkaline phosphatase, RUNX2 and OCN, while the cells stretched at 10 % magnitude rather expressed type III collagen and tenascin-C, which are markers of tenogenic differentiation. Koike *et al*. [55] observed that straining of ST2 bone marrow cells with higher magnitude or for longer periods led to a decrease in RUNX2 expression. Therefore, we hypothesize that the higher FLIPUS acoustic intensity used in this study may have triggered a different signaling pathway than the lower intensity, leading to distinct biological responses in the investigated rMSCs. Similar to results of Koike *et al*. [55] the cellular mechanoresponse to ultrasound could also be dependent on the duration of FLIPUS stimulation. This assumption is supported by our previous observation that activation of mechanosensitive transcription factors AP-1, Sp1 and TEAD was most pronounced in response to 5-min FLIPUS treatment of C2C12 cells at 44.5 mW/cm^2 [56] and longer stimulations returned activation of AP-1 and TEAD to their basal level.

It should be noted that the lower FLIPUS intensity resulted in a reduced expression of RUNX2 in aged rMSCs on day 7 of FLIPUS exposure. The RUNX2 transcription factor, which is usually associated with the expression of osteogenic markers, also regulates proliferation of maturating bone-forming cells. During cellular differentiation from osteoprogenitors to osteoblasts, RUNX2 expression oscillates, i.e., it decreases when cells proliferate and it increases when they differentiate [57]. The expression of RUNX2 goes down on cell-cycle entry, accelerating the transition to the S-phase and results in cell division. However, this phenomenon is not observed in cancer cell-lines, e.g., rat osteosarcoma ROS17/2.8 cells [58]. In our study the acoustic intensity of 11.7 mW/cm^2 may have promoted cellular proliferation on day 7 by temporally delaying the osteogenic differentiation of rMSCs. On day 14 of FLIPUS treatment, the expression of RUNX2 exceeds the one of unstimulated controls by about 25 % in aged rMSCs stimulated with 44 mW/cm^2. In contrast, the expression of OCN remained unchanged for both stimulation intensities in old rMSCs. However, an increase in OCN expression in response to FLIPUS is anticipated at later time points, since the RUNX2 expression was enhanced only on day 14, which needs to be confirmed in future studies. The Alizarin Red S staining of the

mineralized matrix showed the same trend for young rMSCs, i.e., more enhanced matrix mineralization was observed for cells stimulated with lower acoustic intensity.

Our data suggest that FLIPUS regulate functioning of rMSCs of two different age groups through the activation of different mechanisms: younger cells might start maturating soon after the treatment, whereas older cells might first increase in population size and then proceed to differentiation. The observed mechanistic differences could be also attributed to the properties of the ECM synthesized by cells. Extracellular matrix elasticity in direct proximity to the cells and architecture change throughout cell's life [59], altering the biological response of cells to the same mechanical stimuli. McBeath *et al.* [60] showed that confining human MSCs on small islands directs them towards adipocytes, whereas introducing them to larger areas, where cellular spreading occurs, led to osteogenic differentiation of cells, when they were cultured in media with both, osteogenic and adipogenic supplements.

Further studies need to be conducted in order to understand accurately cellular mechanisms in aged and young cells when LIPUS is applied. Moreover, the most optimal stimulation conditions, e.g., duration, average and peak intensity levels, duty cycle and repetitions of LIPUS treatments need to be investigated, which could not be achieved in the current study due to the limited number of freshly isolated cells in the same passage. However, the FLIPUS system, used in this study, should allow a straightforward transfer of an optimized age-dependent "acoustic dose" to an *in-vivo* application, e.g., in a rat osteotomy model.

CONCLUSIONS

From our observations, we conclude that the osteogenic potential of rMSCs isolated from species of two different age groups was influenced by FLIPUS differently: young cells benefited from $I_{SATA} = 11.7\ mW/cm^2$, whereas aged cells experienced delayed osteogenic effects with acoustic intensity of $44.5\ mW/cm^2$. These data might suggest age related differences in mechanisms in response to LIPUS and support our hypothesis of patient-dependent parameter optimization of the employed acoustic stimulation.

ACKNOWLEDGEMENTS

The study was funded by the German Research Foundation (Deutsche Forschungsgemeinschaft, DFG) grant Ra1380/8-1. S.G. received support from DFG grant GE2512/1-2. R.P. received a DFG scholarship through the Berlin-Brandenburg School for Regenerative Therapies GSC 203.

REFERENCES

[1] P. V. Giannoudis, T. A. Einhorn, and D. Marsh, "Fracture healing: the diamond concept," *Injury*, vol. 38 Suppl 4, p. S3-S6, Sept.2007.

[2] R. Gruber, H. Koch, B. A. Doll, F. Tegtmeier, T. A. Einhorn, and J. O. Hollinger, "Fracture healing in the elderly patient," *Exp. Gerontol.*, vol. 41, no. 11, pp. 1080-1093, Nov.2006.

[3] P. Strube, U. Sentuerk, T. Riha, K. Kaspar, M. Mueller, G. Kasper, G. Matziolis, G. N. Duda, and C. Perka, "Influence of age and mechanical stability on bone defect healing: age reverses mechanical effects," *Bone*, vol. 42, no. 4, pp. 758-764, Apr.2008.

[4] N. K. Satija, V. K. Singh, Y. K. Verma, P. Gupta, S. Sharma, F. Afrin, M. Sharma, P. Sharma, R. P. Tripathi, and G. U. Gurudutta, "Mesenchymal stem cell-based therapy: a new paradigm in regenerative medicine," *J. Cell Mol. Med.*, vol. 13, no. 11-12, pp. 4385-4402, Nov.2009.

[5] G. D'Ippolito, P. C. Schiller, C. Ricordi, B. A. Roos, and G. A. Howard, "Age-related osteogenic potential of mesenchymal stromal stem cells from human vertebral bone marrow," *J. Bone Miner. Res.*, vol. 14, no. 7, pp. 1115-1122, July1999.

[6] G. Kasper, L. Mao, S. Geissler, A. Draycheva, J. Trippens, J. Kuhnisch, M. Tschirschmann, K. Kaspar, C. Perka, G. N. Duda, and J. Klose, "Insights into mesenchymal stem cell aging: involvement of antioxidant defense and actin cytoskeleton," *Stem Cells*, vol. 27, no. 6, pp. 1288-1297, June2009.

[7] J. Shen, Y. T. Tsai, N. M. Dimarco, M. A. Long, X. Sun, and L. Tang, "Transplantation of mesenchymal stem cells from young donors delays aging in mice," *Sci. Rep.*, vol. 1, p. 67, 2011.

[8] M. F. Pittenger, A. M. Mackay, S. C. Beck, R. K. Jaiswal, R. Douglas, J. D. Mosca, M. A. Moorman, D. W. Simonetti, S. Craig, and D. R. Marshak, "Multilineage potential of adult human mesenchymal stem cells," *Science*, vol. 284, no. 5411, pp. 143-147, Apr.1999.

[9] T. M. Dexter, E. G. Wright, F. Krizsa, and L. G. Lajtha, "Regulation of haemopoietic stem cell proliferation in long term bone marrow cultures," *Biomedicine.*, vol. 27, no. 9-10, pp. 344-349, Dec.1977.

[10] J. He, B. Jiang, Y. Dai, J. Hao, Z. Zhou, Z. Tian, F. Wu, and Z. Gu, "Regulation of the osteoblastic and chondrocytic differentiation of stem cells by the extracellular matrix and subsequent bone formation modes," *Biomaterials*, vol. 34, no. 28, pp. 6580-6588, Sept.2013.

[11] A. I. Caplan and J. E. Dennis, "Mesenchymal stem cells as trophic mediators," *J. Cell Biochem.*, vol. 98, no. 5, pp. 1076-1084, Aug.2006.

[12] G. Kasper, J. D. Glaeser, S. Geissler, A. Ode, J. Tuischer, G. Matziolis, C. Perka, and G. N. Duda, "Matrix metalloprotease activity is an essential link between mechanical stimulus and mesenchymal stem cell behavior," *Stem Cells*, vol. 25, no. 8, pp. 1985-1994, Aug.2007.

[13] S. Geissler, M. Textor, J. Kuhnisch, D. Konnig, O. Klein, A. Ode, T. Pfitzner, J. Adjaye, G. Kasper, and G. N. Duda, "Functional comparison of chronological and in vitro aging: differential role of the cytoskeleton and mitochondria in mesenchymal stromal cells," *PLoS. One.*, vol. 7, no. 12, p. e52700, 2012.

[14] W. Li, G. Ren, Y. Huang, J. Su, Y. Han, J. Li, X. Chen, K. Cao, Q. Chen, P. Shou, L. Zhang, Z. R. Yuan, A. I. Roberts, S. Shi, A. D. Le, and Y. Shi, "Mesenchymal stem cells: a double-edged sword in regulating immune responses," *Cell Death. Differ.*, vol. 19, no. 9, pp. 1505-1513, Sept.2012.

[15] A. Philippou, M. Maridaki, A. Theos, and M. Koutsilieris, "Cytokines in muscle damage," *Adv. Clin. Chem.*, vol. 58, pp. 49-87, 2012.

[16] D. E. Discher, P. Janmey, and Y. L. Wang, "Tissue cells feel and respond to the stiffness of their substrate," *Science*, vol. 310, no. 5751, pp. 1139-1143, Nov.2005.

[17] E. Hadjipanayi, V. Mudera, and R. A. Brown, "Guiding cell migration in 3D: a collagen matrix with graded directional stiffness," *Cell Motil. Cytoskeleton*, vol. 66, no. 3, pp. 121-128, Mar.2009.

[18] J. P. Winer, P. A. Janmey, M. E. McCormick, and M. Funaki, "Bone marrow-derived human mesenchymal stem cells become quiescent on soft substrates but remain responsive to chemical or mechanical stimuli," *Tissue Eng Part A*, vol. 15, no. 1, pp. 147-154, Jan.2009.

[19] A. J. Engler, S. Sen, H. L. Sweeney, and D. E. Discher, "Matrix elasticity directs stem cell lineage specification," *Cell*, vol. 126, no. 4, pp. 677-689, Aug.2006.

[20] S. Geissler, M. Textor, K. Schmidt-Bleek, O. Klein, M. Thiele, A. Ellinghaus, D. Jacobi, A. Ode, C. Perka, A. Dienelt, J. Klose, G. Kasper, G. N. Duda, and P. Strube, "In serum veritas-in

serum sanitas? Cell non-autonomous aging compromises differentiation and survival of mesenchymal stromal cells via the oxidative stress pathway," *Cell Death. Dis.*, vol. 4, p. e970, 2013.

[21] C. Fehrer and G. Lepperdinger, "Mesenchymal stem cell aging," *Exp. Gerontol.*, vol. 40, no. 12, pp. 926-930, Dec.2005.

[22] A. Stolzing, E. Jones, D. McGonagle, and A. Scutt, "Age-related changes in human bone marrow-derived mesenchymal stem cells: consequences for cell therapies," *Mech. Ageing Dev.*, vol. 129, no. 3, pp. 163-173, Mar.2008.

[23] S. Sethe, A. Scutt, and A. Stolzing, "Aging of mesenchymal stem cells," *Ageing Res. Rev.*, vol. 5, no. 1, pp. 91-116, Feb.2006.

[24] M. M. Bonab, K. Alimoghaddam, F. Talebian, S. H. Ghaffari, A. Ghavamzadeh, and B. Nikbin, "Aging of mesenchymal stem cell in vitro," *BMC. Cell Biol.*, vol. 7, p. 14, 2006.

[25] W. Zhang, G. Ou, M. Hamrick, W. Hill, J. Borke, K. Wenger, N. Chutkan, J. Yu, Q. S. Mi, C. M. Isales, and X. M. Shi, "Age-related changes in the osteogenic differentiation potential of mouse bone marrow stromal cells," *J. Bone Miner. Res.*, vol. 23, no. 7, pp. 1118-1128, July2008.

[26] J. D. Heckman, J. P. Ryaby, J. McCabe, J. J. Frey, and R. F. Kilcoyne, "Acceleration of tibial fracture-healing by non-invasive, low-intensity pulsed ultrasound," *J. Bone Joint Surg. Am.*, vol. 76, no. 1, pp. 26-34, Jan.1994.

[27] T. K. Kristiansen, J. P. Ryaby, J. McCabe, J. J. Frey, and L. R. Roe, "Accelerated healing of distal radial fractures with the use of specific, low-intensity ultrasound. A multicenter, prospective, randomized, double-blind, placebo-controlled study," *J. Bone Joint Surg. Am.*, vol. 79, no. 7, pp. 961-973, July1997.

[28] S. R. Angle, K. Sena, D. R. Sumner, and A. S. Virdi, "Osteogenic differentiation of rat bone marrow stromal cells by various intensities of low-intensity pulsed ultrasound," *Ultrasonics*, vol. 51, no. 3, pp. 281-288, Apr.2011.

[29] H. El-Mowafi and M. Mohsen, "The effect of low-intensity pulsed ultrasound on callus maturation in tibial distraction osteogenesis," *Int. Orthop.*, vol. 29, no. 2, pp. 121-124, Apr.2005.

[30] J. W. Chow, A. J. Wilson, T. J. Chambers, and S. W. Fox, "Mechanical loading stimulates bone formation by reactivation of bone lining cells in 13-week-old rats," *J. Bone Miner. Res.*, vol. 13, no. 11, pp. 1760-1767, Nov.1998.

[31] N. M. Pounder and A. J. Harrison, "Low intensity pulsed ultrasound for fracture healing: a review of the clinical evidence and the associated biological mechanism of action," *Ultrasonics*, vol. 48, no. 4, pp. 330-338, Aug.2008.

[32] F. Y. Wei, K. S. Leung, G. Li, J. Qin, S. K. Chow, S. Huang, M. H. Sun, L. Qin, and W. H. Cheung, "Low intensity pulsed ultrasound enhanced mesenchymal stem cell recruitment through stromal derived factor-1 signaling in fracture healing," *PLoS. One.*, vol. 9, no. 9, p. e106722, 2014.

[33] K. Bandow, Y. Nishikawa, T. Ohnishi, K. Kakimoto, K. Soejima, S. Iwabuchi, K. Kuroe, and T. Matsuguchi, "Low-intensity pulsed ultrasound (LIPUS) induces RANKL, MCP-1, and MIP-1beta expression in osteoblasts through the angiotensin II type 1 receptor," *J. Cell Physiol*, vol. 211, no. 2, pp. 392-398, May2007.

[34] J. Unsworth, S. Kaneez, S. Harris, J. Ridgway, S. Fenwick, D. Chenery, and A. Harrison, "Pulsed low intensity ultrasound enhances mineralisation in preosteoblast cells," *Ultrasound Med. Biol.*, vol. 33, no. 9, pp. 1468-1474, Sept.2007.

[35] X. Roussignol, C. Currey, F. Duparc, and F. Dujardin, "Indications and results for the Exogen ultrasound system in the management of non-union: a 59-case pilot study," *Orthop. Traumatol. Surg. Res.*, vol. 98, no. 2, pp. 206-213, Apr.2012.

[36] F. Padilla, R. Puts, L. Vico, and K. Raum, "Stimulation of bone repair with ultrasound: a review of the possible mechanic effects," *Ultrasonics*, vol. 54, no. 5, pp. 1125-1145, July2014.

[37] A. Suzuki, T. Takayama, N. Suzuki, M. Sato, T. Fukuda, and K. Ito, "Daily low-intensity pulsed ultrasound-mediated osteogenic differentiation in rat osteoblasts," *Acta Biochim. Biophys. Sin. (Shanghai)*, vol. 41, no. 2, pp. 108-115, Feb.2009.

[38] F. Padilla, R. Puts, L. Vico, A. Guignandon, and K. Raum, "Stimulation of Bone Repair with Ultrasound," *Adv. Exp. Med. Biol.*, vol. 880, pp. 385-427, 2016.

[39] R. Puts, K. Ruschke, T. H. Ambrosi, A. Kadow-Romacker, P. Knaus, K. V. Jenderka, and K. Raum, "A Focused Low-Intensity Pulsed Ultrasound (FLIPUS) System for Cell Stimulation: Physical and Biological Proof of Principle," *IEEE Trans. Ultrason. Ferroelectr. Freq. Control*, vol. 63, no. 1, pp. 91-100, Jan.2016.

[40] R. Puts, T.-H. Ambrosi, A. Kadow-Romacker, K. Ruschke, P. Knaus, and K. Raum, "In-vitro stimulation of cells of the musculoskeletal system with focused Low-Intensity Pulsed Ultrasound (FLIPUS): Analyses of cellular activities in response to the optimized acoustic dose.," Ultrasonics Symposium (IUS), 2014 IEEE International: 2014, pp. 1630-1633.

[41] A. Emami, M. Petren-Mallmin, and S. Larsson, "No effect of low-intensity ultrasound on healing time of intramedullary fixed tibial fractures," *J. Orthop. Trauma*, vol. 13, no. 4, pp. 252-257, May1999.

[42] P. H. Lubbert, R. H. van der Rijt, L. E. Hoorntje, and C. van der Werken, "Low-intensity pulsed ultrasound (LIPUS) in fresh clavicle fractures: a multi-centre double blind randomised controlled trial," *Injury*, vol. 39, no. 12, pp. 1444-1452, Dec.2008.

[43] J. P. Rue, D. W. Armstrong, III, F. J. Frassica, M. Deafenbaugh, and J. H. Wilckens, "The effect of pulsed ultrasound in the treatment of tibial stress fractures," *Orthopedics*, vol. 27, no. 11, pp. 1192-1195, Nov.2004.

[44] Y. Watanabe, T. Matsushita, M. Bhandari, R. Zdero, and E. H. Schemitsch, "Ultrasound for fracture healing: current evidence," *J. Orthop. Trauma*, vol. 24 Suppl 1, p. S56-S61, Mar.2010.

[45] J. L. Ramirez-Zacarias, F. Castro-Munozledo, and W. Kuri-Harcuch, "Quantitation of adipose conversion and triglycerides by staining intracytoplasmic lipids with Oil red O," *Histochemistry*, vol. 97, no. 6, pp. 493-497, July1992.

[46] S. Roura, J. Farre, C. Soler-Botija, A. Llach, L. Hove-Madsen, J. J. Cairo, F. Godia, J. Cinca, and A. Bayes-Genis, "Effect of aging on the pluripotential capacity of human CD105+ mesenchymal stem cells," *Eur. J. Heart Fail.*, vol. 8, no. 6, pp. 555-563, Oct.2006.

[47] P. Meunier, J. Aaron, C. Edouard, and G. Vignon, "Osteoporosis and the replacement of cell populations of the marrow by adipose tissue. A quantitative study of 84 iliac bone biopsies," *Clin. Orthop. Relat Res.*, vol. 80, pp. 147-154, Oct.1971.

[48] P. Ducy, R. Zhang, V. Geoffroy, A. L. Ridall, and G. Karsenty, "Osf2/Cbfa1: a transcriptional activator of osteoblast differentiation," *Cell*, vol. 89, no. 5, pp. 747-754, May1997.

[49] G. S. Stein, J. B. Lian, J. L. Stein, A. J. van Wijnen, and M. Montecino, "Transcriptional control of osteoblast growth and differentiation," *Physiol Rev.*, vol. 76, no. 2, pp. 593-629, Apr.1996.

[50] E. J. Moerman, K. Teng, D. A. Lipschitz, and B. Lecka-Czernik, "Aging activates adipogenic and suppresses osteogenic programs in mesenchymal marrow stroma/stem cells: the role of PPAR-gamma2 transcription factor and TGF-beta/BMP signaling pathways," *Aging Cell*, vol. 3, no. 6, pp. 379-389, Dec.2004.

[51] S. E. Ross, N. Hemati, K. A. Longo, C. N. Bennett, P. C. Lucas, R. L. Erickson, and O. A. MacDougald, "Inhibition of adipogenesis by Wnt signaling," *Science*, vol. 289, no. 5481, pp. 950-953, Aug.2000.

[52] D. A. Lowe, H. Degens, K. D. Chen, and S. E. Alway, "Glyceraldehyde-3-phosphate dehydrogenase varies with age in glycolytic muscles of rats," *J. Gerontol. A Biol. Sci. Med. Sci.*, vol. 55, no. 3, p. B160-B164, Mar.2000.

[53] C. D. Touchberry, M. J. Wacker, S. R. Richmond, S. A. Whitman, and M. P. Godard, "Age-related changes in relative expression of real-time PCR housekeeping genes in human skeletal muscle," *J. Biomol. Tech.*, vol. 17, no. 2, pp. 157-162, Apr.2006.

[54] Y. J. Chen, C. H. Huang, I. C. Lee, Y. T. Lee, M. H. Chen, and T. H. Young, "Effects of cyclic mechanical stretching on the mRNA expression of tendon/ligament-related and osteoblast-specific genes in human mesenchymal stem cells," *Connect. Tissue Res.*, vol. 49, no. 1, pp. 7-14, 2008.

[55] M. Koike, H. Shimokawa, Z. Kanno, K. Ohya, and K. Soma, "Effects of mechanical strain on proliferation and differentiation of bone marrow stromal cell line ST2," *J. Bone Miner. Metab*, vol. 23, no. 3, pp. 219-225, 2005.

[56] R. Puts, P. Rikeit, K. Ruschke, A. Kadow-Romacker, S. Hwang, K. V. Jenderka, P. Knaus, and K. Raum, "Activation of Mechanosensitive Transcription Factors in Murine C2C12 Mesenchymal Precursors by Focused Low-Intensity Pulsed Ultrasound (FLIPUS)," *IEEE Trans. Ultrason. Ferroelectr. Freq. Control*, July2016.

[57] J. Pratap, M. Galindo, S. K. Zaidi, D. Vradii, B. M. Bhat, J. A. Robinson, J. Y. Choi, T. Komori, J. L. Stein, J. B. Lian, G. S. Stein, and A. J. van Wijnen, "Cell growth regulatory role of Runx2 during proliferative expansion of preosteoblasts," *Cancer Res.*, vol. 63, no. 17, pp. 5357-5362, Sept.2003.

[58] M. Galindo, J. Pratap, D. W. Young, H. Hovhannisyan, H. J. Im, J. Y. Choi, J. B. Lian, J. L. Stein, G. S. Stein, and A. J. van Wijnen, "The bone-specific expression of Runx2 oscillates during the cell cycle to support a G1-related antiproliferative function in osteoblasts," *J. Biol. Chem.*, vol. 280, no. 21, pp. 20274-20285, May2005.

[59] M. Stolz, R. Gottardi, R. Raiteri, S. Miot, I. Martin, R. Imer, U. Staufer, A. Raducanu, M. Duggelin, W. Baschong, A. U. Daniels, N. F. Friederich, A. Aszodi, and U. Aebi, "Early detection of aging cartilage and osteoarthritis in mice and patient samples using atomic force microscopy," *Nat. Nanotechnol.*, vol. 4, no. 3, pp. 186-192, Mar.2009.

[60] R. McBeath, D. M. Pirone, C. M. Nelson, K. Bhadriraju, and C. S. Chen, "Cell shape, cytoskeletal tension, and RhoA regulate stem cell lineage commitment," *Dev. Cell*, vol. 6, no. 4, pp. 483-495, Apr.2004.

Chapter 3: TRANSCRIPTIONAL MECHANORESPONSE OF MURINE C2C12 MESENCHYMAL PRECURSORS TO FLIPUS

Reprinted with permission from: Puts, R., Rikeit, P., Ruschke, K., Kadow-Romacker, A., Hwang, S., Jenderka, K.V., Knaus, P., and Raum, K. Activation of Mechanosensitive Transcription Factors in Murine C2C12 Mesenchymal Precursors by Focused Low-Intensity Pulsed Ultrasound (FLIPUS), *IEEE Trans. Ultrason. Ferroelectr. Freq. Control*, vol. 63, no. 10, pp. 1505-1513, Oct.2016.
10.1109/TUFFC.2016.2586972

ABSTRACT

In this study we investigated the mechanoresponse of C2C12 mesenchymal precursor cells to focused low-intensity pulsed ultrasound (FLIPUS). The set-up has been developed for *in-vitro* stimulation of adherent cells in the defocused far-field of the ultrasound propagating through the bottom of the well plate. Twenty-four-well tissue culture plates, carrying the cell monolayers, were incubated in a temperature controlled water tank. The ultrasound was applied at 3.6 MHz frequency, pulsed at 100 Hz repetition frequency with a 27.8 % duty cycle, and calibrated output intensity of $I_{SATA} = 44.5 \pm 7.1$ mW/cm^2. Numerical sound propagation simulations showed no generation of standing waves in the well plate. The response of murine C2C12 cells to FLIPUS was evaluated by measuring activation of mechanosensitive transcription factors, i.e., activator protein 1 (AP-1), specificity protein 1 (Sp1) and transcriptional enhancer factor (TEF or TEAD), and expression of mechanosensitive genes, i.e., c-fos, c-jun, HB-GAM, and Cyr-61. FLIPUS induced 50% ($p \leq 0.05$) and 70% ($p \leq 0.05$) increases in AP-1 and TEAD promoter activities, respectively, when stimulated for 5 minutes. The Sp1 activity was enhanced by about 20 % ($p \leq 0.05$) after 5-min FLIPUS exposure and the trend persisted for 30 min ($p \leq 0.05$) and 1 hour ($p \leq 0.05$) stimulation times. Expressions of mechanosensitive genes c-fos ($p \leq 0.05$), c-jun ($p \leq 0.05$), HB-GAM ($p \leq 0.05$) and Cyr61 ($p \leq 0.05$) was enhanced in response to 5-min FLIPUS stimulation. The increase in proliferation of C2C12s occurred after the FLIPUS stimulation ($p \leq 0.05$), with AP-1, SP1 and TEAD possibly regulating the observed cellular activities.

Key Words: LIPUS; QUS; mechanosensation; transcription factors; bone; soft tissue; regeneration

INTRODUCTION

Numerous studies confirmed the beneficial potential of Low-Intensity Pulsed Ultrasound (LIPUS) in fracture healing [1]. Several *in-vitro* and *in-vivo* reports have shown that LIPUS holds as well promise for regeneration of soft tissues [2] and is in demand due to non-invasiveness and safety of the procedure. Until now, the physico-biological mechanisms dictating these promising effects are only partially understood. The interaction of LIPUS with cells and tissues consists of several physical sub-mechanisms, such as cyclic pressure variation at the frequency of the acoustic wave, cyclic variation of an acoustic radiation force at the pulse repetition frequency, and a quasi-static perfusion induced by acoustic streaming [3]. Planar transducers used in most of the *in-vitro* studies create difficulties in reproducing the stimulation conditions and are prone to unwanted physical artifacts, e.g., standing waves, temperature elevations [4;5]. This limits the successful translation of *in-vitro* findings to further *in-vivo* applications.

In our previous study we have shown that focused transducers used for quantitative ultrasound imaging (QUS) also have a bone tissue-regenerative potential [6]. The focused LIPUS (FLIPUS) system used for our experimental procedures enables spatially controlled deposition of the desired intensity and provides a homogenous stimulation, and thereby limiting the induction of aforementioned artifacts.

Mammalian cells represent highly dynamic structures. The cytoskeleton is playing a critical role in translating extracellular stimuli into intracellular responses. Mechanosensitive receptors, e.g., integrins or cadherins, expressed on the cellular surface, transmit physical signals through the membrane by regulation of cytoskeletal activities and signaling pathways [7;8]. Alterations in cytoskeletal structures can persist after cell division, reprogramming the functioning of its offspring many generations after [9]. As a result, mechanical forces cooperate with biological factors and tightly control the transcriptional activity of cells, thereby defining their fate [10]. Dysfunctions in mechanical homeostasis could result in the disruption of normal tissue architecture and lead to various tissue pathologies, contributing to diseases, e.g., osteoarthritis [11], osteoporosis [12] and cancer [13]. Throughout their life time cells can experience a range of mechanical forces generated by fluidal motion, traction forces due to rigidity sensing of the surrounding matrix, or interactions with other cells, which lead to the activation of a number of transcription factors (TFs), e.g., AP-1, Sp1, TEAD, and others [10].

Activator protein-1 (AP-1) is a family of dimeric TFs, consisting of Fos, Jun and activating transcription factor (ATF) leucine-zipper proteins [14]. AP-1s are activated by

mechanical deformations and promoters of a number of mechanosensitive genes. For example, c-fos, c-jun, and HB-GAM were found to have AP-1 binding sites [15][16].

The DNA-interaction domain of the TF Specificity protein 1 (Sp1) consists of zinc-finger proteins, which bind to GC-rich regions [17] in response to fluid shear stress. Fluid shear stress has been shown to activate expression of VEGF receptor 2 [18] and tissue factor [19], both of which are essential proteins for functioning of endothelial cells through the regulation of Sp1 TF.

Transcriptional enhancer factors (TEF or TEAD) regulate tissue homeostasis and organ size growth [20]. Their activity could be affected through the mechanical tensile stress exerted either on extracellular matrix or on cell-cell contacts [21]. TEADs drive expression of genes associated with cell cycle progression and prevention of apoptosis [22].

The murine C2C12 mesenchymal precursor cell line used in our study possesses pronounced mechanosensitivity [23;24] and represents a convenient *in-vitro* model for the investigation of mechanisms, underlying cellular activities in response to LIPUS mechanical stimuli. The pluripotency of C2C12s, i.e., their ability to differentiate into osteoblasts [25], myoblasts [26], and adipose tissue [27] makes them ideal candidates for both, bone and soft tissue research. Recently, we have reported activation of mechanosensitive factors in C2C12 cells by FLIPUS [28]. In this study, we show additional results on mechanosensitive transcriptional response of C2C12 mesenchymal cells after various FLIPUS stimulation times by means of reporter gene sequences of AP-1, Sp1 [29] and TEAD [30], which were subcloned into a minimal Firefly luciferase promoter. Furthermore, we investigated early biological events after FLIPUS stimulation of C2C12 mesenchymal precursor cells, hypothesizing that the applied FLIPUS dose up-regulates the activities of the mechanosensitive transcription factors AP-1, Sp1, and TEAD, which subsequently induces the expression of mechanosensitive pro-mitogenic genes and results in enhanced proliferation of C2C12s. The experimental study is complemented by a numerical sound propagation evaluation for set-ups with planar and focused transducers.

MATERIALS AND METHODS

A. FLIPUS Cell-Stimulation Set-up

C2C12 cells were seeded in 24-well plates and stimulated by our custom FLIPUS set-up (Fig. 1a) [6]. Briefly, twenty-four well plates with the cells were placed into a sealed, autoclavable chamber 13.3 mm above the focus position of an array of five identical transducers

(center frequency: 5 MHz; 141 diameter: 19 mm; epoxy lens with focus distance at 22.8 mm; 142 epoxy backing; STT Richter, Mühlanger, Germany) in a temperature-controlled water tank. Four transducers were used for stimulation and one was used to calibrate the alignment between transducers and bottom of the well plate. A burst signal created by a function generator (33522A, Agilent Technologies, Santa Clara, CA, USA) was amplified (amplifier: 2100L, Electronics & Innovation, Rochester, NY, USA). The amplified signal was then divided by a 4-way splitter (D5855, Werlatone, Inc. Patterson, NY, USA) and delivered to the four focused stimulation transducers. The air/CO_2 concentration and humidity were maintained by an air mixer (FC-5, Life Cell Instrument, Seoul, Korea). The movement in *x*, *y*, and *z* directions was provided by a motion control system (Model XPS, Newport, Spectra-Physics GmbH, Darmstadt, Germany). The following stimulation conditions were used: frequency: 3.6 MHz; peak-to-peak voltage: 400 mV_{pp}; PRF: 100 Hz; duty cycle: 27.8 %, i.e., 2.78 ms "on" and 7.22 ms "off"). All hardware components were controlled by a custom graphical user interface, developed with MATLAB 2009a (The MathWorks, Natick, MA, USA). A detailed description of the set-up and characterization of the acoustic parameters, summarized in Table I, can be found in [6]. Note that in contrast to that study, for the current experiments the above mentioned amplifier was used. The recalibration revealed that an excitation amplitude of 400 mVpp yielded the same acoustic output levels (see table I) as 500 mVpp with the amplifier used in [6].

Table 1. Acoustic Parameters. *a* is the -6-dB cross-sectional beam area measured directly above the well plate bottom. *p+* is the positive peak pressure, *MI* is the mechanical index [6].

	a [cm²]	p_+ [kPa]	MI	I_{SATP} [mW/cm²]	I_{SATA} [mW/cm²]
T1	0.77	83 ± 14	0.066	231.0	49.2
T2	0.81	82 ± 15	0.058	224.3	36.2
T3	0.80	98 ± 18	0.074	323.5	51.4
T4	0.85	93 ± 17	0.070	288.6	41.2
Mean	**0.81**	**89**	**0.067**	**266.8**	**44.5**
SD	**± 0.03**	**± 16**	**± 0.007**	**± 47.5**	**± 7.1**

FLIPUS stimulation experiments were conducted simultaneously in four wells (Fig. 1b). With the current setup, the transducer array can be moved between 4 positions below the 24-well plate.

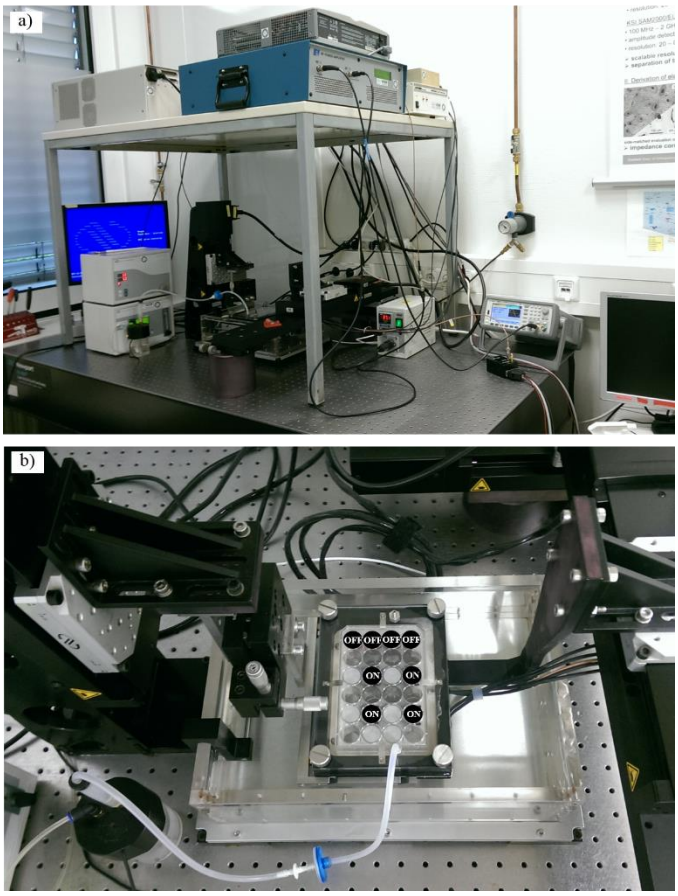

Fig. 1: FLIPUS *in-vitro* cell-stimulation setup (a) and a top view of the 24-well plate placed into an incubation chamber during the FLIPUS stimulation (b). ON and OFF illustrate wells that are simultaneously stimulated, and those that are not reached by the transducer array, respectively.

B. Numerical Simulations of Sound Propagation

Numerical sound propagation simulations through the well-plate were conducted by means of 2D finite-difference time-domain (FDTD) simulations (see supplementary materials of [6]) using the software SimSonic [31]. The model includes a description of the transducer with focusing lens, coupling medium and one well (Fig. 2a) with dimensions and physical properties mimicking the ones used in the experimental setup. The fluids in the stimulation chamber and in the well were assumed to be water (i.e., the bulk modulus, shear modulus, and density are 2.25 GPa, zero and 1000 kg/m^3, respectively). The polystyrene well plate chamber was modeled with bulk modulus, shear modulus, and density of 5.8 GPa, 1.32 GPa and 1050 kg/m^3, respectively. Attenuation values for water and polystyrene were set to 0.002 dB/mm and 0.35

dB/mm, respectively. The simulation box was surrounded by perfectly matched layers to avoid spurious reflections. The simulations were conducted with burst pulses of variable frequency (3.0 – 5.0 MHz) and burst length. A virtual receiver array was placed directly above the well plate bottom. For comparison, Fig. 2b shows the simulations for an unfocused configuration.

C. Cell Culture

Murine C2C12 mesenchymal cells were purchased from ATCC and cultured in expansion media (Dulbecco Modified Eagle's Medium (DMEM), supplemented with 10 % Fetal Calf Serum (FCS), 1 % Penicillin/Streptomycin (Biochrom AG, Berlin, Germany), 2 mM GlutaMax™ (GIBCO, Life Technologies, Darmstadt, Germany) under standard cultivation conditions (37°C, 5 % CO_2, 95 % humidity).

D. Luciferase Reporter Gene Assay

The cells were seeded in 24-well plates at a density of 5×10^4 cells/well in expansion media. Next day the media was changed to DMEM with 5 % FCS, 2 mM GlutaMax™ without antibiotics. One hour later the cells were transfected with AP-1 (5´- ATC TGA CTC AGC ATG CAT GTG ACT CAG CTA - 3´) or Sp1 (5´ - ATC GCG GCG GGG GCG GGC GCC GCA TGC ATG GCG GCG GGG GCG GGC GCC GCT A - 3´) constructs or TEAD-binding sequences (TBS, 14 times GGAATG) reporters by means of Lipofectamine 2000 (Life Technologies, Carlsbad, CA, USA) in 1:2 ratios, respectively. Renilla luciferase constructs (pRL-TK, Promega GmbH, Mannhein, Germany) were co-transfected in cells at 1:5 ratio to the plasmid of interest and used as transfection efficiency controls. Six hours later the medium was changed to one containing 1 % Penicillin/Streptomycin. After 24 hours, the cells were first starved for 3 hours in the expansion medium without FCS in order to eliminate effects of the serum-present growth factors, and then stimulated with FLIPUS for 5 min, 30 min, or 1 h. The cells were lysed with 1x lysis buffer (PJK GmbH, Kleinblittersdorf, Germany) 24 hours later and the activity of the reporters was quantified by addition of Beetle-Juice substrate (PJK GmbH, Kleinblittersdorf, Germany) and measuring Firefly luciferase activity by Mithras LB940, Wildbad, Germany. The activity of Renilla luciferase was measured by Renilla Juice (PJK GmbH, Kleinblittersdorf, Germany). CAGA construct, consisting of twelve CAGA-boxes, cloned into the Firefly luciferase promoter and selectively activated by transforming growth factor-β (TGF-β) proteins and activins [32] was used as mechano-insensitive control. The construct was treated identically to the others. The activity of CAGA-boxes was additionally verified by 1h stimulation of the transfected

C2C12s with 3 ng/mL of porcine TGF-β1. The results of the reporter gene assays should not be affected by changes in cell numbers in response to FLIPUS, since as a result of mitosis, daughter cells produced by the transfected cells do not contain plasmid DNA and therefore cannot interfere with the interpretation of the data.

E. WST-8 Viability Assay

The C2C12s were seeded at density 5×10^4 cells per well. Two days later, the cells were starved for 3 hours in the expansion medium without FCS and stimulated for either 5 min, 30 min, or 1 h with FLIPUS. Right after the stimulation the cells were incubated with Water-soluble Tetrazolium Salt-8 (WST-8) for 1 h at 37 °C according to the manufacturer's protocol (PromoKine GmbH, Heidelberg, Germany). Cell viability was analyzed colorimetrically, i.e., absorbance at a wavelength of 450 nm and a reference wavelength of 600 nm was measured by TECAN infinite, M200 PRO (Maennedorf, Switzerland).

F. Quantification of Gene Expression

The C2C12s were seeded in 24-well plates at a density of 9×10^4 cells/well. Two days later, the cells were starved for 3 hours in the expansion medium without FCS and stimulated for 5 minutes with FLIPUS. Cells were lysed 0 min or 1 h after the stimulation. The mRNA was isolated from cell lysates by NucleoSpin RNA II Kit (Machery Nagel, Düren, Germany). The complementary DNA (cDNA) was transcribed by qScript™ cDNA SuperMix (Quanta Biosciences, Gaithersburg, MD, USA) by means of Mastercycler EP Gradient S (Eppendorf, Hamburg, Germany). The cDNA of the genes of interest was further quantified by Quantitative Real Time Polymerase Chain Reaction (qRT-PCR).

G. qRT-PCR

The gene expression of c-fos, c-jun, HB-Gam and Cyr61 was quantified using PerfeCTa®SYBR®Green SuperMix (Quanta Biosciences, Gaithersburg, USA) with help of LightCycler 480 II (Roche Diagnostics GmbH, Mannheim, Germany). The primers were designed by Primer-BLAST (NCBI) and synthesized by TIB Molbiol (Berlin, Germany). Expression of all target genes was normalized to the expression of house-keeping gene hypoxanthine-guanine phosphoribosyltransferase (HPRT), which accounts for potential changes in cell numbers. The following primers were used: c-fos forward 5´- AATGGTGAAGACCGTGTCAG - 3´ and reverse 5´- CAGCCATCTTATTCCGTTCC - 3´; c-

jun forward 5′– TGTTTGTTTGTTTGGGTGTCC – 3′ and reverse 5′– GAGGTTGGGGGCTACTTTTC – 3′; HB-GAM forward 5′- ACTGGAAGAAGCAGTTTGGA - 3′ and reverse 5′- GCTTGGAGATGGTGACAGTT - 3′; Cyr61 forward 5′- TGCTGTAAGGTCTGCGCTAA - 3′ and reverse 5′- AGGGTCTGCCTTCTGACTGA - 3′; HPRT forward 5′- TGTTGTTGGATATGCCCTTG - 3′ and reverse 5′- ACTGGCAACATCAACAGGACT - 3′. Eukaryotic translation elongation factor 1 α1 (Eef1α1) was used as mechano-insensitive gene control with the following primer sequences: forward 5′- TTGACATCTCCCTGTGGAAA - 3′and reverse 5′- AGCAACAATCAGGACAGCAC - 3′.

H. BrdU-ELISA

In this experiment C2C12 cells were seeded in 24-well plates at 9×10^4 cells/well density in expansion media. Two days later, the cells were starved in 0 % FCS expansion media for 3 h and stimulated for 5 min with FLIPUS. The cells were labeled for 5 hours after the stimulation with BrdU. BrdU-ELISA was performed, as described in the protocol (Roche Diagnostics GmbH, Mannheim, Germany). Cell proliferation was assessed colorimetrically by measuring absorbance at a wavelength of 450 nm and at a reference wavelength of 690 nm on TECAN infinite, M200 PRO (Maennedorf, Switzerland).

I. Statistics

One-way ANOVA followed by *post-hoc* multi-comparison Tukey-Kramer tests were used to evaluate significance of differences in the readout parameters between the groups with help of the MATLAB statistics toolbox (The MathWorks, Natick, MA, USA). All the data were expressed as means and standard deviations. The differences were considered to be significant for *p*-value smaller than 0.05.

RESULTS

A. Numerical Simulation of Sound Propagation

The focused beam provides a smooth transmission of a slightly curved wave front into the well chamber (Fig. 2a). The waves reflected at the upper liquid-air interface do not result in the generation of standing waves, which is the case for the unfocused setup.

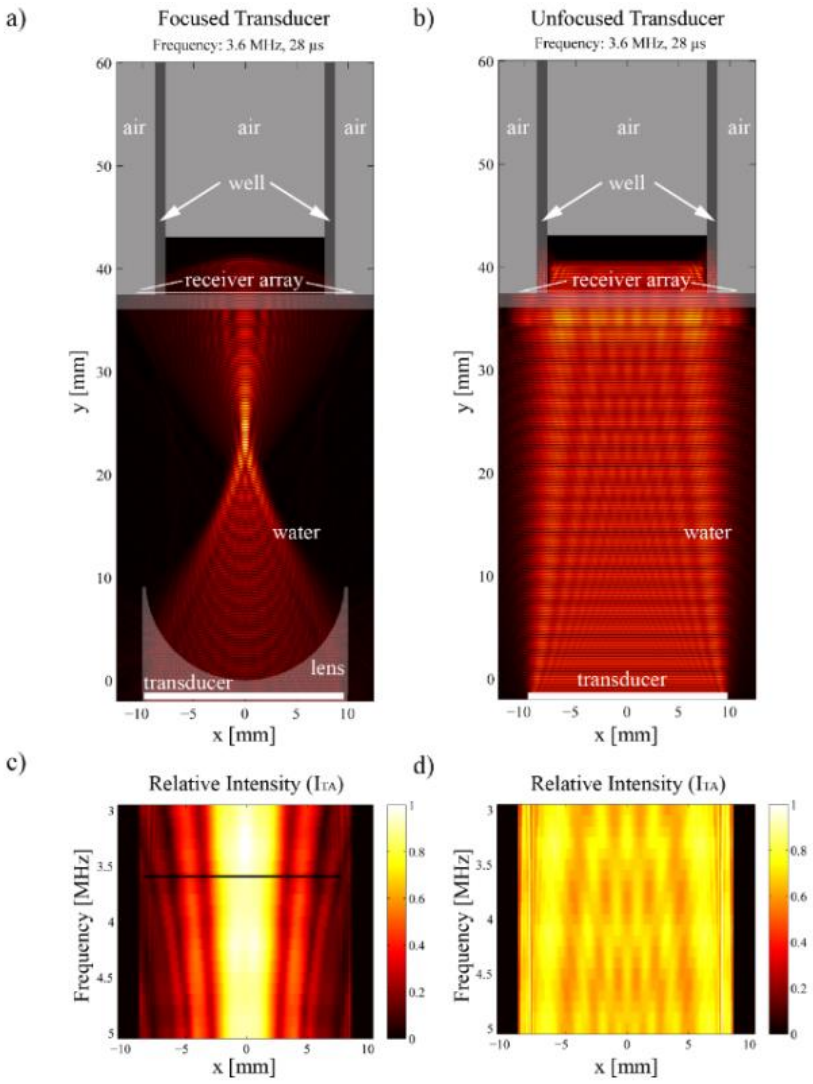

Fig. 2: Sound propagation at 3.6 MHz using a focused (FLIPUS) configuration (a) in comparison to an unfocused (LIPUS) setup (b). For better illustration the snapshot is taken prior to the reflection of the wave front at the upper liquid-air interface. The full animations are provided in the supplementary materials of [6]. The distributions of the temporal average intensity detected by a virtual receiver array directly above the well plate bottom (c-d) exhibit strong variations with respect to lateral position and frequency in the case of the planar transducer (d). For the focused transducer, peaks in the central part of the beam occur at distinct frequencies of 3.3, 3.9, and 4.2 MHz (c). At the frequency used for the stimulation (3.6 MHz, indicated by the black horizontal line), a smooth decrease of the intensity from the center towards the periphery of the well can be seen.

Moreover, much less acoustic energy is coupled into the side walls of the well. The temporally averaged intensity distributions along the virtual receiver array of the focused and unfocused configurations are shown in c) and d), respectively, for frequencies between 3 and 5 MHz. Much less amplitude variation with respect to the excitation frequency are obtained with

the focused beam in comparison with the unfocused beam. For the focused beam, the transmission maxima at the beam axis occur at 3.3, 4.2 and 4.9 MHz. At 3.6 MHz (indicated by the black line in (c)) the lateral intensity profile does not exhibit a strong central peak, providing a more even distribution within the well.

B. Activation of Mechanosensitive Transcription Factors

FLIPUS stimulation for 5 min enhanced the activity of TEAD and AP-1 responsive elements by 70 % and 50 %, respectively (Fig. 3a and 3b). Activation of Sp1 responsive elements was enhanced by 20 % and the increase persisted for 30 min and 1 h stimulation times (Fig. 3c). Interestingly, longer stimulation times (30 min and 1 h) did not result in an enhanced activity of TEAD and AP-1 TFs. Activation of CAGA-boxes, sensitive to TGF-β proteins and activins, was not observed in response to FLIPUS, as it was expected (Fig. 3d).

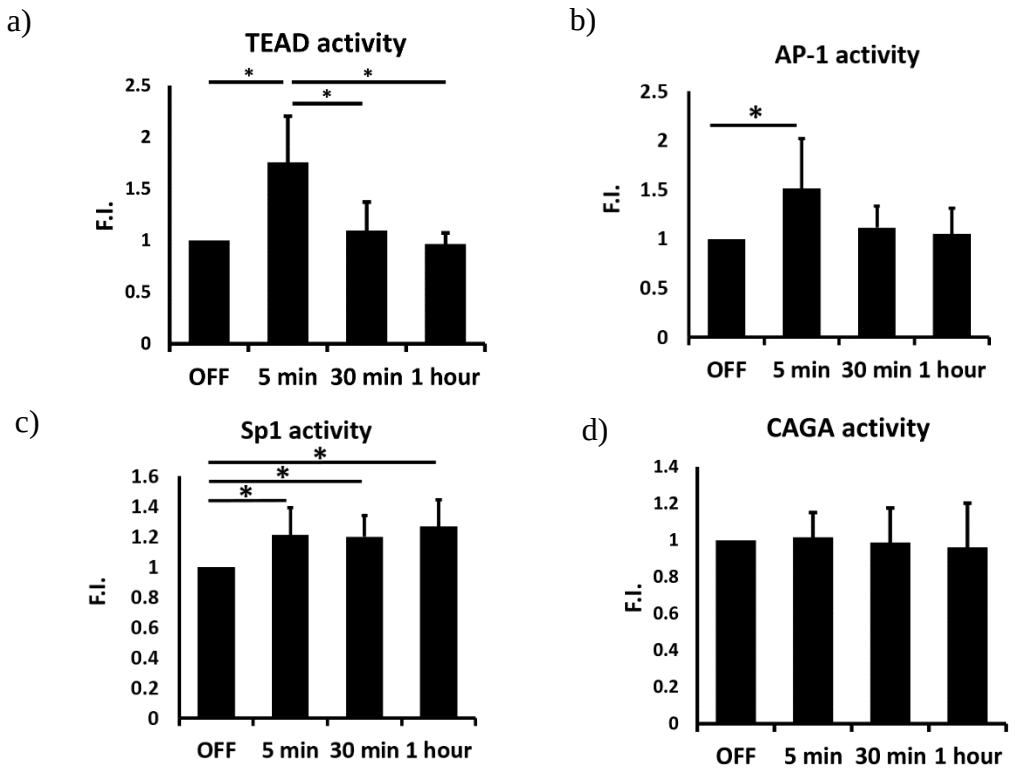

Fig. 3: Activation of TEAD (a), AP-1 (b), Sp1 (c) TFs, and binding to CAGA boxes (d) after FLIPUS-treatment in C2C12 cells. All data are presented as mean ± SD of minimum 5 independent experiments and correspond to fold induction (F.I.) relative to unstimulated controls (OFF). *$p \leq 0.05$.

The activity of CAGA-boxes was measured in response to 3 ng/mL incubation with porcine TGF-β1 (Fig.4) to confirm the functionalty of the construct.

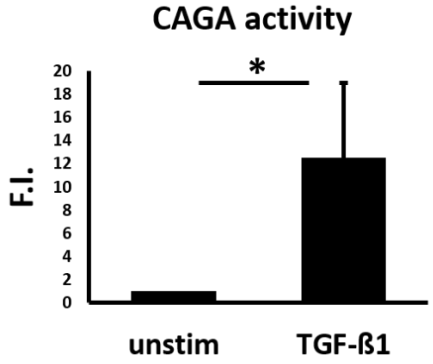

Fig. 4: Activation of CAGA-boxes by 1 h stimulation with porcine TGF-β1. Data are presented as mean ± SD of 3 independent experiments and expressed as fold induction (F.I.) relative to controls not stimulated with the ligand (unstim). *$p \leq 0.05$.

C. FLIPUS Slightly Enhances Cellular Viability

In order to eliminate possibility of negative effects of FLIPUS on cellular viability, a WST-8 assay was performed. Stimulation with FLIPUS improved viability of the cells by approximately 4.6 %, regardless of stimulation time (Fig. 5).

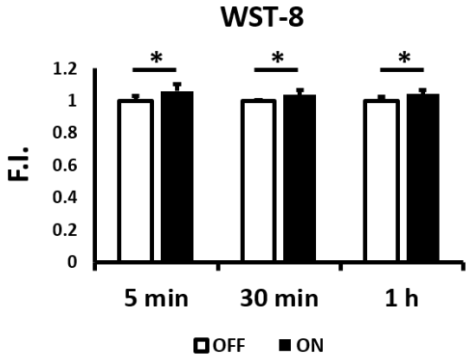

Fig. 5: WST-8 cell viability assay in response to 5 min, 30 min and 1 h FLIPUS stimulation (ON). All data are presented as mean ± SD of 3 independent experiments, each performed in duplicate. The values represent fold induction (F.I.) relative to unstimulated controls (OFF). *$p \leq 0.05$.

D. FLIPUS Affects Expression of Mechanosensitive Genes

A 5-min FLIPUS stimulation increased expressions of c-fos, c-jun, Cyr61 and HB-GAM 1 h after the stimulation, compared to unstimulated controls (Fig. 6). The increase was also statistically significant for Cyr61 and HB-GAM compared to the 0-min post-stimulation time

point. Expression of Eef1α1, which is involved in the process of protein synthesis, remained unchanged after 5-min FLIPUS stimulation at both time points:

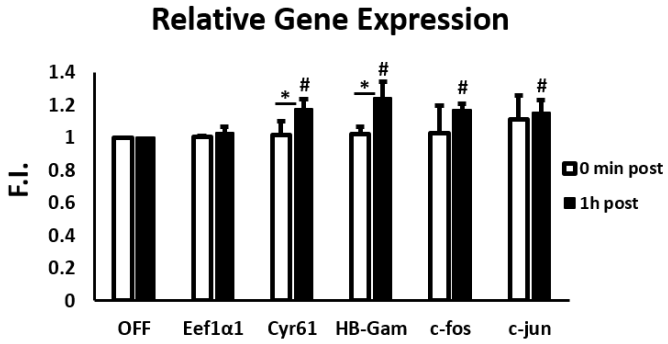

Fig. 6: Expression of mechanosensitive genes in response to 5-min-long FLIPUS stimulation of C2C12 cells. All data are presented as mean ± SD of 3 independent experiments and corresponds to fold induction (F.I.) relative to unstimulated controls (OFF). * and # denote significant differences ($p \leq 0.05$) between post-stimulation time points and in comparison to unstimulated controls, respectively.

E. Pro-proliferative Effect of FLIPUS

FLIPUS, introduced for 5 min, up-regulated proliferation of C2C12s (Fig. 7), which was measured by BrdU incorporation 5 hours after FLIPUS-exposure.

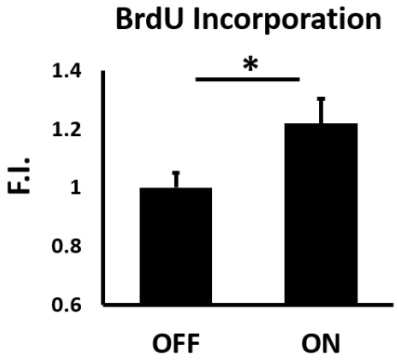

Fig.7: BrdU incorporation in C2C12s, stimulated for 5 min with FLIPUS (ON) and labeled for 5 hours with BrdU. All data are presented as mean ± SD of 4 independent experiments, each performed in duplicate, and correspond to fold induction (F.I.) relative to unstimulated controls (OFF). *$p \leq 0.05$.

DISCUSSION

For about two decades LIPUS has been successfully used in clinics for the non-invasive management of bone defects [33]. More recently, an increasing number of reports also

demonstrate regeneration of other mechanosensitive tissues, e.g., cartilage, muscle, and ligaments by LIPUS stimulation [2]. These promising reports emphasize the need to understand the mechanisms dictating the observed beneficial biological effects. Recently, a number of studies expressed the demand for the development of LIPUS-stimulation set-ups that allow for better control of the applied acoustic intensity and are minimizing the artifacts, which can be introduced by planar transducers, both *in vitro* and in small animal models [4;5;34;35]. In this study, we have stimulated pluripotent murine mesenchymal precursor C2C12 cells in the diverging, defocused far-field of a novel focused LIPUS system, which ensured precise alignment of the cross-sectional ultrasound field area with the area of a well in 24-well plate for either 5 minutes or 30 minutes or 1 hour. The acoustic intensity delivered by this system to the cells has been investigated previously both, experimentally and numerically [6]. The set-up does not elevate temperature in the cell region and does not introduce standing waves. All three stimulation periods with the described here FLIPUS parameters had no negative effect on the viability of C2C12s, as examined by WST-8 assay. This system was then used to investigate LIPUS-induced changes in the activity of mechanosensitive TFs AP-1, Sp1 and TEAD.

Transcription factors AP-1, Sp1 and TEAD can be activated by various stress stimuli, including mechanical forces. They regulate many aspects of cellular behavior, e.g., proliferation, migration, apoptosis, and differentiation [10]. Our data indicate that the acoustic intensity of 44.5 mW/cm^2 introduced by FLIPUS activated all three described mechanosensitive TFs, which in turn up-regulated the proliferation rate of C2C12s.

Very striking is the observation that the activation profile of the analyzed TF was highly dependent on the length of FLIPUS stimulation. Activation of all three TFs was most enhanced after the 5-minute long treatment with FLIPUS. However, longer stimulation times (30 min and 1 h) did not lead to significant activation of AP-1 and TEAD, whereas Sp1 was activated similarly throughout all three stimulation periods. It could be hypothesized that prolonged stimulation with ultrasound activates other, so far unknown signaling pathways, which oppose the observed effects of the mechanical stimulation on AP-1 and TEAD. This hypothesis is consistent with the observation summarized in the review of Chaqour and Goppelt-Struebe [36], in which they described that expression of TEAD target genes Cyr61 and CTGF, activated by mechanical stimulation, declined back to their basal levels when the mechanical deformation of cells persisted for longer times. This suggests that cells can adapt to certain stresses by turning on negative feedback loop mechanisms in order to maintain the homeostasis of the living system. On the other hand, Sp1 activation was not affected by the length of stimulation in our study, which

emphasizes the complexity of biological responses to physical sub-mechanisms introduced by LIPUS. Sp1 has been explicitly shown to be activated by shear stress [18;19;37], whereas AP-1 [38;39] and TEAD [40;41] have been reported to be more sensitive to mechanical strain.

By performing genome-wide analyses, Zanconato *et al.* [42] established that binding of AP-1 TF overlaps with most of the TEAD binding sites, forming a transcriptional complex with TEAD and synergizing at gene transcription. Similar results were reported by Stein *et al.* [43], who concluded that AP-1 might be a cooperative co-factor of TEAD. This could also partially explain similar activation patterns of AP-1 and TEAD TFs. FLIPUS might activate the described here mechanosensitive TFs, which in turn synergistically regulate cellular activities.

To ensure that 5-min long LIPUS stimulation leads to activation of the mechanosensitive response on the transcriptional level, expressions of several mechanosensitive genes, i.e., c-fos, c-jun, HB-GAM and Cyr61 were verified. Heparin binding growth associated molecule (HB-GAM) is a mechanosensitive gene, known to play role in proliferation and differentiation of bone cells [44]. c-fos and c-jun are early-response genes, which comprise functional subunits of AP-1 TF [15]. The AP-1 complex regulates genes associated with cell cycle and survival [45]. The abolished expression of c-fos in mice results in bone pathologies [46] and expression of osteocalcin gene is decreased by binding of Fos-Jun proteins to its promoter in proliferating osteoblasts [47]. The functioning of cystein-rich protein 61 (Cyr61), another early response gene [48], is mediated by mechanical stimuli, i.e., shear stress and stretching [36]. Cyr61 is known to be pro-angiogenic [49] and pro-mitogenic [50] and both, Sp1 [51] and TEAD [52] TFs can regulate Cyr61 expression. Our data indicate that expression of all four genes was up-regulated after the FLIPUS treatment, whereas expression of translational elongation factor Eef1α1 remained unaffected by mechanostimulation.

It had been shown that myogenic differentiation of C2C12 cells is inhibited, when the activity of AP-1 and Sp1 TFs is elevated, whereas proliferative potential of the cells is enhanced [53]. Thus, the observed increase in Sp1 and AP-1 binding activity after FLIPUS treatment might imply that ultrasound delays the myogenic differentiation of C2C12s, promoting other cellular functions, e.g., proliferation or, eventually, osteogenic differentiation of cells, which ultimately could result in tissue growth or enhanced osteogenesis, leading to improved tissue regeneration. The former process was verified by BrdU-incorporation assay and led to the conclusion that FLIPUS enhances proliferation of C2C12s. The study of Ikeda *et al.* [54] showed that application of LIPUS alone could redirect C2C12 cells into an osteogenic lineage. It is important to note that in this study 70 mW/cm^2 intensity was used and the set-up itself (transducer from the top) could

have amplified the signal due to the encountered reflective interfaces. Therefore, the findings obtained in that study should be confirmed with our setup. We are not excluding the possibility of osteogenic effects of FLIPUS in C2C12s at later time points and this should be verified in a separate study.

Future studies should investigate, how different intensity levels can regulate the activity of these factors. This is easily achievable with our FLIPUS set-up. Our data suggest that the use of FLIPUS is not only limited to *in-vitro* investigations of bone healing potential, but can also be used for mechanistic studies of soft tissue regeneration. Particularly, it is known that avascular soft-tissues, like articular cartilage, intervertebral disks, ligaments and tendons have very limited regeneration capacities, which could result in impaired healing and permanent disabilities. The FLIPUS-stimulation conditions described here were previously found to provide well-controlled *in-vitro* cell-stimulation and demonstrated to elicit cellular responses in rat mesenchymal stem cells [6] and in cardiac mesoangioblasts isolated from mouse and human ventricle explants [55]. Although frequency, pulse repetition frequency (PRF), and acoustic intensity deviate from the most common LIPUS protocol using unfocused transducers, i.e., 1.5 MHz frequency, 1 kHz PRF at 20 % duty cycle and I_{SATA} = 30 mW/cm^2, they are within the range of other published LIPUS studies [54;56-58]. Therefore, the reported findings obtained with our FLIPUS setup represent an initial study of a larger research direction, aimimg at the examination of regenerative biological mechanisms by FLIPUS stimulation in primary cells isolated from mechanosensitive tissues. Moreover, FLIPUS holds a great promise for local *in-vivo* applications [59],[60], as subsurface repair regions can easily be reached by ultrasound, the size of the stimulated area can be adjusted (down to less than 1 mm cross-sectional diameter in the focal plane), and the applied acoustic intensity can be well controlled.

ACKNOWLEDGEMENTS

The study was funded by the German Research Foundation (Deutsche Forschungsgemeinschaft, DFG) grant Ra1380/8-1. P.K. was supported by the DFG grant FOR2165. The authors thank the laboratory of Franz Jakob, especially Regina Ebert and Sigrid Müller-Deubert, from Würzburg University, Germany for providing AP-1 and Sp1 mechanosensitive constructs and Fernando Camargo from Boston's Children Hospital, Harvard

University for TBS gene reporter. Porcine TGF-β1 was a kind gift of Alf Hamann from German Rheumatism Research Center Berlin.

REFERENCES

[1] Pounder, N. M. and Harrison, A. J., "Low intensity pulsed ultrasound for fracture healing: a review of the clinical evidence and the associated biological mechanism of action," *Ultrasonics*, vol. 48, no. 4, pp. 330-338, 2008.

[2] Khanna, A., Nelmes, R. T., Gougoulias, N., Maffulli, N., and Gray, J., The effects of LIPUS on soft-tissue healing: a review of literature," *Br.Med.Bull.*, vol. 89 pp. 169-182, 2009.

[3] Padilla, F., Puts, R., Vico, L., Guignandon, A., and Raum, K., "Stimulation of Bone Repair with Ultrasound," *Adv.Exp.Med.Biol.*, vol. 880 pp. 385-427, 2016.

[4] Leskinen, J. J. and Hynynen, K., "Study of factors affecting the magnitude and nature of ultrasound exposure with in vitro set-ups," *Ultrasound Med.Biol.*, vol. 38, no. 5, pp. 777-794, 2012.

[5] Leskinen, J. J., Olkku, A., Mahonen, A., and Hynynen, K., "Nonuniform temperature rise in in vitro osteoblast ultrasound exposures with associated bioeffect," *IEEE Trans.Biomed.Eng*, vol. 61, no. 3, pp. 920-927, 2014.

[6] Puts, R., Ruschke, K., Ambrosi, T. H., Kadow-Romacker, A., Knaus, P., Jenderka, K. V., and Raum, K., "A Focused Low-Intensity Pulsed Ultrasound (FLIPUS) System for Cell Stimulation: Physical and Biological Proof of Principle," *IEEE Trans.Ultrason.Ferroelectr.Freq. Control*, vol. 63, no. 1, pp. 91-100, 2016.

[7] Iqbal, J. and Zaidi, M., "Molecular regulation of mechanotransduction," *Biochem.Biophys.Res.Commun.*, vol. 328, no. 3, pp. 751-755, 2005.

[8] Liedert, A., Kaspar, D., Blakytny, R., Claes, L., and Ignatius, A., "Signal transduction pathways involved in mechanotransduction in bone cells," *Biochem.Biophys. Res.Commun.*, vol. 349, no. 1, pp. 1-5, 2006.

[9] Fletcher, D. A. and Mullins, R. D., "Cell mechanics and the cytoskeleton," *Nature*, vol. 463, no. 7280, pp. 485-492, 2010.

[10] Mammoto, A., Mammoto, T., and Ingber, D. E., "Mechanosensitive mechanisms in transcriptional regulation," *J.Cell Sci.*, vol. 125, no. Pt 13, pp. 3061-3073, 2012.

[11] Agarwal, S., Deschner, J., Long, P., Verma, A., Hofman, C., Evans, C. H., and Piesco, N., "Role of NF-kappaB transcription factors in antiinflammatory and proinflammatory actions of mechanical signals," *Arthritis Rheum.*, vol. 50, no. 11, pp. 3541-3548, 2004.

[12] Gass, M. and Dawson-Hughes, B., "Preventing osteoporosis-related fractures: an overview," *Am.J.Med.*, vol. 119, no. 4 Suppl 1, pp. S3-S11, 2006.

[13] Suresh, S., "Biomechanics and biophysics of cancer cells," *Acta Biomater.*, vol. 3, no. 4, pp. 413-438, 2007.

[14] Karin, M., Liu, Z., and Zandi, E., "AP-1 function and regulation," *Curr.Opin.Cell Biol.*, vol. 9, no. 2, pp. 240-246, 1997.

[15] Karin, M., "The regulation of AP-1 activity by mitogen-activated protein kinases," *J.Biol.Chem.*, vol. 270, no. 28, pp. 16483-16486, 1995.

[16] Liedert, A., Kassem, M., Claes, L., and Ignatius, A., "Mechanosensitive promoter region in the human HB-GAM gene," *Biochem.Biophys.Res.Commun.*, vol. 387, no. 2, pp. 289-293, 2009.

[17] Suske, G., "The Sp-family of transcription factors," *Gene*, vol. 238, no. 2, pp. 291-300, 1999.

[18] Urbich, C., Stein, M., Reisinger, K., Kaufmann, R., Dimmeler, S., and Gille, J., "Fluid shear stress-induced transcriptional activation of the vascular endothelial growth factor receptor-2 gene requires Sp1-dependent DNA binding," *FEBS Lett.*, vol. 535, no. 1-3, pp. 87-93, 2003.

[19] Lin, M. C., Almus-Jacobs, F., Chen, H. H., Parry, G. C., Mackman, N., Shyy, J. Y., and Chien, S., "Shear stress induction of the tissue factor gene," *J.Clin.Invest*, vol. 99, no. 4, pp. 737-744, 1997.

[20] Zhao, B., Tumaneng, K., and Guan, K. L., "The Hippo pathway in organ size control, tissue regeneration and stem cell self-renewal," *Nat.Cell Biol.*, vol. 13, no. 8, pp. 877-883, 2011.

[21] Low, B. C., Pan, C. Q., Shivashankar, G. V., Bershadsky, A., Sudol, M., and Sheetz, M., "YAP/TAZ as mechanosensors and mechanotransducers in regulating organ size and tumor growth," *FEBS Lett.*, vol. 588, no. 16, pp. 2663-2670, 2014.

[22] Ota, M. and Sasaki, H., "Mammalian Tead proteins regulate cell proliferation and contact inhibition as transcriptional mediators of Hippo signaling," *Development*, vol. 135, no. 24, pp. 4059-4069, 2008.

[23] Sbrana, F., Sassoli, C., Meacci, E., Nosi, D., Squecco, R., Paternostro, F., Tiribilli, B., Zecchi-Orlandini, S., Francini, F., and Formigli, L., "Role for stress fiber contraction in surface tension development and stretch-activated channel regulation in C2C12 myoblasts," *Am.J.Physiol Cell Physiol*, vol. 295, no. 1, pp. C160-C172, 2008.

[24] Wedhas, N., Klamut, H. J., Dogra, C., Srivastava, A. K., Mohan, S., and Kumar, A., "Inhibition of mechanosensitive cation channels inhibits myogenic differentiation by suppressing the expression of myogenic regulatory factors and caspase-3 activity," *FASEB J.*, vol. 19, no. 14, pp. 1986-1997, 2005.

[25] Burattini, S., Ferri, P., Battistelli, M., Curci, R., Luchetti, F., and Falcieri, E., "C2C12 murine myoblasts as a model of skeletal muscle development: morpho-functional characterization," *Eur.J.Histochem.*, vol. 48, no. 3, pp. 223-233, 2004.

[26] Yaffe, D. and Saxel, O., "Serial passaging and differentiation of myogenic cells isolated from dystrophic mouse muscle," *Nature*, vol. 270, no. 5639, pp. 725-727, 1977.

[27] Fux, C., Mitta, B., Kramer, B. P., and Fussenegger, M., "Dual-regulated expression of C/EBP-alpha and BMP-2 enables differential differentiation of C2C12 cells into adipocytes and osteoblasts," *Nucleic Acids Res.*, vol. 32, no. 1, pp. e1, 2004.

[28] Puts, R., Rikeit, P., Ruschke, K., Kadow-Romacker, A., Hwang, S., Jenderka, K.-V., Knaus, P., and Raum, K. Activation of Mechanosensitive Transcription Factors in Murine C2C12 Myoblasts by Focused Low-Intensity Pulsed Ultrasound (FLIPUS). 1-4. 2015. Ultrasonics Symposium (IUS), 2015 IEEE International.

[29] Seefried, L., Mueller-Deubert, S., Schwarz, T., Lind, T., Mentrup, B., Kober, M., Docheva, D., Liedert, A., Kassem, M., Ignatius, A., Schieker, M., Claes, L., Wilke, W., Jakob, F., and Ebert, R., "A small scale cell culture system to analyze mechanobiology using reporter gene constructs and polyurethane dishes," *Eur.Cell Mater.*, vol. 20 pp. 344-355, 2010.

[30] Schlegelmilch, K., Mohseni, M., Kirak, O., Pruszak, J., Rodriguez, J. R., Zhou, D., Kreger, B. T., Vasioukhin, V., Avruch, J., Brummelkamp, T. R., and Camargo, F. D., "Yap1 acts downstream of alpha-catenin to control epidermal proliferation," *Cell*, vol. 144, no. 5, pp. 782-795, 2011.

[31] Bossy, E., Talmant, M., and Laugier, P., "Effect of bone cortical thickness on velocity measurements using ultrasonic axial transmission: a 2D simulation study," *J.Acoust.Soc.Am.*, vol. 112, no. 1, pp. 297-307, 2002.

[32] Dennler, S., Itoh, S., Vivien, D., ten, D. P., Huet, S., and Gauthier, J. M., "Direct binding of Smad3 and Smad4 to critical TGF beta-inducible elements in the promoter of human plasminogen activator inhibitor-type 1 gene," *EMBO J.*, vol. 17, no. 11, pp. 3091-3100, 1998.

[33] Romano, C. L., Romano, D., and Logoluso, N., "Low-intensity pulsed ultrasound for the treatment of bone delayed union or nonunion: a review," *Ultrasound Med.Biol.*, vol. 35, no. 4, pp. 529-536, 2009.

[34] Hensel, K., Mienkina, M. P., and Schmitz, G., "Analysis of ultrasound fields in cell culture wells for in vitro ultrasound therapy experiments," *Ultrasound Med.Biol.*, vol. 37, no. 12, pp. 2105-2115, 2011.

[35] Padilla, F., Puts, R., Vico, L., and Raum, K., "Stimulation of bone repair with ultrasound: a review of the possible mechanic effects," *Ultrasonics*, vol. 54, no. 5, pp. 1125-1145, 2014.

[36] Chaqour, B. and Goppelt-Struebe, M., "Mechanical regulation of the Cyr61/CCN1 and CTGF/CCN2 proteins," *FEBS J.*, vol. 273, no. 16, pp. 3639-3649, 2006.

[37] Yun, S., Dardik, A., Haga, M., Yamashita, A., Yamaguchi, S., Koh, Y., Madri, J. A., and Sumpio, B. E., "Transcription factor Sp1 phosphorylation induced by shear stress inhibits membrane type 1-matrix metalloproteinase expression in endothelium," *J.Biol.Chem.*, vol. 277, no. 38, pp. 34808-34814, 2002.

[38] Peverali, F. A., Basdra, E. K., and Papavassiliou, A. G., "Stretch-mediated activation of selective MAPK subtypes and potentiation of AP-1 binding in human osteoblastic cells," *Mol.Med.*, vol. 7, no. 1, pp. 68-78, 2001.

[39] Haasper, C., Jagodzinski, M., Drescher, M., Meller, R., Wehmeier, M., Krettek, C., and Hesse, E., "Cyclic strain induces FosB and initiates osteogenic differentiation of mesenchymal cells," *Exp.Toxicol.Pathol.*, vol. 59, no. 6, pp. 355-363, 2008.

[40] Maller, O., DuFort, C. C., and Weaver, V. M., "YAP forces fibroblasts to feel the tension," *Nat.Cell Biol.*, vol. 15, no. 6, pp. 570-572, 2013.

[41] Halder, G., Dupont, S., and Piccolo, S., "Transduction of mechanical and cytoskeletal cues by YAP and TAZ," *Nat.Rev.Mol.Cell Biol.*, vol. 13, no. 9, pp. 591-600, 2012.

[42] Zanconato, F., Forcato, M., Battilana, G., Azzolin, L., Quaranta, E., Bodega, B., Rosato, A., Bicciato, S., Cordenonsi, M., and Piccolo, S., "Genome-wide association between YAP/TAZ/TEAD and AP-1 at enhancers drives oncogenic growth," *Nat.Cell Biol.*, vol. 17, no. 9, pp. 1218-1227, 2015.

[43] Stein, C., Bardet, A. F., Roma, G., Bergling, S., Clay, I., Ruchti, A., Agarinis, C., Schmelzle, T., Bouwmeester, T., Schubeler, D., and Bauer, A., "YAP1 Exerts Its Transcriptional Control via TEAD-Mediated Activation of Enhancers," *PLoS.Genet.*, vol. 11, no. 8, pp. e1005465, 2015.

[44] Liedert, A., Augat, P., Ignatius, A., Hausser, H. J., and Claes, L., "Mechanical regulation of HB-GAM expression in bone cells," *Biochem.Biophys.Res.Commun.*, vol. 319, no. 3, pp. 951-958, 2004.

[45] Shaulian, E. and Karin, M., "AP-1 in cell proliferation and survival," *Oncogene*, vol. 20, no. 19, pp. 2390-2400, 2001.

[46] Wang, Z. Q., Ovitt, C., Grigoriadis, A. E., Mohle-Steinlein, U., Ruther, U., and Wagner, E. F., "Bone and haematopoietic defects in mice lacking c-fos," *Nature*, vol. 360, no. 6406, pp. 741-745, 1992.

[47] Owen, T. A., Bortell, R., Yocum, S. A., Smock, S. L., Zhang, M., Abate, C., Shalhoub, V., Aronin, N., Wright, K. L., van Wijnen, A. J., and ., "Coordinate occupancy of AP-1 sites in the vitamin D-responsive and CCAAT box elements by Fos-Jun in the osteocalcin gene: model for phenotype suppression of transcription," *Proc.Natl.Acad.Sci.U.S.A*, vol. 87, no. 24, pp. 9990-9994, 1990.

[48] Latinkic, B. V., O'Brien, T. P., and Lau, L. F., "Promoter function and structure of the growth factor-inducible immediate early gene cyr61," *Nucleic Acids Res.*, vol. 19, no. 12, pp. 3261-3267, 1991.

[49] Lau, L. F. and Lam, S. C., "The CCN family of angiogenic regulators: the integrin connection," *Exp.Cell Res.*, vol. 248, no. 1, pp. 44-57, 1999.

[50] Kireeva, M. L., MO, F. E., Yang, G. P., and Lau, L. F., "Cyr61, a product of a growth factor-inducible immediate-early gene, promotes cell proliferation, migration, and adhesion," *Mol.Cell Biol.*, vol. 16, no. 4, pp. 1326-1334, 1996.

[51] Schutze, N., Rucker, N., Muller, J., Adamski, J., and Jakob, F., "5' flanking sequence of the human immediate early responsive gene ccn1 (cyr61) and mapping of polymorphic CA repeat sequence motifs in the human ccn1 (cyr61) locus," *Mol.Pathol.*, vol. 54, no. 3, pp. 170-175, 2001.

[52] Zhang, H., Pasolli, H. A., and Fuchs, E., "Yes-associated protein (YAP) transcriptional coactivator functions in balancing growth and differentiation in skin," *Proc.Natl.Acad.Sci.U.S.A*, vol. 108, no. 6, pp. 2270-2275, 2011.

[53] Lehtinen, S. K., Rahkila, P., Helenius, M., Korhonen, P., and Salminen, A., "Down-regulation of transcription factors AP-1, Sp-1, and NF-kappa B precedes myocyte differentiation," *Biochem.Biophys.Res.Commun.*, vol. 229, no. 1, pp. 36-43, 1996.

[54] Ikeda, K., Takayama, T., Suzuki, N., Shimada, K., Otsuka, K., and Ito, K., "Effects of low-intensity pulsed ultrasound on the differentiation of C2C12 cells," *Life Sci.*, vol. 79, no. 20, pp. 1936-1943, 2006.

[55] Bernal, A., Perez, L. M., De, L. B., Martin, N. S., Kadow-Romacker, A., Plaza, G., Raum, K., and Galvez, B. G., "Low-Intensity Pulsed Ultrasound Improves the Functional Properties of Cardiac Mesoangioblasts," *Stem Cell Rev.*, 2015.

[56] Fu, S. C., Shum, W. T., Hung, L. K., Wong, M. W., Qin, L., and Chan, K. M., "Low-intensity pulsed ultrasound on tendon healing: a study of the effect of treatment duration and treatment initiation," *Am.J.Sports Med.*, vol. 36, no. 9, pp. 1742-1749, 2008.

[57] Marvel, S., Okrasinski, S., Bernacki, S. H., Loboa, E., and Dayton, P. A., "The development and validation of a LIPUS system with preliminary observations of ultrasonic effects on human adult stem cells," *IEEE Trans.Ultrason.Ferroelectr.Freq.Control*, vol. 57, no. 9, pp. 1977-1984, 2010.

[58] Katiyar, A., Duncan, R. L., and Sarkar, K., "Ultrasound stimulation increases proliferation of MC3T3-E1 preosteoblast-like cells," *J.Ther.Ultrasound*, vol. 2 pp. 1, 2014.

[59] Rohrbach, D., Preininger, B., Hesse, B., Gerigk, H., Perka, C., and Raum, K., "The early phases of bone healing can be differentiated in a rat osteotomy model by focused transverse-transmission ultrasound," *Ultrasound Med.Biol.*, vol. 39, no. 9, pp. 1642-1653, 2013.

[60] Jung, Y. J., Kim, R., Ham, H. J., Park, S. I., Lee, M. Y., Kim, J., Hwang, J., Park, M. S., Yoo, S. S., Maeng, L. S., Chang, W., and Chung, Y. A., "Focused low-intensity pulsed ultrasound enhances bone regeneration in rat calvarial bone defect through enhancement of cell proliferation," *Ultrasound In Medicine And Biology*, vol. 41, no. 4, pp. 999-1007, 2015.

Chapter 4: THE ROLE OF YAP IN THE MECHANISM OF MECHANOTRANSDUCTION IN RESPONSE TO FLIPUS IN C2C12 CELLS

Puts, R., Rikeit, P., Ruschke, K., Knaus, P., and Raum, K. Focused Low-Intensity Pulsed Ultrasound (FLIPUS) Enhances Proliferation of Murine C2C12 Mesenchymal Precursor Cells through Activation of YAP Mechanosensitive Protein (in preparation).

ABSTRACT

The mechanotransduction potential of Yes-associated protein (YAP) in the cellular fate of murine C2C12 mesenchymal precursors was investigated after stimulation with Focused Low-Intensity Pulsed Ultrasound (FLIPUS). The signal was supplied at 3.6 MHz frequency, 100 Hz pulse repetition frequency (PRF) delivered at 20 % duty cycle (DC), and 44.5 mW/cm^2 acoustic intensity (I_{SATA}). C2C12s were stimulated for 5 minutes with ultrasound and early cellular events were evaluated. FLIPUS decreased phospho-YAP(Ser127) to total YAP ratio, releasing and translocating higher quantities of the active YAP into the nucleus. This in turn enhanced the expression of YAP-target genes, associated with actin nucleation and stabilization, cytokinesis, and cell cycle progression. FLIPUS enhanced proliferation of C2C12s and silencing the YAP expression abolished the beneficial effects of ultrasound. The expression of the transcription factor MyoD, defining myogenic differentiation, was inhibited by mechanical stimulation. Further investigation of the FLIPUS-mediated mechanotransduction mechanism upstream of YAP is underway.

Key Words: LIPUS, YAP, mechanotransduction, proliferation

INTRODUCTION

Proper functioning of organ-forming tissues, during both embryonic and adult-development, significantly relies on the cells' mechanical environment defining their fate along with biochemical cues. The differentiation potential of Mesenchymal Stem Cells (MSCs) can be directed into various tissues solely by alteration of the substrate stiffness [1], tumor growth and progression decelerates with softening of the microenvironment [2] and cellular proliferation can be enhanced with the stiffening of the carrier matrix [3]. Normal tissue homeostasis highly depends on the mechanical forces exhibited by the cells [4]. However, the mechanisms relaying conversion of the mechanical signals experienced by the cell into a biochemical outcome, namely, the mechanotransduction signaling pathways, currently remain unclear. The discovery of the mechanosensitive properties of protein YAP and its structural homologue TAZ has shed some light on the mechanistic events directing cellular commitment in response to mechanical stimuli [3;5].

YAP, or Yes-associated protein, was originally isolated bound to Yes-protein-tyrosine kinase [6] and later found to be a critical mediator of the Hippo signaling pathway, controlling organ homeostasis and tissue regeneration [7]. If the Hippo cascade is inactive, then YAP, which lacks DNA-binding domains, enters the nucleus and binds a number of transcription factors with TEAD being one of the most wide-spread partners [8-10], thereby regulating cellular proliferation, apoptosis, differentiation, migration, etc.

The functioning of YAP was originally found to be regulated by contact inhibition of proliferation (CIP), when the study of Dupont *et al.* [3] elegantly demonstrated that the mechanism of mechanotransduction of YAP is dependent on cell geometry: cells, able to spread over large area had YAP in their nuclei, whereas the confined cellular morphology retained YAP in the cytoplasm. This was later supported by a study of Aragona *et al.* [5], who reported that epithelial cells, grown densely and stretched on a monolayer stretching device, had YAP translocated in the nucleus and proliferated faster, in comparison to the static controls.

Cellular morphology is dictated by the functioning of cytoskeleton, namely, through the dynamics of contractile actomyosin filaments [11]. A direct link has been established between YAP functioning and the formation of actin stress fibers. Thick F-actin fibers modulate the nuclear transportation of YAP, whereas actin and myosin disrupting drugs, latrunculin A and blebbistatin, respectively, ablate YAP activity [12]. Inhibition of actin capping proteins, such as Cofilin, Gelosin, and CapZ, leads to F-actin bundle formation, thus, increasing YAP activity [5].

Treatment of cells with the actin polymerizing drug jasplakinolide drives YAP into the nucleus [13].

Throughout its life a cell can experience a range of mechanical stimuli: compression, tension, hydrostatic pressure, shear force, etc., each influencing its fate [14]. Low-Intensity Pulsed Ultrasound (LIPUS) represents a mechanical technique, eliciting complex physical phenomena, which is used in clinic for bone healing [15] and holds a potential for regeneration of soft tissues [16]. The mechanisms leading to the observed regenerative effects still remain contentious [17]. The focused LIPUS (FLIPUS) used in our experiments represents a well-characterized *in-vitro* set-up, enabling quantification of the mechanical dose by minimizing the introduced physical artifacts, i.e., standing waves, temperature elevations, and near-field interferences [18], usually associated with *in-vitro* devices employing planar transducers [17]. We have previously demonstrated that FLIPUS generates mechanotranscriptional response in murine C2C12 mesenchymal precursors through the activation of AP-1, Sp1, and TEAD transcription factors [19]. Due to the tight connection between the functioning of the TEAD and YAP transcriptional co-activator, in the current study we investigated whether YAP is the link transducing the FLIPUS mechanical signal into the nucleus and regulating the proliferation of C2C12s in response to the spatial average temporal average intensity I_{SATA} = 44.5 mW/cm^2.

MATERIALS AND METHODS

A. FLIPUS in-vitro Cell Stimulation Set-up

The FLIPUS cell-stimulation set-up was calibrated and previously described elsewhere [18]. Briefly, the set-up consists of an array of four focused transducers positioned at the bottom of a temperature-controlled (37 °C) water tank, which is filled with deionized degassed water. The 24-well-plate, carrying C2C12 cell-monolayers, was submerged in the water above the transducer array, so that the diverging defocused far-field of each of the four probes overlapped with the area of a well. The set-up enabled homogenous intensity distribution within the well. No temperature changes were detected directly above the bottom of the well and no standing waves were observed. The cells in the chamber were supplied with 5 % CO_2 and 95 % air mixture. In our experimental set-up C2C12s were seeded at $9*10^4$ cells/mL density (if not mentioned otherwise) in order to maintain a circular cellular morphology. Forty eight hours later the cells were starved for 3 h in the expansion media (see below) without fetal calf serum (FCS) and stimulated for 5 min with FLIPUS. The FLIPUS signal consisted of 3.6 MHz frequency,

100 Hz pulse repetition frequency (PRF), 20 % duty cycle (DC) and spatial average temporal average intensity I_{SATA} = 44.5 mW/cm^2.

B. Cell Culturing

Murine C2C12 mesenchymal precursors were obtained from ATCC. The cells were expanded in Dulbecco Modified Eagle's Medium (DMEM), supplemented with 10 % FCS, 1 % Penicillin/Streptomycin (Biochrom AG, Berlin, Germany), 2 mM GlutaMaxTM (GIBCO, Life Technologies, Darmstadt, Germany) under standard cultivation conditions (37°C, 5 % CO2, 95 % humidity).

C. *Western Blotting*

The cells were lysed 0 h, 1 h, 2 h, 3 h, 4 h and 5 h after the sonication with 2X Laemmli Sample Buffer. Each individual time point had its own negative control, which did not receive FLIPUS exposure. The cell lysates were separated on 12.5 % polyacrylamide gels and transferred for 2 h to a nitrocellulose membrane with 0.45 µm pore-size (neoLab Migge GmbH, Heidelberg, Germany). The membranes were blocked in TBST buffer (TBS buffer with 0.1 % Tween-20 (Sigma-Aldrich, Munich, Germany)) at pH 8, containing 3 % Bovine Serum Albumin (BSA) (Carl Roth GmbH + Co. KG, Karlsruhe, Germany) for 1 h at room temperature. Then the membranes were incubated overnight at 4 °C in either rabbit phospho-YAP(Ser127) (Cell Signaling Technology, Inc., Danvers, MA, USA) or rabbit GAPDH (Cell Signaling Technology, Inc., Danvers, MA, USA) or mouse YAP (Santa Cruz Biotechnology, Dallas, TX, USA) antibody. The next day the membranes were washed 3 times in TBST buffer and incubated for 50 min at room temperature in TBST buffer containing 3 % BSA and either IRDye® 800CW Goat (polyclonal) Anti-Rabbit IgG (H+L) or 680RD Goat (polyclonal) Anti-Mouse IgG(H+L), Highly Cross Adsorbed secondary antibody (LI-COR, Lincoln, NE, USA). The membranes were washed twice with TBST and once with TBS buffer. The near-infrared fluorescence signal was imaged and quantified by LI-COR Odyssey system.

D. Immunofluorescence Staining

The C2C12s were seeded at a density of 5*10^4 cells/well. The next day the cells were starved for 3 h in the expansion media containing no FCS and stimulated for 5 min with FLIPUS. Two hours after the stimulation the cells were fixed in 4 % paraformaldehyde solution. The cells were rinsed with phosphate buffered saline, PBS (Biochrom AG, Berlin, Germany) and

permeabilized for 30 min in 0.1 % Triton™ X-100 (Sigma Aldrich, Steinheim, Germany). This was followed by blocking the cells in PBS containing 3 % BSA (Carl Roth GmbH + Co. KG, Karlsruhe, Germany) for 1 h. After the blocking, primary mouse YAP antibody (Santa Cruz Biotechnology, Dallas, TX, USA) was diluted in 1 % BSA-containing PBS at 1:300 ratio, added to the fixed cells, and incubated for 1 h. The cells then were rinsed with PBS 3 times and incubated for 1 h in secondary Alexa Fluor 594 goat anti-mouse (H+L) antibody (Thermo Fischer Scientific, Rockford, IL, USA) at 1:150 ratio, prepared in PBS with 1 % BSA. Up until this point the procedure was carried out at room temperature. Then the cells were rinsed again and stained with 5 µM Hoechst 33342 (Thermo Fischer Scientific, Eugene, OR, USA) solution for 20 min at 37 ºC. Traces of the staining were removed by PBS and the cells were mounted in Flouromount-G® (Southern Biotech, Birmingham, AL, USA) medium. The stainings were visualized with Zeiss Axio Obsever. Z1.

E. Cell Fractionation Assay

After the FLIPUS exposure was complete, the cells were scraped off the bottom 2 h and 3 h after the stimulation in 600 µl PBS. The rest of the procedure was performed according to the manufacturer protocol NE-PER™ Nuclear and Cytoplasmic Extraction Reagents (Thermo Fischer Scientific, Darmstadt, Germany). The western blotting procedure was performed as described above with few modifications. Rabbit histone antibody (Cell Signaling Technology, Inc., Danvers, MA, USA) was used for loading controls in the nuclear fractions. Horseradish peroxidase-conjugated goat-anti-mouse IgG + IgM [H+L] and goat-anti-rabbit IgG [H+L] secondary antibodies (Dianova GmbH, Hamburg, Germany) were used in the protocol. The antibodies were diluted at 1:2000 ratio in TBST containing 3 % BSA and the membranes were incubated for 1 h at room temperature. The HRP-juice (PJK GmbH, Kleinblittersdorf, Germany) was added and the membranes were visualized on Fusion Fx-7. The images were quantified with help of ImageJ software.

F. RNA Extraction and Quantitative Real Time PCR (qRT-PCR)

The cells were lysed 0 min, 1 h, 3 h, 5 h and 7 h after the FLIPUS stimulation. Each individual time point had its own negative control, which did not receive FLIPUS exposure. The mRNA isolation was performed by NucleoSpin RNA II Kit (Machery Nagel, Düren, Germany). The mRNA was transcribed to the complementary DNA (cDNA) with help of qScriptTM cDNA SuperMix (Quanta Biosciences, Gaithersburg, MD, USA) using Mastercycler EP Gradient S

(Eppendorf, Hamburg, Germany). The quantities of cysteine-rich angiogenic inducer 61 (Cyr61), CyclinD1, amphiregulin (AREG), anillin (ANLN), diaphanous 1 and 3 formins (Diaph1 and Diaph3), Ras-homolog gene family, member A (RhoA), Rho-associated coiled-coil containing protein kinase (Rock1), cell division controlling homolog 42 (CDC42), Ras-related C3 botulinum toxin substrate 1 (Rac1), connective tissue growth factor (CTGF), myogenic factor 3 (MyoD) and YAP were measured using PerfeCTa®SYBR®Green SuperMix (Quanta Biosciences, Gaithersburg, USA) on LightCycler 480 II (Roche Diagnostics GmbH, Mannheim, Germany). The primers were designed by Primer3 Input software and ordered from TIB Molbiol (Berlin, Germany). The expression of all target genes was normalized to the expression of house-keeping gene hypoxanthine-guanine phosphoribosyltransferase (HPRT). The primers used for the experiments are summarized in Table 1.

Table 1. Primers List

Gene Name	Forward Sequence	Reverse Sequence
CyclinD1	5´- CGTGGCCTCTAAGATGAAGG – 3´	5´- CCACTTGAGCTTGTTCACCA – 3´
AREG	5´- CTGCTGGTCTTAGGCTCAGG – 3´	5´- TTTCGCTTATGGTGGAAACC – 3´
Cyr61	5´- TGCTGTAAGGTCTGCGCTAA – 3´	5´- AGGGTCTGCCTTCTGACTGA – 3´
CTGF	5´- CCACCCGAGTTACCAATGAC – 3´	5´- GACAGGCTTGGCGATTTTAG – 3´
ANLN	5´- TCAATAGCAGCAGTGTTCAGC -3´	5´- GATTTTGTGCCTCACGGTTT -3´
Diaph3	5´- TAATGGGCTACTATGCTGTCG -3´	5´- CTCTTTCTCTGCTCGCTCTTT -3´
Diaph1	5´- CCCTTTGGATTTGGGGTTC – 3´	5´ - AGCGGTCCTCCTTCACCTT – 3´
RhoA	5´- GAAGTCAAGCATTTCTGTCCA – 3´	5´- CTCACTCCATCTTTGGTCTTTG – 3´
Rock1	5´- TTCTGGGAAGAAAGGGACATC – 3´	5´- AGGCACGTCATAGTTGCTCAT – 3´
Rac1	5´- TGTCCCAATACTCCTATCATCC – 3´	5´- TACAACAGCAGGCATTTTCTC – 3´
CDC42	5´- AGTGTGTTGTTGTTGGTGATG – 3´	5´- GAGTCTTTGGACAGTGGTGAG – 3´
MyoD	5´- CTACCCAAGGTGGAGATCCTG – 3´	5´- CACTGTAGTAGGCGGTGTCGT – 3´
YAP	5´- AAGGAGAGACTGCGGTTGAA – 3´	5´- CCTGAGACATCCCAGGAGAA – 3´
HPRT	5´- TGTTGTTGGATATGCCCTTG – 3´	5´- ACTGGCAACATCAACAGGACT – 3´

G. BrdU-ELISA

After the successful stimulation, the cells were labeled for 12 h with BrdU solution. The BrdU-ELISA was performed after the labeling as described by the provider (Roche Diagnostics GmbH, Mannheim, Germany). The amount of the incorporated BrdU was then quantified

colorimetrically. Absorbance values were measured at 450 nm with a reference to 690 nm reference on TECAN infinite, M200 PRO (Maennedorf, Switzerland).

H. Preparation of YAP Knock-Down

The C2C12s were seeded at a density of $5*10^4$ cells/mL. Twenty four hours later the cells were transfected either with YAP-knock-down (YAP-KD) siRNA (stock 20 µM) or YAP-scrambled (YAP-SCR) (stock 100 µM) siRNA at a final concentration of 50 nM per well. The YAP-KD and YAP-SCR siRNAs were mixed with Lipofectamine RNAiMAX (Invitrogen, ThermoFisher Scientific, Waltham, MA, USA) at 2.5 µl of the transfection agent per well. The next day the cells were starved for 3 h, stimulated for 5 min with FLIPUS, and analyzed by BrdU-ELISA as it is described above.

I. Scratch-Wound Migration Assay

The C2C12s were seeded at a density of $1*10^4$ cells per 80 µl in each of the two compartments of ibidi Culture-inserts (ibidi GmbH, Planegg, Martinsried, Germany). Forty eight hours later the inserts were removed and each well was rinsed twice with PBS. The cells were starved for 3 h in expansion media containing 1 % FCS and inhibitor of DNA synthesis Mitomycin C (Sigma-Aldrich, Munich, Germany) added at 1:300 ratio. Then the cells were stimulated for 5 min with FLIPUS and images visualizing the gap closure were taken directly before and 2 h, 4 h, 6 h, 8 h, and 24 h after the stimulation. The cells incubated in expansion media with 10 % FCS were used as a positive control. The gap area at each time point then was evaluated by ImageJ software and the migration rate (MR) was calculated as following:

$$MR = \frac{Gap\ Area\ Prestim - Gap\ Area\ Poststim}{Gap\ Area\ Prestim} * 100\%.$$

J. Statistical Analysis

Significance of differences in the evaluated parameters was assessed by one-way ANOVA followed by post-hoc multi-comparison Tukey-Kramer tests using the MATLAB statistics toolbox (The MathWorks, Natick, MA, USA). All data were expressed as mean plus/minus standard deviation. The differences were considered to be significant if *p*-value was smaller than 0.05.

RESULTS

A. *FLIPUS Reduces Phosphorylation State of YAP on Ser127*

Due to our recent finding that the activation of TEAD binding sequences is enhanced after 5-min-long FLIPUS exposure [19], we explored whether these observations are related to changes in the YAP(Ser127) phosphorylation state. The time point kinetics after 5 min FLIPUS stimulation revealed that the p-YAP(Ser127) amounts start reducing 2 h after the stimulation, reaching a minimum at 3 h, returning to basal level 4 h after the FLIPUS exposure, whereas total YAP levels remained unchanged (Fig.1a&b). There was also a subtle, but statistically significant, decrease in p-YAP(Ser127) observed right after the stimulation.

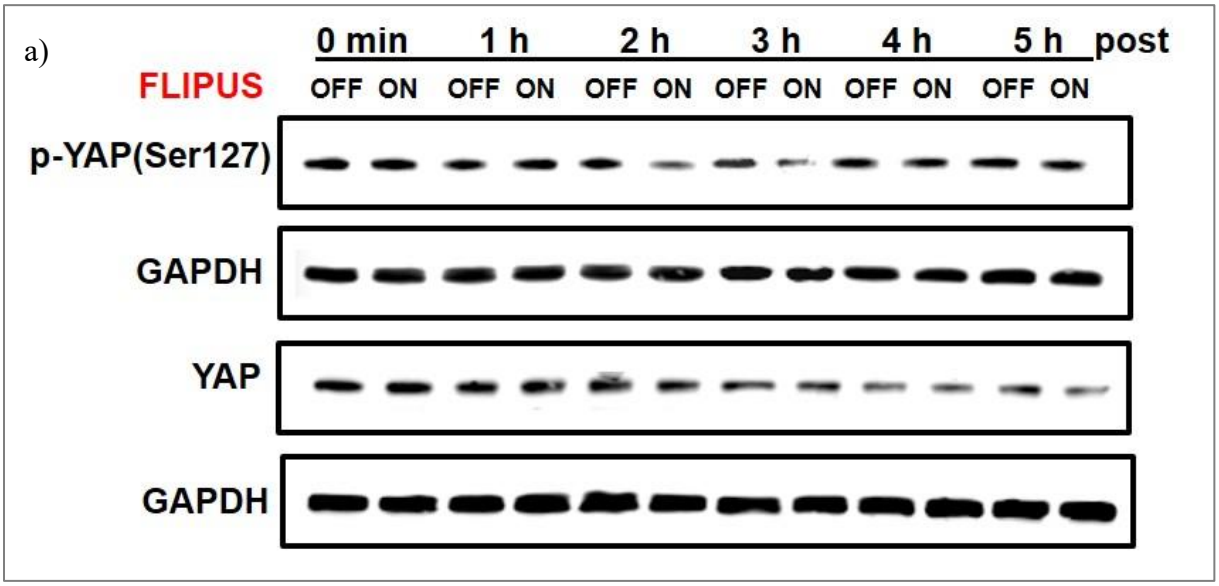

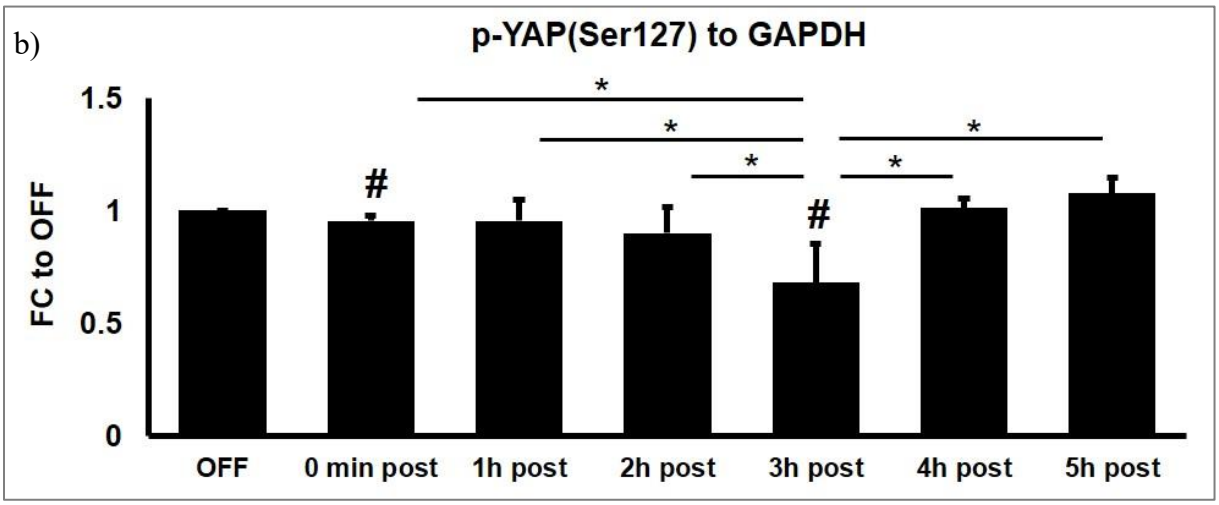

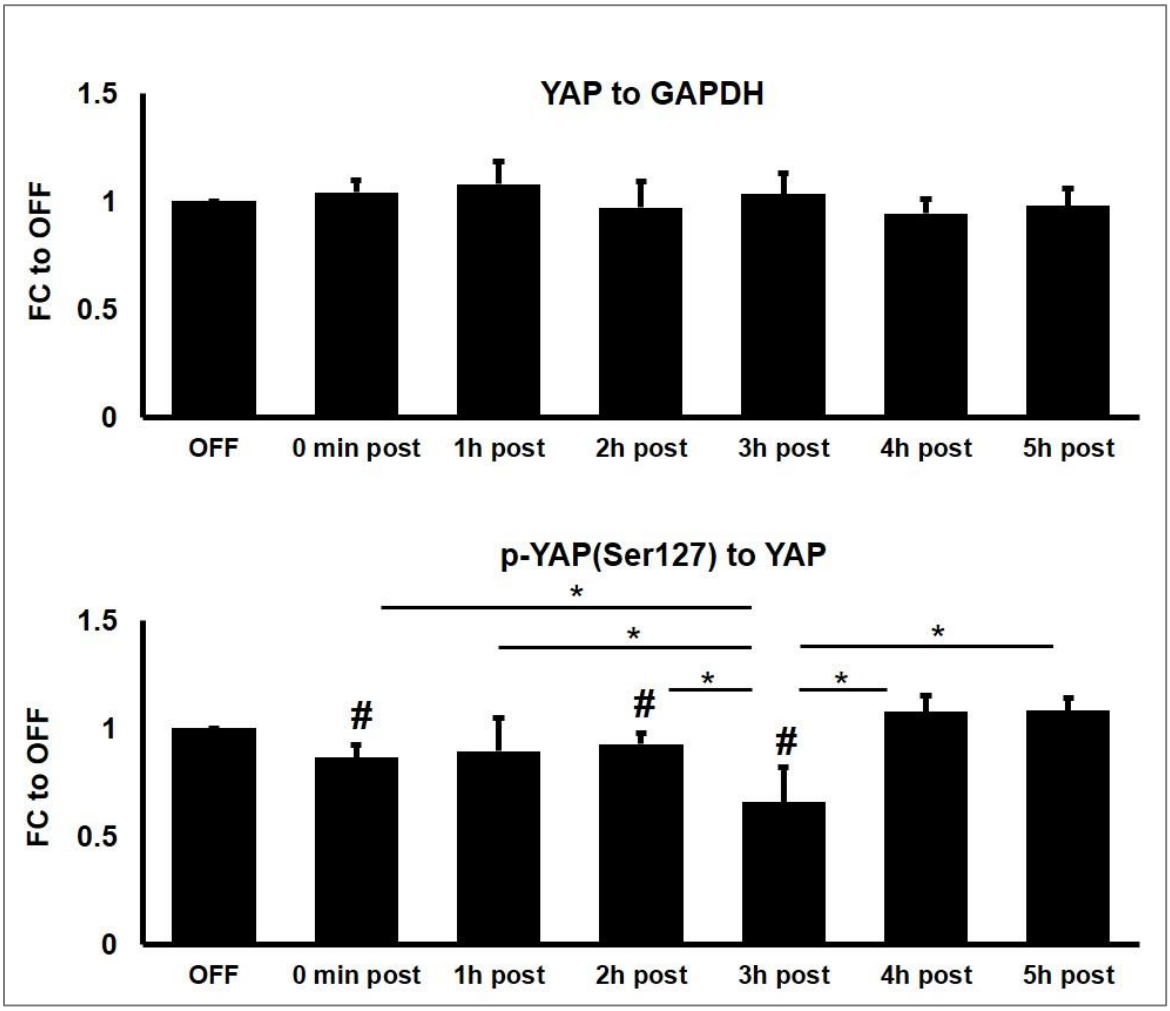

Fig.1: Exemplary pictures of western blotting analysis of C2C12 cell-lysates, prepared 0 min, 1 h, 2 h, 3 h, 4 h, and 5 h after 5-min-long FLIPUS stimulation (a). The quantified amounts of blots presented in graphs and expressed as fold change (FC) in average intensity values of FLIPUS treated cells when compared to non-sonicated controls (OFF) (b). Each time point had its own unstimulated control (OFF) and is averaged from minimum three biological trials. *$p < 0.05$ signify changes between the time points and $^{\#}p < 0.05$ indicate changes between FLIPUS-treated and untreated cells for a selected time point.

B. FLIPUS Supports YAP Nuclear Translocation

FLIPUS stimulation resulted in YAP primarily localized in the nucleus, whereas unstimulated cells had a number of cells with YAP found in the cytoplasm (Fig.2a)

The results of the cell fractionation assay supported findings of the immunofluorescence stainings (Fig.2b), revealing increase in nuclear and decrease in cytosolic YAP content 2 h after the stimulation. Three hours post-FLIPUS the amounts of YAP equalize with unstimulated groups, leaving nuclear vs cytosolic difference minimal. A cellular morphology also changed

after the FLIPUS stimulation, with the sonicated cells appearing spread as opposed to the constrained semblance of the untreated cells (Fig.2a).

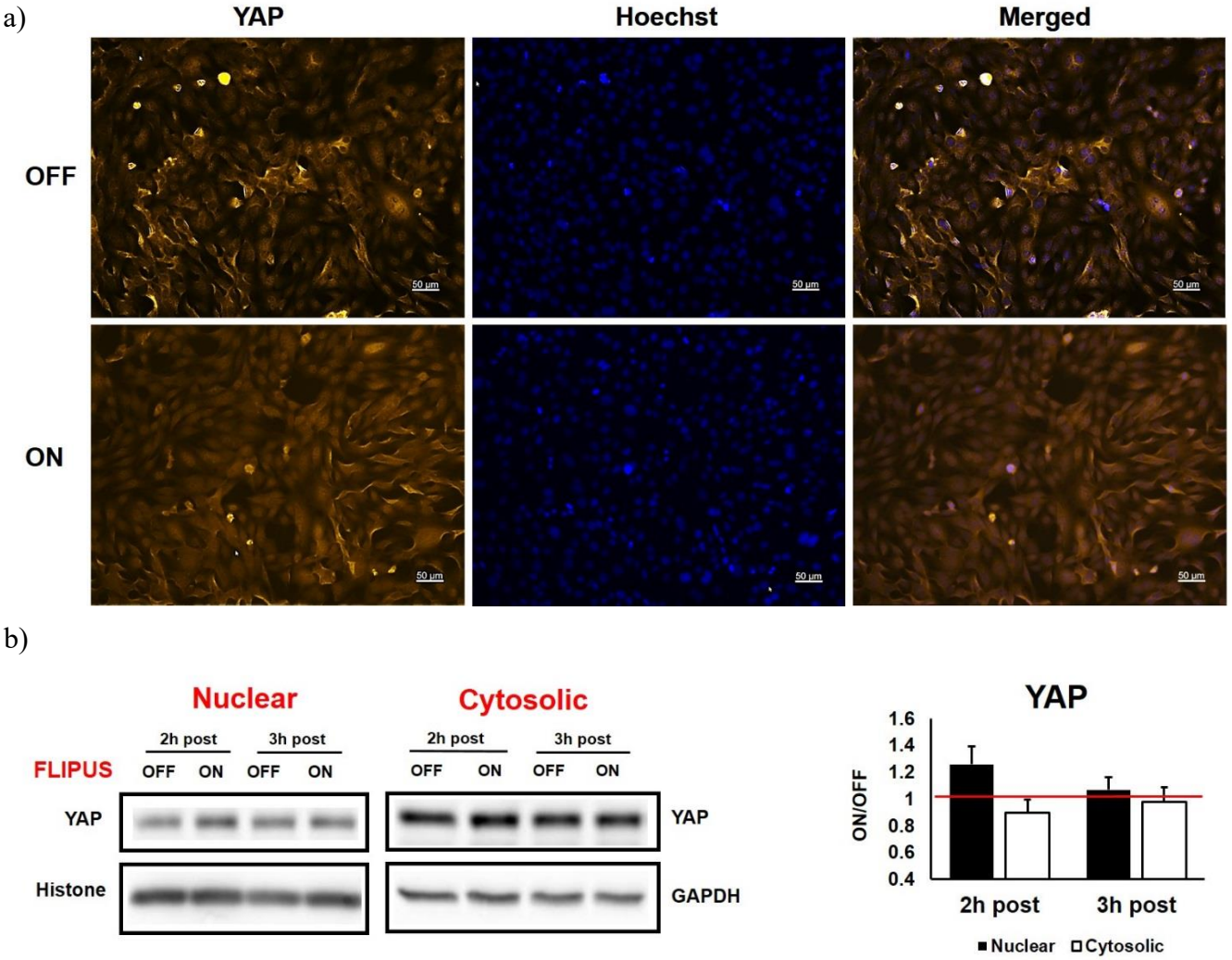

Fig.2: FLIPUS supports nuclear translocation of YAP in C2C12s: exemplary immunofluorescence images of YAP localization (a); western blot images of cell fractionation assay (left) and the quantification results (right) averaged from 3 biological trials (b).

C. YAP-Knock-Down and YAP Target Genes

In order to establish YAP target genes, several cell-cycle-related and cytoskeletal genes were quantified in C2C12s, transfected either with YAP-knock-down (YAP-KD) or YAP-scrambled (YAP-SCR) siRNAs (Fig.3). The gene expression of CyclinD1, Cyr61, and AREG were the most affected by the KD (Fig.3a). In addition, cytoskeleton stabilizing genes ANLN, Diaph3, and Diaph1 were significantly decreased by YAP silencing (Fig.3a). The RhoA, Rock1,

Rac1, and CDC42 did not change their expression patterns after the treatment (Fig.3b). The expression of the MyoD transcriptional factor, which defines the myogenic differentiation of cells of the musculoskeletal system [20], was increased in the YAP-KD samples (Fig.3c). Strikingly, the expression of CTGF was also upregulated in the YAP-silenced cells (Fig.3c).

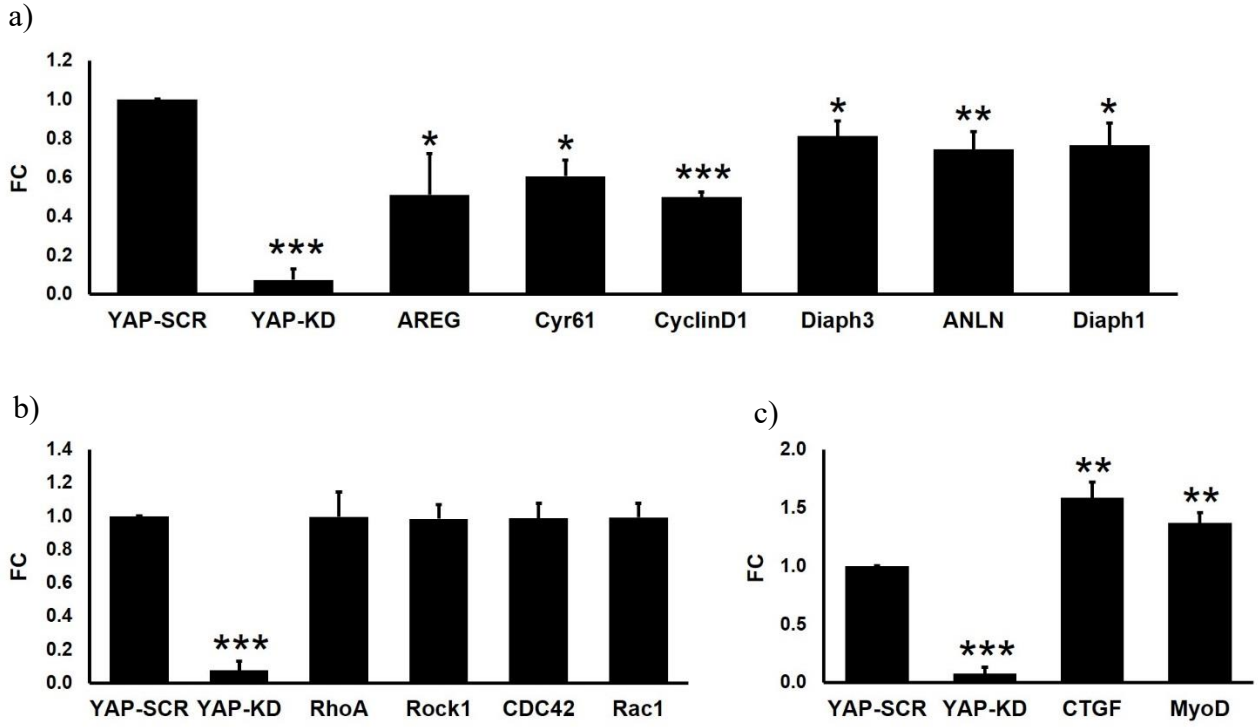

Fig.3: Fold change (FC) in the mean normalized expression values of genes in YAP-KD C2C12s in comparison to the YAP-SCR cells, where (a), (b), and (c) represent genes downregulated, unaffected, and upregulated by the KD, respectively. The results are averaged from three biological trials, where *$p < 0.05$, **$p < 0.01$, and ***$p < 0.001$.

D. Gene Expression in Response to FLIPUS

The expression of ANLN, Diaph3, and Cyr61 was enhanced already 1 h after FLIPUS (Fig.4a). Interestingly, the expression of these genes exhibited cyclic regulation with another boost 5 h to 7 h after the stimulation with ultrasound. The mRNA quantity of Diaph1 remained unchanged within 3 h after the exposure and the increase occurred 5 h after FLIPUS, which reached significance 7 h post-sonication (Fig.4a). CyclinD1 was similarly regulated by ultrasound to Diaph1, whereas the expression of AREG was the most significant 5 h after the mechanical stimulation (Fig.4a).

a)

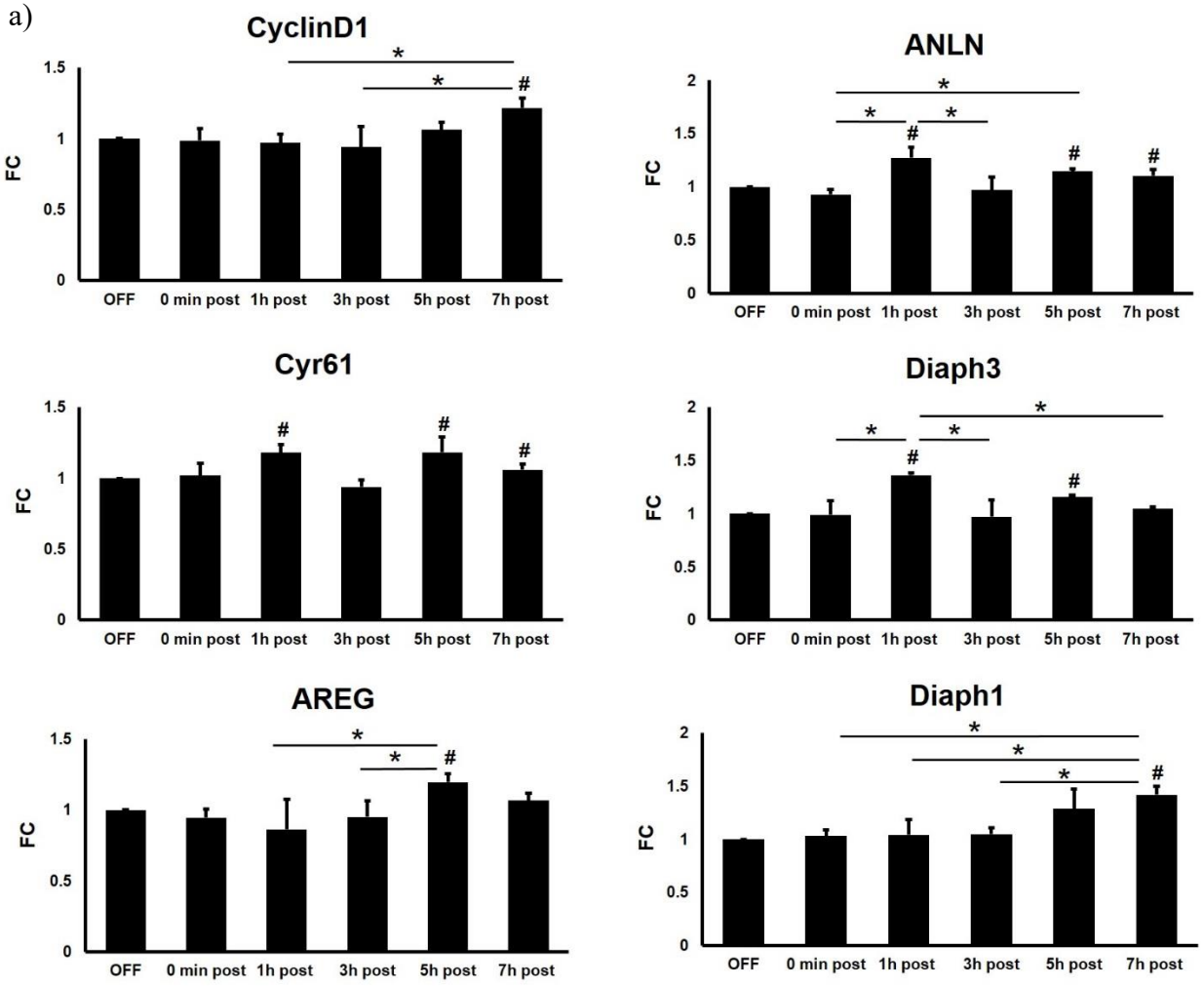
CyclinD1
ANLN
Cyr61
Diaph3
AREG
Diaph1
FC
OFF
0 min post
1h post
3h post
5h post
7h post

b)

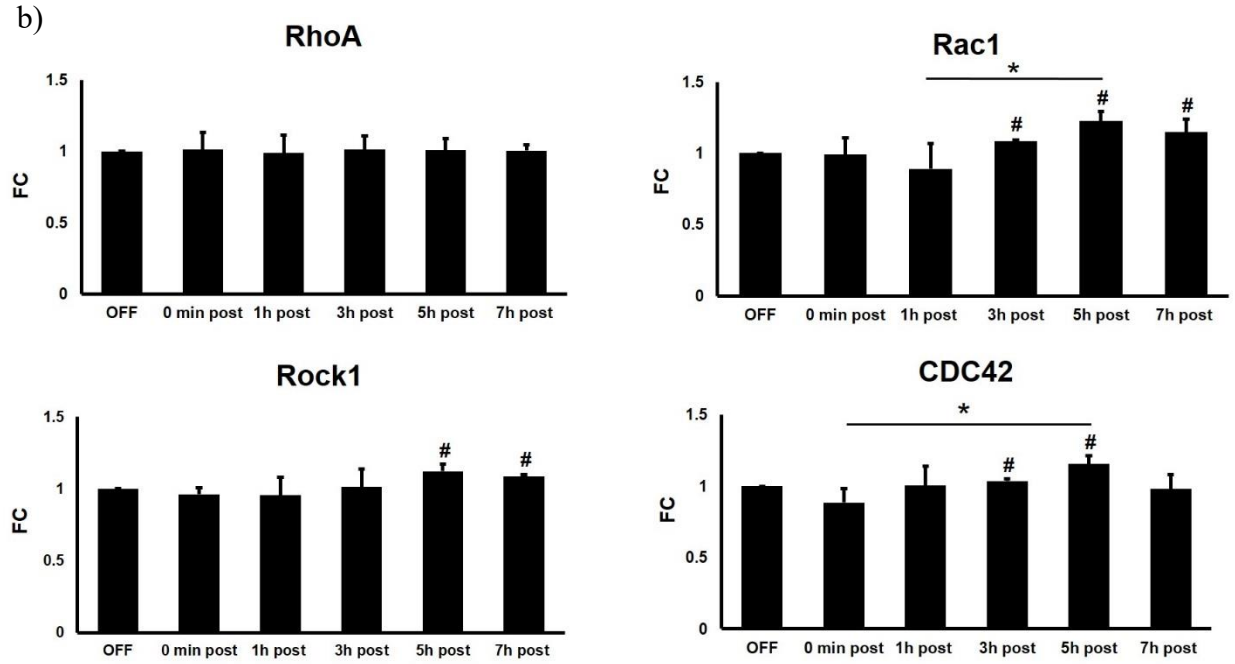
RhoA
Rac1
Rock1
CDC42
FC
OFF
0 min post
1h post
3h post
5h post
7h post

c)

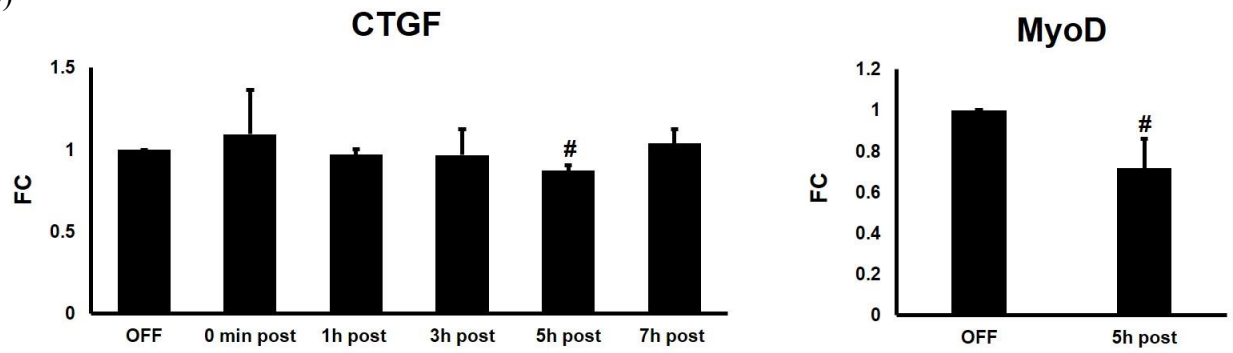

Fig.4: Gene expression in C2C12s in response to FLIPUS, analyzed 0 min, 1 h, 3 h, 5 h and 7 h after the stimulation, where (a), (b), and (c) represent genes downregulated, unaffected, and upregulated by the KD, respectively. Each data point represents a fold change (FC) of gene expression of FLIPUS-stimulated cells when compared to non-sonicated controls (OFF) and averaged from three independent experiments. *$p < 0.05$ signify changes between the time points and $^{\#}p < 0.05$ indicate changes between FLIPUS-treated and untreated cells for a selected time point.

The expression of the small GTPases RhoA, Rac1, and CDC42, and the effector of RhoA, Rock1 kinase, did not change early after stimulation. However, the mRNA of CDC42 and Rac1 started accumulating 3 h after FLIPUS, peaking at 5 h and persisting at 7 h without yielding the significance for CDC42 (Fig.4b). The expression of RhoA remained static throughout all post-stimulation time points; whereas Rock1 exhibited slight increase 5 h and 7 h after the sonication (Fig.4b). The expression of MyoD was decreased 5 h after the ultrasound treatment (Fig.4c). In agreement with previously found regulation of CTGF in YAP-KD samples, the expression of the gene was slightly, but significantly, reduced 5 h after the FLIPUS introduction (Fig.4c).

E. FLIPUS Enhances Cell Proliferation YAP-Dependently

Since the genes that were affected by FLIPUS stimulation are associated with cytokinesis and cell cycle progression, we verified whether proliferation of the cells is influenced by the mechanical stimulation and whether YAP mediates the observed cell growth. The BrdU-ELISA assay revealed that FLIPUS indeed enhanced the proliferation of C2C12s and that the YAP-KD cells could no longer benefit from the ultrasound stimulation (Fig.5a). The YAP-KD efficiency was evaluated by western blotting (Fig.5b).

From our findings, the hypothetical mechanism of FLIPUS mechanotransduction in C2C12s consists of following steps: a) mechanical stimulation results in actin nucleation and stabilization of the cytoskeleton, which leads to stretched morphology of the cells; b) causing YAP dephosphorylation on Ser127 and its consequent nuclear translocation; c) which promotes

the expression of cell cycle-promoting genes and cellular proliferation. The upstream components of the mechanism, i.e., the receptors and cytoplasmic signaling proteins, still remain a matter of investigation. A schematic view of the hypothesized mechanism is presented in Fig.6.

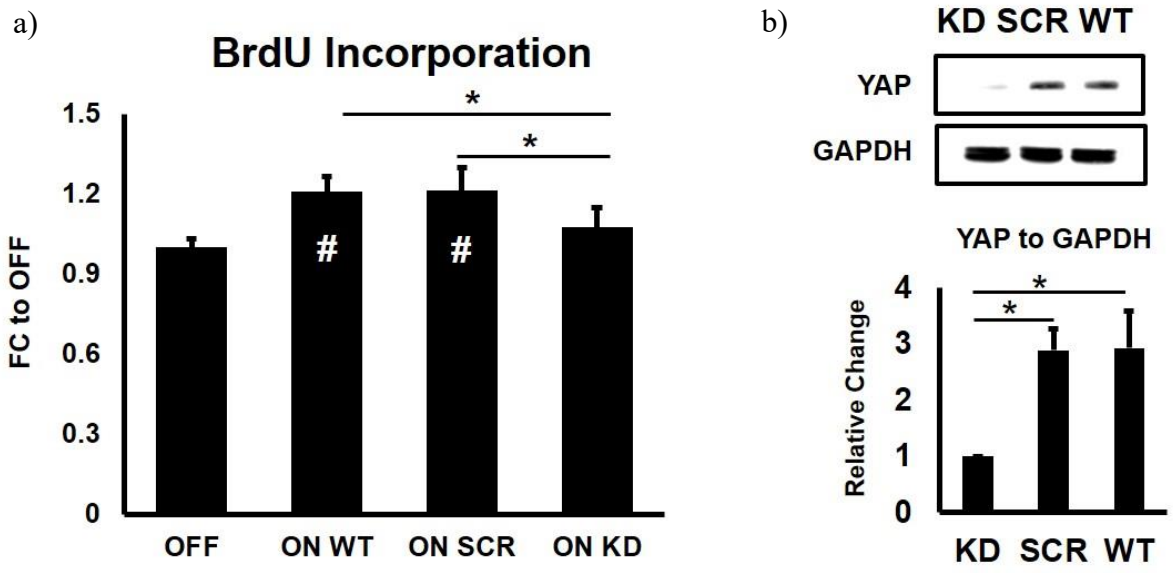

Fig.5: BrdU incorporation in FLIPUS-treated wild type (ON WT), YAP-SCR (ON SCR), YAP-KD (ON KD), and non-sonicated (OFF) C2C12s (a). Each experiment was repeated four times and performed in duplicate. The controls of transfection efficiencies analyzed by western blotting for three biological trials are summarized in (b), $^{\#}p < 0.05$ indicate changes between FLIPUS-treated and untreated cells for a selected time point and $*p < 0.05$ indicate changes between the sonicated groups.

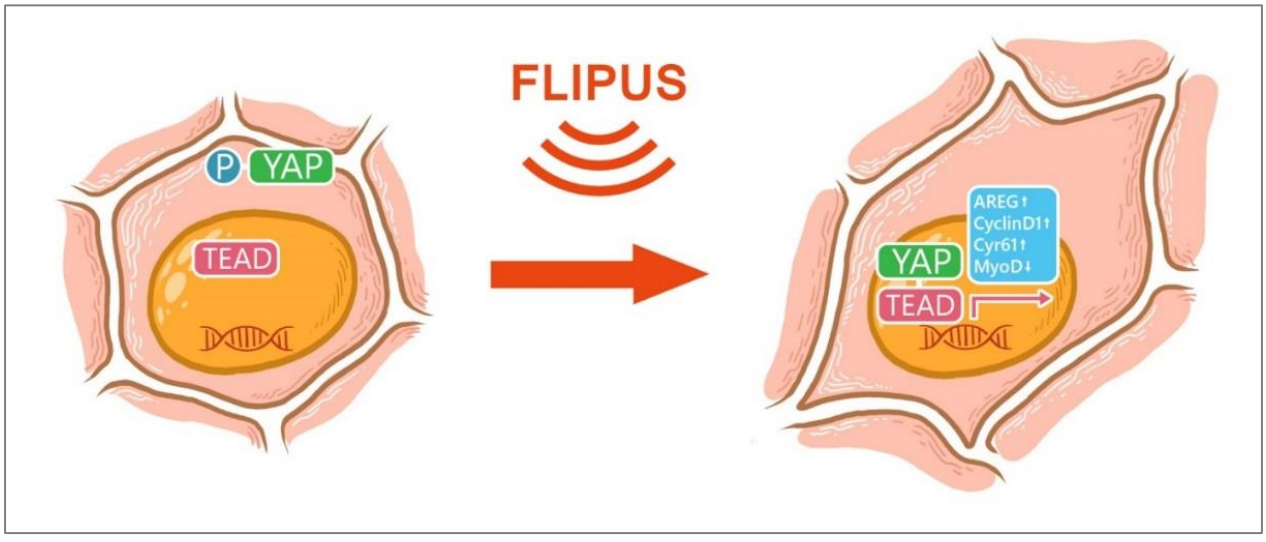

Fig.6: Hypothesized mechanotransduction mechanism regulating the pro-proliferative response of C2C12 to FLIPUS through regulation of YAP activity.

DISCUSSION

The process of tissue regeneration heavily relies upon the proliferative potential of cells, required to reconstruct the impaired site [4]. Inadequate cellular functioning eventually leads to tissue deterioration and significant organ disabilities. The YAP transcriptional coactivator, regulated by mechanical stimuli, determines the cellular proliferative potential, which in turn decides the outcome of successful tissue regeneration [21]. Our recent findings suggest that the YAP's fate can be affected by Focused Low-Intensity Pulsed Ultrasound (FLIPUS) mechanical stimulation, resulting in enhanced cellular proliferation of murine C2C12 mesenchymal progenitor cells.

Inspired by our previous results, that the TEAD binding activity increases in response to 5-min-long FLIPUS exposure in C2C12s [19], we next investigated whether these changes were associated with the YAP functioning. It was found that FLIPUS mechanical stimulation, indeed, reduced the phosphorylation state of YAP on Ser127. The critical role of YAP in defining the cellular commitment of C2C12s has been recently demonstrated by Watt *et al.* [22]. This study emphasized that the YAP(S127A) mutant, which avoids cytoplasmic retention, delayed the myogenic differentiation of cells and promoted their proliferation, suggesting that the phosphorylated state of YAP on Ser127 is crucial for muscle maturation. Similarly, the role of YAP in the functioning of primary murine satellite cells has been investigated by Judson *et al.* [23], who showed that the YAP expression was elevated during the cellular activation, while it was reduced when the cells underwent differentiation. To verify the observations made by Watt *et al.*, we selected several genes known to be regulated by YAP and investigated whether their expression is affected by YAP-KD. CyclinD1, Cyr61 and AREG have been numerously demonstrated to be YAP target genes with cell cycle promoting properties (reviewed in [24]). The transcriptional regulation of Diaph1, Diaph3, and ANLN by YAP has been previously shown by Calvo *et al.* [25], who suggested that these proteins contributed to the extracellular matrix (ECM) stiffening, promoting YAP and TEAD nuclear activity. Diaph1, the effector of RhoA, is actin nucleating formin, which regulates the filaments elongation at actin barbed ends [26]. ANLN protein regulates bundling of F-actin and is also enriched and co-localized with myosin II in cleavage furrow during cytokinesis [27]. ANLN binding to Daiph3 formin stabilizes its conformation crucial for cell division [28]. As a result, we established that the pro-proliferative genes CyclinD1, Cyr61, AREG, as well as the cytoskeleton stabilizing and cytokinesis-associated genes Diaph1, Diaph3 and ANLN, were downregulated in YAP-KD C2C12s. The expression of other cytoskeletal genes, such as small GTPases RhoA, CDC42, and Rac1, as well as RhoA's

effector Rock1 kinase, were not affected by YAP suppression. On the contrary, the expression of the MyoD myogenic transcriptional factor was enhanced upon YAP silencing. These results agree with those of Watt *et al.*, who identified YAP as a negative regulator of myogenesis in C2C12.

The expression of the described above genes was next analyzed after being exposed to FLIPUS stimulation. Six target genes, - CyclinD1, Cyr61, AREG, Diaph1, Diaph3, and ANLN, were found to be enhanced 5 h to 7 h after 5-min-long sonication. Stimulation with FLIPUS reduced expression of MyoD 5 h after the stimulation, suggesting that, as an early effect, FLIPUS rather supports stress filaments formation, cytokinesis and proliferation of C2C12s, while delaying cellular specification.

Interestingly, the expressions of Rock1, CDC42, and Rac1 were also upregulated after the FLIPUS introduction. Previous studies have shown that enhanced activity of CDC42, Rac1 [29], and Rock1 [30] attenuates myogenic differentiation, suggesting that FLIPUS could inhibit myogenesis through an additional mechanism, which is not, or indirectly, mediated by YAP. The enhanced expression of the filopodia- and lamellipodia-inducing genes CDC42 and Rac1 [31] could also suggest the increased migratory potential of C2C12s. This is in agreement with our findings that FLIPUS enhances migration of C2C12s (Supplementary Fig.1).

Strikingly, the expression of the CTGF gene - the most described YAP target in the literature [5;8;10] - was negatively regulated by the FLIPUS stimulation and CTGF experienced elevated expression in our YAP-KD samples. This implies that increased expression of CTGF should be critically evaluated as a universal indicator of the enhanced YAP activity. Our observations could be also supported by Hishikawa *et al.* [32], who found that CTGF suppresses cellular viability and induces apoptosis in smooth muscle cells via activation of caspase 3 cascade. A reduced expression of CTGF mediated by YAP and TEAD has been also very recently shown by Wang *et al.* [33], who demonstrated that YAP downregulates CTGF in order to preserve the stem-like cells in a pluripotent state. Thus, FLIPUS could be affecting the fate of C2C12 not only through improvement of cellular proliferation, but also by maintenance of cellular pluripotency. However, further experimental work is required in order to draw any firmer conclusions.

Our findings that FLIPUS induces YAP activity were supported further by the observation of the YAP nuclear localization after the mechanical stimulation. These results were additionally quantified by fractionation assay, revealing higher nuclear YAP-content after the sonication. Our results agree with the study by Reddy *et al.* [13], where intensified actin

polymerization resulted in decrease of YAP phosphorylation on Ser127 and in increase of the total YAP to p-YAP(Ser127) ratio, providing more available YAP to be translocated to the nucleus. Similarly to our data, the study by Zhong *et al.* [34] demonstrated that rat MSCs and chondrocytes subjected to the gradual increase of shear-stress, which was generated by a microfluidic bioreactor, led to more intensive YAP nuclear localization through the formation of stress-fibers. This in turn enhanced the proliferative potential of the cells.

It is important to note that FLIPUS-stimulation of C2C12s along with YAP-nuclear status also modified cellular appearance: unstimulated cells looked more confined in size, whereas mechanostimulated cells exhibited spread morphology (Fig.2a). FLIPUS-induced change in cellular shape and YAP activity are in line with the original work of the group of Stefano Piccolo [24], first demonstrating the link between cell-geometry and YAP-mediated cellular fate. The diminution of YAP expression in our experimental work abolished pro-proliferative influence of FLIPUS in C2C12s.

Our results put all together suggest that FLIPUS reduces phosphorylation of YAP on Ser127 through possible alternation of cellular geometry. This activates YAP and translocates it to the nucleus, where the expression of ECM-remodeling, cytokinesis-related, and pro-proliferative genes occurs, which in turn drives division of C2C12s. These findings represent not only great importance from a biological, but also from a physical point of view, by suggesting that the FLIPUS submechanism, which significantly regulates cellular fate is cell stretching, caused by, e.g., pressure gradients of acoustic radiation force.

Most certainly further investigation of the mechanism is necessary to expand our knowledge on LIPUS-triggered biological and physical cues. Firstly, it is crucial to understand the upstream events from YAP signaling, namely, the involvement of evolutionary conserved Hippo pathway in transmission of the FLIPUS mechanical signal. Furthermore, although we observed enhanced expression of stress-fiber and actin stabilizing genes after cellular sonication, fluorescence stainings of the cytoskeleton would complement the study very well. Due to the high cell density used in the study, which constrained the cellular shape to a circle, we were not able to obtain pictures of cytoskeletal staining of optimal quality, which was further worsened by polystyrene plates possessing strong autofluorescence. The glass slips were not suitable for the cell growth, since glass reflects ultrasound and no signal would be transmitted to the cells in our set-up. Therefore, we would like to shift further investigation of the mechanism to 3D cultures in scaffolds, where changes in cellular morphology and actin properties can be visualized without impairing data interpretation. The 3D experimental set-up will also permit to vary the substrate

stiffness in order to evaluate changes in FLIPUS-induced cellular mechanoresponse, more closely mimicking natural tissue architecture and revealing ultrasound-mediated regenerative mechanisms.

SUPPLEMENTARY MATERIAL

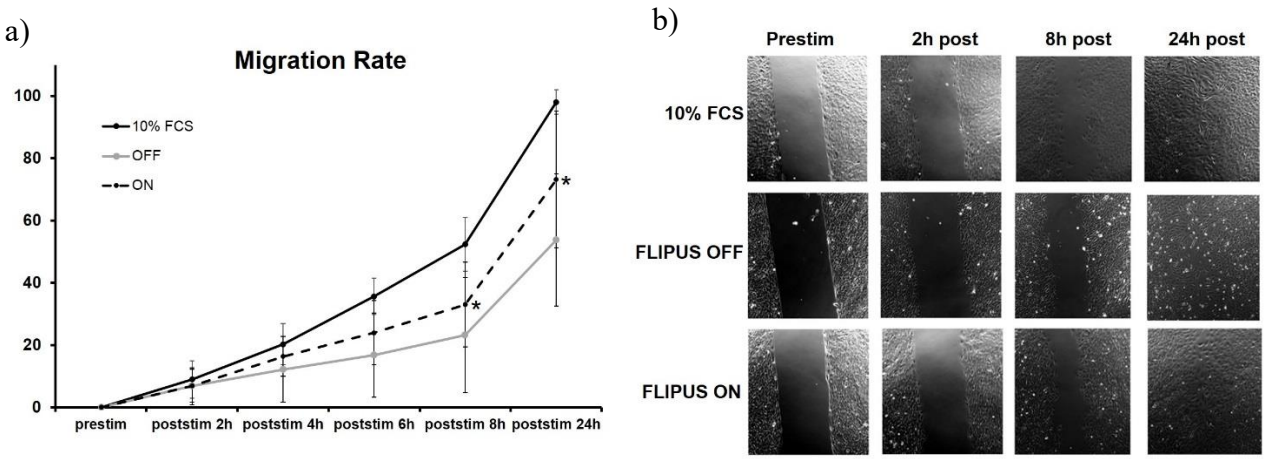

Fig. S1: FLIPUS enhances migration rate of C2C12s, analyzed by scratch-wound assay 2 h, 4 h, 6 h, 8 h and 24 h after 5-min-long stimulation (a), where 10 % FCS, ON and OFF represent cells cultivated in normal expansion media, starved FLIPUS-stimulated, and starved non-sonicated cells, respectively. Each data point represents the mean of three independent experiments. *p < 0.05 indicates significant difference between ON and OFF groups. Exemplary snapshots of the gap closure are illustrated in (b).

ACKNOWLEDGEMENTS

The presented here study was funded by the German Research Foundation (Deutsche Forschungsgemeinschaft, DFG) grant Ra1380/8-1. P.K. was supported by the DFG grant FOR2165. The authors thank Ruslan Puts for the design of Figure 6.

REFERENCES

[1] D. E. Discher, D. J. Mooney, and P. W. Zandstra, "Growth factors, matrices, and forces combine and control stem cells," *Science*, vol. 324, no. 5935, pp. 1673-1677, June2009.

[2] K. R. Levental, H. Yu, L. Kass, J. N. Lakins, M. Egeblad, J. T. Erler, S. F. Fong, K. Csiszar, A. Giaccia, W. Weninger, M. Yamauchi, D. L. Gasser, and V. M. Weaver, "Matrix crosslinking forces tumor progression by enhancing integrin signaling," *Cell*, vol. 139, no. 5, pp. 891-906, Nov.2009.

[3] S. Dupont, L. Morsut, M. Aragona, E. Enzo, S. Giulitti, M. Cordenonsi, F. Zanconato, D. J. Le, M. Forcato, S. Bicciato, N. Elvassore, and S. Piccolo, "Role of YAP/TAZ in mechanotransduction," *Nature*, vol. 474, no. 7350, pp. 179-183, June2011.

[4] D. E. Jaalouk and J. Lammerding, "Mechanotransduction gone awry," *Nat. Rev. Mol. Cell Biol.*, vol. 10, no. 1, pp. 63-73, Jan.2009.

[5] M. Aragona, T. Panciera, A. Manfrin, S. Giulitti, F. Michielin, N. Elvassore, S. Dupont, and S. Piccolo, "A mechanical checkpoint controls multicellular growth through YAP/TAZ regulation by actin-processing factors," *Cell*, vol. 154, no. 5, pp. 1047-1059, Aug.2013.

[6] M. Sudol, "Yes-associated protein (YAP65) is a proline-rich phosphoprotein that binds to the SH3 domain of the Yes proto-oncogene product," *Oncogene*, vol. 9, no. 8, pp. 2145-2152, Aug.1994.

[7] B. Zhao, X. Wei, W. Li, R. S. Udan, Q. Yang, J. Kim, J. Xie, T. Ikenoue, J. Yu, L. Li, P. Zheng, K. Ye, A. Chinnaiyan, G. Halder, Z. C. Lai, and K. L. Guan, "Inactivation of YAP oncoprotein by the Hippo pathway is involved in cell contact inhibition and tissue growth control," *Genes Dev.*, vol. 21, no. 21, pp. 2747-2761, Nov.2007.

[8] B. Zhao, X. Ye, J. Yu, L. Li, W. Li, S. Li, J. Yu, J. D. Lin, C. Y. Wang, A. M. Chinnaiyan, Z. C. Lai, and K. L. Guan, "TEAD mediates YAP-dependent gene induction and growth control," *Genes Dev.*, vol. 22, no. 14, pp. 1962-1971, July2008.

[9] A. Vassilev, K. J. Kaneko, H. Shu, Y. Zhao, and M. L. DePamphilis, "TEAD/TEF transcription factors utilize the activation domain of YAP65, a Src/Yes-associated protein localized in the cytoplasm," *Genes Dev.*, vol. 15, no. 10, pp. 1229-1241, May2001.

[10] M. Ota and H. Sasaki, "Mammalian Tead proteins regulate cell proliferation and contact inhibition as transcriptional mediators of Hippo signaling," *Development*, vol. 135, no. 24, pp. 4059-4069, Dec.2008.

[11] D. A. Fletcher and R. D. Mullins, "Cell mechanics and the cytoskeleton," *Nature*, vol. 463, no. 7280, pp. 485-492, Jan.2010.

[12] K. Wada, K. Itoga, T. Okano, S. Yonemura, and H. Sasaki, "Hippo pathway regulation by cell morphology and stress fibers," *Development*, vol. 138, no. 18, pp. 3907-3914, Sept.2011.

[13] P. Reddy, M. Deguchi, Y. Cheng, and A. J. Hsueh, "Correction: Actin Cytoskeleton Regulates Hippo Signaling," *PLoS. One.*, vol. 8, no. 9 2013.

[14] A. Mammoto, T. Mammoto, and D. E. Ingber, "Mechanosensitive mechanisms in transcriptional regulation," *J. Cell Sci.*, vol. 125, no. Pt 13, pp. 3061-3073, July2012.

[15] F. Padilla, R. Puts, L. Vico, A. Guignandon, and K. Raum, "Stimulation of Bone Repair with Ultrasound," *Adv. Exp. Med. Biol.*, vol. 880, pp. 385-427, 2016.

[16] A. Khanna, R. T. Nelmes, N. Gougoulias, N. Maffulli, and J. Gray, "The effects of LIPUS on soft-tissue healing: a review of literature," *Br. Med. Bull.*, vol. 89, pp. 169-182, 2009.

[17] F. Padilla, R. Puts, L. Vico, and K. Raum, "Stimulation of bone repair with ultrasound: a review of the possible mechanic effects," *Ultrasonics*, vol. 54, no. 5, pp. 1125-1145, July2014.

[18] R. Puts, K. Ruschke, T. H. Ambrosi, A. Kadow-Romacker, P. Knaus, K. V. Jenderka, and K. Raum, "A Focused Low-Intensity Pulsed Ultrasound (FLIPUS) System for Cell Stimulation: Physical and Biological Proof of Principle," *IEEE Trans. Ultrason. Ferroelectr. Freq. Control*, vol. 63, no. 1, pp. 91-100, Jan.2016.

[19] R. Puts, P. Rikeit, K. Ruschke, A. Kadow-Romacker, S. Hwang, K. V. Jenderka, P. Knaus, and K. Raum, "Activation of Mechanosensitive Transcription Factors in Murine C2C12 Mesenchymal Precursors by Focused Low-Intensity Pulsed Ultrasound (FLIPUS)," *IEEE Trans. Ultrason. Ferroelectr. Freq. Control*, July2016.

[20] M. A. Rudnicki, P. N. Schnegelsberg, R. H. Stead, T. Braun, H. H. Arnold, and R. Jaenisch, "MyoD or Myf-5 is required for the formation of skeletal muscle," *Cell*, vol. 75, no. 7, pp. 1351-1359, Dec.1993.

[21] X. Varelas, "The Hippo pathway effectors TAZ and YAP in development, homeostasis and disease," *Development*, vol. 141, no. 8, pp. 1614-1626, Apr.2014.

[22] K. I. Watt, R. Judson, P. Medlow, K. Reid, T. B. Kurth, J. G. Burniston, A. Ratkevicius, B. C. De, and H. Wackerhage, "Yap is a novel regulator of C2C12 myogenesis," *Biochem. Biophys. Res. Commun.*, vol. 393, no. 4, pp. 619-624, Mar.2010.

[23] R. N. Judson, A. M. Tremblay, P. Knopp, R. B. White, R. Urcia, B. C. De, P. S. Zammit, F. D. Camargo, and H. Wackerhage, "The Hippo pathway member Yap plays a key role in influencing fate decisions in muscle satellite cells," *J. Cell Sci.*, vol. 125, no. Pt 24, pp. 6009-6019, Dec.2012.

[24] S. Piccolo, S. Dupont, and M. Cordenonsi, "The biology of YAP/TAZ: hippo signaling and beyond," *Physiol Rev.*, vol. 94, no. 4, pp. 1287-1312, Oct.2014.

[25] F. Calvo, N. Ege, A. Grande-Garcia, S. Hooper, R. P. Jenkins, S. I. Chaudhry, K. Harrington, P. Williamson, E. Moeendarbary, G. Charras, and E. Sahai, "Mechanotransduction and YAP-dependent matrix remodelling is required for the generation and maintenance of cancer-associated fibroblasts," *Nat. Cell Biol.*, vol. 15, no. 6, pp. 637-646, June2013.

[26] F. Li and H. N. Higgs, "The mouse Formin mDia1 is a potent actin nucleation factor regulated by autoinhibition," *Curr. Biol.*, vol. 13, no. 15, pp. 1335-1340, Aug.2003.

[27] C. M. Field and B. M. Alberts, "Anillin, a contractile ring protein that cycles from the nucleus to the cell cortex," *J. Cell Biol.*, vol. 131, no. 1, pp. 165-178, Oct.1995.

[28] S. Watanabe, K. Okawa, T. Miki, S. Sakamoto, T. Morinaga, K. Segawa, T. Arakawa, M. Kinoshita, T. Ishizaki, and S. Narumiya, "Rho and anillin-dependent control of mDia2 localization and function in cytokinesis," *Mol. Biol. Cell*, vol. 21, no. 18, pp. 3193-3204, Sept.2010.

[29] R. Gallo, M. Serafini, L. Castellani, G. Falcone, and S. Alema, "Distinct effects of Rac1 on differentiation of primary avian myoblasts," *Mol. Biol. Cell*, vol. 10, no. 10, pp. 3137-3150, Oct.1999.

[30] L. Castellani, E. Salvati, S. Alema, and G. Falcone, "Fine regulation of RhoA and Rock is required for skeletal muscle differentiation," *J. Biol. Chem.*, vol. 281, no. 22, pp. 15249-15257, June2006.

[31] A. Hall, "Rho GTPases and the actin cytoskeleton," *Science*, vol. 279, no. 5350, pp. 509-514, Jan.1998.

[32] K. Hishikawa, T. Nakaki, and T. Fujii, "Connective tissue growth factor induces apoptosis via caspase 3 in cultured human aortic smooth muscle cells," *Eur. J. Pharmacol.*, vol. 392, no. 1-2, pp. 19-22, Mar.2000.

[33] X. Wang, K. Zhang, L. Yang, S. Wan, and Y. Liu, "YAP down-regulated its target CTGF to maintain stem cell pluripotency in human ovarian cancer stem-like cells," *Int J Clin Exp Pathol*, vol. 9, no. 6, pp. 6210-6216, 2016.

[34] W. Zhong, K. Tian, X. Zheng, L. Li, W. Zhang, S. Wang, and J. Qin, "Mesenchymal stem cell and chondrocyte fates in a multishear microdevice are regulated by Yes-associated protein," *Stem Cells Dev.*, vol. 22, no. 14, pp. 2083-2093, July2013.

Discussion

This thesis was dedicated to the development and characterization of Focused Low-Intensity Pulsed Ultrasound (FLIPUS) *in-vitro* set-up. Analyses of generated physical effects and triggered biological responses in cells of musculoskeletal system were performed, in order to understand the regenerative abilities of this technique. It was established that FLIPUS accelerated the osteogenic differentiation of rMSCs, with both the donor age and the selected acoustic dose having an impact. Mesenchymal precursor cell line C2C12 also displayed mechanosensitivity to FLIPUS, which was quantified by the activity of AP-1, Sp1, and TEAD transcription factors and the expression of mechanoresponsive genes. The mechanism of mechanotransduction in C2C12s by FLIPUS was investigated further and for the first time it was identified that YAP signaling protein is a crucial mediator of the process.

1. Future Directions

A. The involvement of actin cytoskeleton in mechanoresponsive YAP functioning has been well established. However, the implication of the evolutionary conserved Hippo cascade in this process to-date remains debatable. Several studies observed that knocking down Lats1/2, the immediate signaling kinase up-stream of YAP in Hippo cascade, had no effect on the mechanically-regulated YAP functioning in mammary epithelial cells and MSCs (Dupont et al., 2011; Aragona et al., 2013). Calvo *et al.* (Calvo et al., 2013) found that the stress-fibers activated YAP's functioning is rather regulated by Rho small GTPases, which activate Scr-family kinases and hinder binding of YAP to 14-3-3 proteins, promoting nuclear translocation of the former in cancer-associated fibroblasts. On the contrary, Wada *et al.* (Wada et al., 2011) demonstrated that Hippo signaling is inhibited by stress fibers up-stream or at Lats kinase in NIH3T3 fibroblasts and MTD-1A epithelial cells. Similarly, Zhao *et al.* (Zhao et al., 2012) established that anoikis, induced by cell-detachment, is mediated by the phosphorylation state of YAP on Ser127, involving activity of Lats1/2. *Thus, further investigation of the FLIPUS-induced YAP-regulated mechanotransduction in C2C12s is an immediate goal of future research. This includes understanding of the role of Hippo cascade or other signaling proteins, e.g., AMOT, ZO-1/2, catenins, as well as the implication of cytoskeleton in the mechanism.*

B. The experimental work presented in this thesis involved mechanical stimulation of cell cultures in monolayers, which had certain limitations. The matrix stiffness used to grow cells can

regulate differentiation of MSCs into various lineages (Discher et al., 2009). The Young Modulus of polystyrene cell culture plates is in the GPa range, which is significantly stiffer than the stiffest tissues found in the human body (Wells, 2008). Therefore, I believe that the polystyrene plates utilized in my work might have dampened the FLIPUS-mediated biological effects and, thus, depressed their appreciation. This also made it challenging to analyze the functioning of YAP, whose activity is strongly affected by the matrix stiffness (Dupont et al., 2011). In order to achieve a more constrained cellular geometry, C2C12s were grown at very high densities in my experimental designs (Chapter 3&4). This compromised the successful performance of the cytoskeleton and protein-localization stainings, which were difficult to achieve to begin with, due to polystyrene-associated autofluorescence (Torkelson et al., 1981). Moreover, for the densely-seeded cells it was challenging to rule out whether the YAP's fate was solely regulated by cell geometry or by the cell-cell junctional proteins. *Therefore, as a next step, investigation of FLIPUS-associated mechanisms is planned in 3D Col-1 scaffolds, in collaboration with Dr. Ansgar Petersen from the Julius Wolff Institute, Berlin-Brandenburg School for Regenerative Therapies*. The stiffness of the Col-1 scaffolds can be varied, which is particularly favorable for investigation of the mechanoresponsive YAP signaling. Optimization of the FLIPUS set-up for 3D culture stimulation is already in progress.

C. One of the challenges faced by the field of regenerative therapies is to provide patient-oriented tissue engineering procedure, while preserving sterility of the designed explants. Most of the described in the literature bioreactors with chemical and mechanical conditioning require extensive manipulations of the patient-isolated cells, which eventually jeopardize the sterility of the explants (Martin et al., 2009). The FLIPUS set-up presented in my thesis has the advantage of mechanical conditioning of the cells with the defined dose, while preserving sterility of the designed constructs. This could be achieved due to the fact that the mechanical stimuli are transmitted through a tissue culture plate and no direct contact of the set-up with the cells is required. Moreover, the mechanical dose delivered to the cells can be stringently controlled, enabling cell stimulation with a signal corresponding to the tissue-specific differentiation path. *Therefore, the application of FLIPUS as a technique with mechanical conditioning for preparation of ex-vivo tissue explants is another promising future prospect of the research.*

D. The application of FLIPUS *in vivo* has two big advantages: firstly, control of the input intensity and secondly, control of the irradiated volume without co-stimulation of several adjacent tissues in a small animal, which is usually unachievable with planar transducers (Naito et al., 2010; Hasuike et al., 2011). The stimulation of defined regions of a small animal with

FLIPUS will enable establishing correlations between the biological observations dictating regenerative processes and the specific mechanical dose. *Thus, the next significant goal of our research is application of FLIPUS for in-vivo stimulation of damaged tissues (e.g., bone, tendon, cartilage, etc.) in a small animal model.*

E. The use of FLIPUS in combination with growth factors, e.g., BMPs, has the potential to decrease the concentration of the biological component, which often leads to side-effects in clinic (Argintar et al., 2011). The synergistic effect of BMP-2/BMP-7/TGFβ-1 and LIPUS has been demonstrated before. However, the mechanism determining it still remains elusive (Sant'Anna et al., 2005; Wijdicks et al., 2009; Lee et al., 2013; Ebisawa et al., 2004). The cooperative effect of BMP-2 and mechanical cyclic loading, through the activation of BMP-2 canonical signaling, has been previously demonstrated by Dr. Jessica Kopf (Kopf et al., 2012). Similarly, I initiated the examination of the FLIPUS and BMP-2 synergistic mechanism in human fetal osteoblasts (hFOBs 1.19). Preliminary results showed that decrease of BMP-2 concentration by 10 fold and simultaneous application of FLIPUS increased the phosphorylation of Smad1/5/8 (downstream signaling proteins in the canonical BMP-2 pathway) and the activity of the BMP-responsive element (BRE) by 25 %, when compared to the BMP-2 treatment alone (results are not shown). *Further understanding of the synergistic mechanism of FLIPUS and BMPs in 2D and 3D cultures is another prospective direction of the research. The co-application of FLIPUS and BMPs is also planned in small animals in vivo.*

2. Distribution of Tasks

The FLIPUS set-up, described in Chapter 1, was initially engineered by my supervisor Prof. Kay Raum, and was further characterized, analyzed, and improved with my participation. The calibration of the most recent version of the set-up presented in my thesis was performed by me and former master student Thomas Ambrosi. Prof. Klaus-Vitold Jenderka from the Merseburg University of Applied Science kindly provided his equipment to gain a detailed insight into the mechanical dose generated by FLIPUS. The experimental work of FLIPUS stimulation of rMSCs and gene quantification were completed with the help of Mr. Ambrosi and technician Anke Kadow-Romacker. The computational SimSonic simulations confirming the lack of standing waves introduced by FLIPUS were performed by Prof. Raum.

The isolation of fresh MSCs from young and aged rat donors, generously provided by Dr. Sven Geißler, was carried out by Josefine Albers, a medical student at Charité Medical

University. Ms. Albers worked under my guidance on her thesis and performed the stimulation of the cells with FLIPUS, the quantification of gene expression, and the ECM stainings. The biological experimental designs and data analyzes were achieved in a cooperative effort of Ms. Kadow-Romacker, Ms. Albers, and me. Dr. Geißler further shared his extensive experience on the age impact on MSCs functioning and provided very detailed comments for the second manuscript (Chapter 2).

The mechanosensitive response of murine C2C12 mesenchymal precursors to FLIPUS, described in Chapter 3, was evaluated with the use of Luciferase-containing mechanosensitive constructs (AP-1 and Sp1), gifted by Prof. Franz Jakob from Würzburg University, and TEAD-responsive plasmid, provided by Dr. Fernando Camargo from the Boston's Children Hospital at Harvard University. Paul Rikeit trained me in reporter gene assay (RGA) technique and shared his experience in working with the constructs, along with his vast knowledge in protein signaling pathways. Soyoung Hwang, was a student from South Korea under my supervision, who joined our laboratory to complete her bachelor thesis. She helped to achieve biological repetitions of RGAs. The rest of the work was performed by me. That includes: design of the experimental set-ups; establishment of the FLIPUS parameters and stimulation times; optimization of the used biochemical techniques; selection of controls; performance of transfections, RGAs, BrdU ELISAs, WST-8 assays, primer designs, and qRT-PCRs.

Further investigation of the mechanotransductive mechanism in C2C12s (Chapter 4) was completed in close collaboration with Mr. Rikeit. He shared his knowledge and experimental findings on YAP-associated signaling pathway, gained while researching on a cross-talk between Hippo and BMP cascades. He established a YAP knock-down procedure, shared some of the primers sequences and performed fractionation assays. I have accomplished the following work described in the manuscript: development of the FLIPUS cell-stimulation protocols; establishment of the experimental designs; optimization of the used biochemical techniques; selection of YAP target genes (also supported by Mr. Rikeit) and controls; performance of western blotting procedures, primer designs, qRT-PCRs, BrdU-ELISAs, immunofluorescence stainings, migration assays, and stimulation and analyses of knock-down samples.

It is important to note that the manuscripts were not to happen without regular discussions with Prof. Kay Raum, Prof. Petra Knaus and Dr. Karen Ruschke, who provided invaluable support with the experimental designs and analyses of biological responses. Dr. Ruschke arranged a very detailed laboratory training at Free University of Berlin soon after my arrival, which was hosted by Prof. Knaus and helped me to learn and improve a number of biochemical

techniques. Ms. Kadow-Romacker assisted with study designs and repetition of the experiments for statistical purposes throughout my entire PhD work. All of the manuscripts presented in Chapters 1-4 were written by me and supported by the critical comments of every participant.

Bibliography

Akimoto,T., Ushida,T., Miyaki,S., Akaogi,H., Tsuchiya,K., Yan,Z., Williams,R.S., and Tateishi,T. (2005). Mechanical stretch inhibits myoblast-to-adipocyte differentiation through Wnt signaling. Biochem. Biophys. Res. Commun. *329*, 381-385.

Altman,G.H., Horan,R.L., Martin,I., Farhadi,J., Stark,P.R., Volloch,V., Richmond,J.C., Vunjak-Novakovic,G., and Kaplan,D.L. (2002a). Cell differentiation by mechanical stress. FASEB J. *16*, 270-272.

Altman,G.H., Lu,H.H., Horan,R.L., Calabro,T., Ryder,D., Kaplan,D.L., Stark,P., Martin,I., Richmond,J.C., and Vunjak-Novakovic,G. (2002b). Advanced bioreactor with controlled application of multi-dimensional strain for tissue engineering. J. Biomech. Eng *124*, 742-749.

Angele,P., Yoo,J.U., Smith,C., Mansour,J., Jepsen,K.J., Nerlich,M., and Johnstone,B. (2003). Cyclic hydrostatic pressure enhances the chondrogenic phenotype of human mesenchymal progenitor cells differentiated in vitro. J. Orthop. Res. *21*, 451-457.

Angle,S.R., Sena,K., Sumner,D.R., and Virdi,A.S. (2011). Osteogenic differentiation of rat bone marrow stromal cells by various intensities of low-intensity pulsed ultrasound. Ultrasonics *51*, 281-288.

Aragona,M., Panciera,T., Manfrin,A., Giulitti,S., Michielin,F., Elvassore,N., Dupont,S., and Piccolo,S. (2013). A mechanical checkpoint controls multicellular growth through YAP/TAZ regulation by actin-processing factors. Cell *154*, 1047-1059.

Argintar,E., Edwards,S., and Delahay,J. (2011). Bone morphogenetic proteins in orthopaedic trauma surgery. Injury *42*, 730-734.

Arnsdorf,E.J., Tummala,P., Kwon,R.Y., and Jacobs,C.R. (2009). Mechanically induced osteogenic differentiation--the role of RhoA, ROCKII and cytoskeletal dynamics. J. Cell Sci. *122*, 546-553.

Azhari,H. (2010). Basics of Biomedical Ultrasound for Engineers. (A John Wiley & Sons, Inc.).

Baker,K.G., Robertson,V.J., and Duck,F.A. (2001). A review of therapeutic ultrasound: biophysical effects. Phys. Ther. *81*, 1351-1358.

Bandow,K., Nishikawa,Y., Ohnishi,T., Kakimoto,K., Soejima,K., Iwabuchi,S., Kuroe,K., and Matsuguchi,T. (2007). Low-intensity pulsed ultrasound (LIPUS) induces RANKL, MCP-1, and MIP-1beta expression in osteoblasts through the angiotensin II type 1 receptor. J. Cell Physiol *211*, 392-398.

Bass,M.D., Morgan,M.R., and Humphries,M.J. (2007). Integrins and syndecan-4 make distinct, but critical, contributions to adhesion contact formation. Soft. Matter *3*, 372-376.

Bellin,R.M., Kubicek,J.D., Frigault,M.J., Kamien,A.J., Steward,R.L., Jr., Barnes,H.M., Digiacomo,M.B., Duncan,L.J., Edgerly,C.K., Morse,E.M., Park,C.Y., Fredberg,J.J., Cheng,C.M.,

and LeDuc,P.R. (2009). Defining the role of syndecan-4 in mechanotransduction using surface-modification approaches. Proc. Natl. Acad. Sci. U. S. A *106*, 22102-22107.

Beyth,S., Borovsky,Z., Mevorach,D., Liebergall,M., Gazit,Z., Aslan,H., Galun,E., and Rachmilewitz,J. (2005). Human mesenchymal stem cells alter antigen-presenting cell maturation and induce T-cell unresponsiveness. Blood *105*, 2214-2219.

Bozec,A., Bakiri,L., Jimenez,M., Schinke,T., Amling,M., and Wagner,E.F. (2010). Fra-2/AP-1 controls bone formation by regulating osteoblast differentiation and collagen production. J. Cell Biol. *190*, 1093-1106.

Butler,D.L., Juncosa-Melvin,N., Boivin,G.P., Galloway,M.T., Shearn,J.T., Gooch,C., and Awad,H. (2008). Functional tissue engineering for tendon repair: A multidisciplinary strategy using mesenchymal stem cells, bioscaffolds, and mechanical stimulation. J. Orthop. Res. *26*, 1-9.

Calvo,F., Ege,N., Grande-Garcia,A., Hooper,S., Jenkins,R.P., Chaudhry,S.I., Harrington,K., Williamson,P., Moeendarbary,E., Charras,G., and Sahai,E. (2013). Mechanotransduction and YAP-dependent matrix remodelling is required for the generation and maintenance of cancer-associated fibroblasts. Nat. Cell Biol. *15*, 637-646.

Caplan,A.I. (1991). Mesenchymal stem cells. J. Orthop. Res. *9*, 641-650.

Carvalho,F., Cintra,T., and Chammas,M. (2015). Elastography: Principles and considerations for clinical research in veterinary medicine. Veterinary Medicine and Animal Health *7*, 99-110.

Chang,S.F., Chang,C.A., Lee,D.Y., Lee,P.L., Yeh,Y.M., Yeh,C.R., Cheng,C.K., Chien,S., and Chiu,J.J. (2008). Tumor cell cycle arrest induced by shear stress: Roles of integrins and Smad. Proc. Natl. Acad. Sci. U. S. A *105*, 3927-3932.

Chao,Y.H., Tsuang,Y.H., Sun,J.S., Cheng,C.K., and Chen,M.H. (2011). The cross-talk between transforming growth factor-beta1 and ultrasound stimulation during mechanotransduction of rat tenocytes. Connect. Tissue Res. *52*, 313-321.

Chen,W., Lou,J., Evans,E.A., and Zhu,C. (2012). Observing force-regulated conformational changes and ligand dissociation from a single integrin on cells. J. Cell Biol. *199*, 497-512.

Chen,Z., Gibson,T.B., Robinson,F., Silvestro,L., Pearson,G., Xu,B., Wright,A., Vanderbilt,C., and Cobb,M.H. (2001). MAP kinases. Chem. Rev. *101*, 2449-2476.

Couchman,J.R. (2003). Syndecans: proteoglycan regulators of cell-surface microdomains? Nat. Rev. Mol. Cell Biol. *4*, 926-937.

D'Addario,M., Arora,P.D., Ellen,R.P., and McCulloch,C.A. (2002). Interaction of p38 and Sp1 in a mechanical force-induced, beta 1 integrin-mediated transcriptional circuit that regulates the actin-binding protein filamin-A. J. Biol. Chem. *277*, 47541-47550.

Denhez,F., Wilcox-Adelman,S.A., Baciu,P.C., Saoncella,S., Lee,S., French,B., Neveu,W., and Goetinck,P.F. (2002). Syndesmos, a syndecan-4 cytoplasmic domain interactor, binds to the focal adhesion adaptor proteins paxillin and Hic-5. J. Biol. Chem. *277*, 12270-12274.

Dingal,P.C., Wells,R.G., and Discher,D.E. (2014). Simple insoluble cues specify stem cell differentiation. Proc. Natl. Acad. Sci. U. S. A *111*, 18104-18105.

Discher,D.E., Mooney,D.J., and Zandstra,P.W. (2009). Growth factors, matrices, and forces combine and control stem cells. Science *324*, 1673-1677.

Doan,N., Reher,P., Meghji,S., and Harris,M. (1999). In vitro effects of therapeutic ultrasound on cell proliferation, protein synthesis, and cytokine production by human fibroblasts, osteoblasts, and monocytes. J. Oral Maxillofac. Surg. *57*, 409-419.

Dupont,S., Morsut,L., Aragona,M., Enzo,E., Giulitti,S., Cordenonsi,M., Zanconato,F., Le,D.J., Forcato,M., Bicciato,S., Elvassore,N., and Piccolo,S. (2011). Role of YAP/TAZ in mechanotransduction. Nature *474*, 179-183.

Ebisawa,K., Hata,K., Okada,K., Kimata,K., Ueda,M., Torii,S., and Watanabe,H. (2004). Ultrasound enhances transforming growth factor beta-mediated chondrocyte differentiation of human mesenchymal stem cells. Tissue Eng *10*, 921-929.

Echtermeyer,F., Streit,M., Wilcox-Adelman,S., Saoncella,S., Denhez,F., Detmar,M., and Goetinck,P. (2001). Delayed wound repair and impaired angiogenesis in mice lacking syndecan-4. J. Clin. Invest *107*, R9-R14.

Ferrara,N., Gerber,H.P., and LeCouter,J. (2003). The biology of VEGF and its receptors. Nat. Med. *9*, 669-676.

Fitzgerald,J.B., Jin,M., Chai,D.H., Siparsky,P., Fanning,P., and Grodzinsky,A.J. (2008). Shear- and compression-induced chondrocyte transcription requires MAPK activation in cartilage explants. J. Biol. Chem. *283*, 6735-6743.

Fortier,L.A., Barker,J.U., Strauss,E.J., McCarrel,T.M., and Cole,B.J. (2011). The role of growth factors in cartilage repair. Clin. Orthop. Relat Res. *469*, 2706-2715.

Freedman,B.R., Bade,N.D., Riggin,C.N., Zhang,S., Haines,P.G., Ong,K.L., and Janmey,P.A. (2015). The (dys)functional extracellular matrix. Biochim. Biophys. Acta *1853*, 3153-3164.

Garvin,J., Qi,J., Maloney,M., and Banes,A.J. (2003). Novel system for engineering bioartificial tendons and application of mechanical load. Tissue Eng *9*, 967-979.

Gemmiti,C.V. and Guldberg,R.E. (2006). Fluid flow increases type II collagen deposition and tensile mechanical properties in bioreactor-grown tissue-engineered cartilage. Tissue Eng *12*, 469-479.

Gimbrone,M.A., Jr., Topper,J.N., Nagel,T., Anderson,K.R., and Garcia-Cardena,G. (2000). Endothelial dysfunction, hemodynamic forces, and atherogenesis. Ann. N. Y. Acad. Sci. *902*, 230-239.

Gleizal,A., Li,S., Pialat,J.B., and Beziat,J.L. (2006). Transcriptional expression of calvarial bone after treatment with low-intensity ultrasound: an in vitro study. Ultrasound Med. Biol. *32*, 1569-1574.

Griffith,L.G. and Naughton,G. (2002). Tissue engineering--current challenges and expanding opportunities. Science *295*, 1009-1014.

Hall,A. (1998). Rho GTPases and the actin cytoskeleton. Science *279*, 509-514.

Hanke,N., Kubis,H.P., Scheibe,R.J., Berthold-Losleben,M., Husing,O., Meissner,J.D., and Gros,G. (2010). Passive mechanical forces upregulate the fast myosin heavy chain IId/x via integrin and p38 MAP kinase activation in a primary muscle cell culture. Am. J. Physiol Cell Physiol *298*, C910-C920.

Hao,Y., Chun,A., Cheung,K., Rashidi,B., and Yang,X. (2008). Tumor suppressor LATS1 is a negative regulator of oncogene YAP. J. Biol. Chem. *283*, 5496-5509.

Harle,J., Mayia,F., Olsen,I., and Salih,V. (2005). Effects of ultrasound on transforming growth factor-beta genes in bone cells. Eur. Cell Mater. *10*, 70-76.

Hasegawa,T., Miwa,M., Sakai,Y., Niikura,T., Kurosaka,M., and Komori,T. (2009). Osteogenic activity of human fracture haematoma-derived progenitor cells is stimulated by low-intensity pulsed ultrasound in vitro. J. Bone Joint Surg. Br. *91*, 264-270.

Hasuike,A., Sato,S., Udagawa,A., Ando,K., Arai,Y., and Ito,K. (2011). In vivo bone regenerative effect of low-intensity pulsed ultrasound in rat calvarial defects. Oral Surg. Oral Med. Oral Pathol. Oral Radiol. Endod. *111*, e12-e20.

Hauff,P., Reinhardt,M., and Foster,S. (2008). Ultrasound basics. Handb. Exp. Pharmacol. 91-107.

Hayton,M.J., Dillon,J.P., Glynn,D., Curran,J.M., Gallagher,J.A., and Buckley,K.A. (2005). Involvement of adenosine 5'-triphosphate in ultrasound-induced fracture repair. Ultrasound Med. Biol. *31*, 1131-1138.

Hensel,K., Mienkina,M.P., and Schmitz,G. (2011). Analysis of ultrasound fields in cell culture wells for in vitro ultrasound therapy experiments. Ultrasound Med. Biol. *37*, 2105-2115.

Huang,C.Y., Hagar,K.L., Frost,L.E., Sun,Y., and Cheung,H.S. (2004). Effects of cyclic compressive loading on chondrogenesis of rabbit bone-marrow derived mesenchymal stem cells. Stem Cells *22*, 313-323.

Huang,J., Wu,S., Barrera,J., Matthews,K., and Pan,D. (2005). The Hippo signaling pathway coordinately regulates cell proliferation and apoptosis by inactivating Yorkie, the Drosophila Homolog of YAP. Cell *122*, 421-434.

Humphrey,J.D., Dufresne,E.R., and Schwartz,M.A. (2014). Mechanotransduction and extracellular matrix homeostasis. Nat. Rev. Mol. Cell Biol. *15*, 802-812.

Ikeda,K., Takayama,T., Suzuki,N., Shimada,K., Otsuka,K., and Ito,K. (2006). Effects of low-intensity pulsed ultrasound on the differentiation of C2C12 cells. Life Sci. *79*, 1936-1943.

Iqbal,J. and Zaidi,M. (2005). Molecular regulation of mechanotransduction. Biochem. Biophys. Res. Commun. *328*, 751-755.

Iwabuchi,S., Ito,M., Hata,J., Chikanishi,T., Azuma,Y., and Haro,H. (2005). In vitro evaluation of low-intensity pulsed ultrasound in herniated disc resorption. Biomaterials *26*, 7104-7114.

Jang,K.W., Ding,L., Seol,D., Lim,T.H., Buckwalter,J.A., and Martin,J.A. (2014). Low-intensity pulsed ultrasound promotes chondrogenic progenitor cell migration via focal adhesion kinase pathway. Ultrasound Med. Biol. *40*, 1177-1186.

Jansen,J.H., Eijken,M., Jahr,H., Chiba,H., Verhaar,J.A., van Leeuwen,J.P., and Weinans,H. (2010). Stretch-induced inhibition of Wnt/beta-catenin signaling in mineralizing osteoblasts. J. Orthop. Res. *28*, 390-396.

Karin,M., Liu,Z., and Zandi,E. (1997). AP-1 function and regulation. Curr. Opin. Cell Biol. *9*, 240-246.

Katsumi,A., Orr,A.W., Tzima,E., and Schwartz,M.A. (2004). Integrins in mechanotransduction. J. Biol. Chem. *279*, 12001-12004.

Kemler,R. (1993). From cadherins to catenins: cytoplasmic protein interactions and regulation of cell adhesion. Trends Genet. *9*, 317-321.

Khachigian,L.M., Collins,T., and Fries,J.W. (1995). Nuclear factor-kappa B mediates induction of vascular cell adhesion molecule-1 in glomerular mesangial cells. Biochem. Biophys. Res. Commun. *206*, 462-467.

Khanna,A., Nelmes,R.T., Gougoulias,N., Maffulli,N., and Gray,J. (2009). The effects of LIPUS on soft-tissue healing: a review of literature. Br. Med. Bull. *89*, 169-182.

Kim,T.J., Seong,J., Ouyang,M., Sun,J., Lu,S., Hong,J.P., Wang,N., and Wang,Y. (2009). Substrate rigidity regulates Ca2+ oscillation via RhoA pathway in stem cells. J. Cell Physiol *218*, 285-293.

Kirstein,M. and Baglioni,C. (1988). Tumor necrosis factor stimulates proliferation of human osteosarcoma cells and accumulation of c-myc messenger RNA. J. Cell Physiol *134*, 479-484.

Kobayashi,Y., Sakai,D., Iwashina,T., Iwabuchi,S., and Mochida,J. (2009). Low-intensity pulsed ultrasound stimulates cell proliferation, proteoglycan synthesis and expression of growth factor-related genes in human nucleus pulposus cell line. Eur. Cell Mater. *17*, 15-22.

Koch,A.E., Polverini,P.J., Kunkel,S.L., Harlow,L.A., DiPietro,L.A., Elner,V.M., Elner,S.G., and Strieter,R.M. (1992). Interleukin-8 as a macrophage-derived mediator of angiogenesis. Science *258*, 1798-1801.

Kook,S.H., Hwang,J.M., Park,J.S., Kim,E.M., Heo,J.S., Jeon,Y.M., and Lee,J.C. (2009). Mechanical force induces type I collagen expression in human periodontal ligament fibroblasts through activation of ERK/JNK and AP-1. J. Cell Biochem. *106*, 1060-1067.

Kopf,J., Petersen,A., Duda,G.N., and Knaus,P. (2012). BMP2 and mechanical loading cooperatively regulate immediate early signalling events in the BMP pathway. BMC Biol. *10*, 37.

Kumagai,K., Takeuchi,R., Ishikawa,H., Yamaguchi,Y., Fujisawa,T., Kuniya,T., Takagawa,S., Muschler,G.F., and Saito,T. (2012). Low-intensity pulsed ultrasound accelerates fracture healing

by stimulation of recruitment of both local and circulating osteogenic progenitors. J. Orthop. Res. *30*, 1516-1521.

Lai,C.F. and Cheng,S.L. (2005). Alphavbeta integrins play an essential role in BMP-2 induction of osteoblast differentiation. J. Bone Miner. Res. *20*, 330-340.

Lai,Z.C., Wei,X., Shimizu,T., Ramos,E., Rohrbaugh,M., Nikolaidis,N., Ho,L.L., and Li,Y. (2005). Control of cell proliferation and apoptosis by mob as tumor suppressor, mats. Cell *120*, 675-685.

Laugier,P. and Haiat,G. (2011). Introduction to the Physics of Ultrasound.

Le,H.Q., Ghatak,S., Yeung,C.Y., Tellkamp,F., Gunschmann,C., Dieterich,C., Yeroslaviz,A., Habermann,B., Pombo,A., Niessen,C.M., and Wickstrom,S.A. (2016). Mechanical regulation of transcription controls Polycomb-mediated gene silencing during lineage commitment. Nat. Cell Biol. *18*, 864-875.

Leckband,D.E., le,D.Q., Wang,N., and de,R.J. (2011). Mechanotransduction at cadherin-mediated adhesions. Curr. Opin. Cell Biol. *23*, 523-530.

Lee,H.J., Choi,B.H., Min,B.H., Son,Y.S., and Park,S.R. (2006). Low-intensity ultrasound stimulation enhances chondrogenic differentiation in alginate culture of mesenchymal stem cells. Artif. Organs *30*, 707-715.

Lee,S.Y., Koh,A., Niikura,T., Oe,K., Koga,T., Dogaki,Y., and Kurosaka,M. (2013). Low-intensity pulsed ultrasound enhances BMP-7-induced osteogenic differentiation of human fracture hematoma-derived progenitor cells in vitro. J. Orthop. Trauma *27*, 29-33.

Leskinen,J.J. and Hynynen,K. (2012). Study of factors affecting the magnitude and nature of ultrasound exposure with in vitro set-ups. Ultrasound Med. Biol. *38*, 777-794.

Li,J., Zhao,Z., Yang,J., Liu,J., Wang,J., Li,X., and Liu,Y. (2009). p38 MAPK mediated in compressive stress-induced chondrogenesis of rat bone marrow MSCs in 3D alginate scaffolds. J. Cell Physiol *221*, 609-617.

Liedert,A., Kaspar,D., Blakytny,R., Claes,L., and Ignatius,A. (2006). Signal transduction pathways involved in mechanotransduction in bone cells. Biochem. Biophys. Res. Commun. *349*, 1-5.

Liu,J., Zhao,Z., Li,J., Zou,L., Shuler,C., Zou,Y., Huang,X., Li,M., and Wang,J. (2009). Hydrostatic pressures promote initial osteodifferentiation with ERK1/2 not p38 MAPK signaling involved. J. Cell Biochem. *107*, 224-232.

Loufrani,L., Retailleau,K., Bocquet,A., Dumont,O., Danker,K., Louis,H., Lacolley,P., and Henrion,D. (2008). Key role of alpha(1)beta(1)-integrin in the activation of PI3-kinase-Akt by flow (shear stress) in resistance arteries. Am. J. Physiol Heart Circ. Physiol *294*, H1906-H1913.

Low,B.C., Pan,C.Q., Shivashankar,G.V., Bershadsky,A., Sudol,M., and Sheetz,M. (2014). YAP/TAZ as mechanosensors and mechanotransducers in regulating organ size and tumor growth. FEBS Lett. *588*, 2663-2670.

MacKenna,D.A., Dolfi,F., Vuori,K., and Ruoslahti,E. (1998). Extracellular signal-regulated kinase and c-Jun NH2-terminal kinase activation by mechanical stretch is integrin-dependent and matrix-specific in rat cardiac fibroblasts. J. Clin. Invest *101*, 301-310.

Maddi,A., Hai,H., Ong,S.T., Sharp,L., Harris,M., and Meghji,S. (2006). Long wave ultrasound may enhance bone regeneration by altering OPG/RANKL ratio in human osteoblast-like cells. Bone *39*, 283-288.

Mahoney,C.M., Morgan,M.R., Harrison,A., Humphries,M.J., and Bass,M.D. (2009). Therapeutic ultrasound bypasses canonical syndecan-4 signaling to activate rac1. J. Biol. Chem. *284*, 8898-8909.

Mammoto,A., Mammoto,T., and Ingber,D.E. (2012). Mechanosensitive mechanisms in transcriptional regulation. J. Cell Sci. *125*, 3061-3073.

Man,J., Shelton,R.M., Cooper,P.R., Landini,G., and Scheven,B.A. (2012). Low intensity ultrasound stimulates osteoblast migration at different frequencies. J. Bone Miner. Metab *30*, 602-607.

Margadant,C. and Sonnenberg,A. (2010). Integrin-TGF-beta crosstalk in fibrosis, cancer and wound healing. EMBO Rep. *11*, 97-105.

Martin,I., Smith,T., and Wendt,D. (2009). Bioreactor-based roadmap for the translation of tissue engineering strategies into clinical products. Trends Biotechnol. *27*, 495-502.

Martin,I., Wendt,D., and Heberer,M. (2004). The role of bioreactors in tissue engineering. Trends Biotechnol. *22*, 80-86.

Maruthamuthu,V., Sabass,B., Schwarz,U.S., and Gardel,M.L. (2011). Cell-ECM traction force modulates endogenous tension at cell-cell contacts. Proc. Natl. Acad. Sci. U. S. A *108*, 4708-4713.

Marvel,S., Okrasinski,S., Bernacki,S.H., Loboa,E., and Dayton,P.A. (2010). The development and validation of a LIPUS system with preliminary observations of ultrasonic effects on human adult stem cells. IEEE Trans. Ultrason. Ferroelectr. Freq. Control *57*, 1977-1984.

Mauney,J.R., Sjostorm,S., Blumberg,J., Horan,R., O'Leary,J.P., Vunjak-Novakovic,G., Volloch,V., and Kaplan,D.L. (2004). Mechanical stimulation promotes osteogenic differentiation of human bone marrow stromal cells on 3-D partially demineralized bone scaffolds in vitro. Calcif. Tissue Int. *74*, 458-468.

Mikuni-Takagaki,Y. (1999). Mechanical responses and signal transduction pathways in stretched osteocytes. J. Bone Miner. Metab *17*, 57-60.

Morgan,M.R., Humphries,M.J., and Bass,M.D. (2007). Synergistic control of cell adhesion by integrins and syndecans. Nat. Rev. Mol. Cell Biol. *8*, 957-969.

Mukai,S., Ito,H., Nakagawa,Y., Akiyama,H., Miyamoto,M., and Nakamura,T. (2005). Transforming growth factor-beta1 mediates the effects of low-intensity pulsed ultrasound in chondrocytes. Ultrasound Med. Biol. *31*, 1713-1721.

Naito,K., Watari,T., Muta,T., Furuhata,A., Iwase,H., Igarashi,M., Kurosawa,H., Nagaoka,I., and Kaneko,K. (2010). Low-intensity pulsed ultrasound (LIPUS) increases the articular cartilage type II collagen in a rat osteoarthritis model. J. Orthop. Res. *28*, 361-369.

Nakao,J., Fujii,Y., Kusuyama,J., Bandow,K., Kakimoto,K., Ohnishi,T., and Matsuguchi,T. (2014). Low-intensity pulsed ultrasound (LIPUS) inhibits LPS-induced inflammatory responses of osteoblasts through TLR4-MyD88 dissociation. Bone *58*, 17-25.

Naruse,K., Mikuni-Takagaki,Y., Azuma,Y., Ito,M., Oota,T., Kameyama,K., and Itoman,M. (2000). Anabolic response of mouse bone-marrow-derived stromal cell clone ST2 cells to low-intensity pulsed ultrasound. Biochem. Biophys. Res. Commun. *268*, 216-220.

Naruse,K., Miyauchi,A., Itoman,M., and Mikuni-Takagaki,Y. (2003). Distinct anabolic response of osteoblast to low-intensity pulsed ultrasound. J. Bone Miner. Res. *18*, 360-369.

Naughton,G.K., Tolbert,W.R., and Grillot,T.M. (1995). Emerging developments in tissue engineering and cell technology. Tissue Eng *1*, 211-219.

Nomura,S. and Takano-Yamamoto,T. (2000). Molecular events caused by mechanical stress in bone. Matrix Biol. *19*, 91-96.

Ogasawara,A., Arakawa,T., Kaneda,T., Takuma,T., Sato,T., Kaneko,H., Kumegawa,M., and Hakeda,Y. (2001). Fluid shear stress-induced cyclooxygenase-2 expression is mediated by C/EBP beta, cAMP-response element-binding protein, and AP-1 in osteoblastic MC3T3-E1 cells. J. Biol. Chem. *276*, 7048-7054.

Ota,M. and Sasaki,H. (2008). Mammalian Tead proteins regulate cell proliferation and contact inhibition as transcriptional mediators of Hippo signaling. Development *135*, 4059-4069.

Padilla,F., Puts,R., Vico,L., Guignandon,A., and Raum,K. (2016). Stimulation of Bone Repair with Ultrasound. Adv. Exp. Med. Biol. *880*, 385-427.

Padilla,F., Puts,R., Vico,L., and Raum,K. (2014). Stimulation of bone repair with ultrasound: a review of the possible mechanic effects. Ultrasonics *54*, 1125-1145.

Pantalacci,S., Tapon,N., and Leopold,P. (2003). The Salvador partner Hippo promotes apoptosis and cell-cycle exit in Drosophila. Nat. Cell Biol. *5*, 921-927.

Papachristou,D.J., Papachroni,K.K., Basdra,E.K., and Papavassiliou,A.G. (2009). Signaling networks and transcription factors regulating mechanotransduction in bone. Bioessays *31*, 794-804.

Parvizi,J., Parpura,V., Greenleaf,J.F., and Bolander,M.E. (2002). Calcium signaling is required for ultrasound-stimulated aggrecan synthesis by rat chondrocytes. J. Orthop. Res. *20*, 51-57.

Pertz,O. (2010). Spatio-temporal Rho GTPase signaling - where are we now? J. Cell Sci. *123*, 1841-1850.

Piccolo,S., Dupont,S., and Cordenonsi,M. (2014). The biology of YAP/TAZ: hippo signaling and beyond. Physiol Rev. *94*, 1287-1312.

Pisanti,P., Yeatts,A.B., Cardea,S., Fisher,J.P., and Reverchon,E. (2012). Tubular perfusion system culture of human mesenchymal stem cells on poly-L-lactic acid scaffolds produced using a supercritical carbon dioxide-assisted process. J. Biomed. Mater. Res. A *100*, 2563-2572.

Pittenger,M.F., Mackay,A.M., Beck,S.C., Jaiswal,R.K., Douglas,R., Mosca,J.D., Moorman,M.A., Simonetti,D.W., Craig,S., and Marshak,D.R. (1999). Multilineage potential of adult human mesenchymal stem cells. Science *284*, 143-147.

Poh,Y.C., Na,S., Chowdhury,F., Ouyang,M., Wang,Y., and Wang,N. (2009). Rapid activation of Rac GTPase in living cells by force is independent of Src. PLoS. One. *4*, e7886.

Potier,E., Ferreira,E., Andriamanalijaona,R., Pujol,J.P., Oudina,K., Logeart-Avramoglou,D., and Petite,H. (2007). Hypoxia affects mesenchymal stromal cell osteogenic differentiation and angiogenic factor expression. Bone *40*, 1078-1087.

Pounder,N.M. and Harrison,A.J. (2008). Low intensity pulsed ultrasound for fracture healing: a review of the clinical evidence and the associated biological mechanism of action. Ultrasonics *48*, 330-338.

Radomsky,M.L., Thompson,A.Y., Spiro,R.C., and Poser,J.W. (1998). Potential role of fibroblast growth factor in enhancement of fracture healing. Clin. Orthop. Relat Res. S283-S293.

Reher,P., Doan,N., Bradnock,B., Meghji,S., and Harris,M. (1998). Therapeutic ultrasound for osteoradionecrosis: an in vitro comparison between 1 MHz and 45 kHz machines. Eur. J. Cancer *34*, 1962-1968.

Reher,P., Elbeshir,e., Harvey,W., Meghji,S., and Harris,M. (1997). The stimulation of bone formation in vitro by therapeutic ultrasound. Ultrasound Med. Biol. *23*, 1251-1258.

Reher,P., Harris,M., Whiteman,M., Hai,H.K., and Meghji,S. (2002). Ultrasound stimulates nitric oxide and prostaglandin E2 production by human osteoblasts. Bone *31*, 236-241.

Ren,L., Yang,Z., Song,J., Wang,Z., Deng,F., and Li,W. (2013). Involvement of p38 MAPK pathway in low intensity pulsed ultrasound induced osteogenic differentiation of human periodontal ligament cells. Ultrasonics *53*, 686-690.

Roper,J., Harrison,A., and Bass,M.D. (2012). Induction of adhesion-dependent signals using low-intensity ultrasound. J. Vis. Exp. e4024.

Sant'Anna,E.F., Leven,R.M., Virdi,A.S., and Sumner,D.R. (2005). Effect of low intensity pulsed ultrasound and BMP-2 on rat bone marrow stromal cell gene expression. J. Orthop. Res. *23*, 646-652.

Sarvazyan,A.P., Rudenko,O.V., and Nyborg,W.L. (2010). Biomedical applications of radiation force of ultrasound: historical roots and physical basis. Ultrasound Med. Biol. *36*, 1379-1394.

Sawai,Y., Murata,H., Koto,K., Matsui,T., Horie,N., Ashihara,E., Maekawa,T., Fushiki,S., and Kubo,T. (2012). Effects of low-intensity pulsed ultrasound on osteosarcoma and cancer cells. Oncol. Rep. *28*, 481-486.

Schlegelmilch,K., Mohseni,M., Kirak,O., Pruszak,J., Rodriguez,J.R., Zhou,D., Kreger,B.T., Vasioukhin,V., Avruch,J., Brummelkamp,T.R., and Camargo,F.D. (2011). Yap1 acts downstream of alpha-catenin to control epidermal proliferation. Cell *144*, 782-795.

Schumann,D., Kujat,R., Zellner,J., Angele,M.K., Nerlich,M., Mayr,E., and Angele,P. (2006). Treatment of human mesenchymal stem cells with pulsed low intensity ultrasound enhances the chondrogenic phenotype in vitro. Biorheology *43*, 431-443.

Seefried,L., Mueller-Deubert,S., Schwarz,T., Lind,T., Mentrup,B., Kober,M., Docheva,D., Liedert,A., Kassem,M., Ignatius,A., Schieker,M., Claes,L., Wilke,W., Jakob,F., and Ebert,R. (2010). A small scale cell culture system to analyze mechanobiology using reporter gene constructs and polyurethane dishes. Eur. Cell Mater. *20*, 344-355.

Sena,K., Leven,R.M., Mazhar,K., Sumner,D.R., and Virdi,A.S. (2005). Early gene response to low-intensity pulsed ultrasound in rat osteoblastic cells. Ultrasound Med. Biol. *31*, 703-708.

Shah, N., Morsi, Y., Manuelpillai, U., Barry, T., and Manasseh, R. Elucidating the effects of low-intensity ultrasound on mesenchymal stem cell proliferation and viability. 2013.
Ref Type: Conference Proceeding

Song,H., Mak,K.K., Topol,L., Yun,K., Hu,J., Garrett,L., Chen,Y., Park,O., Chang,J., Simpson,R.M., Wang,C.Y., Gao,B., Jiang,J., and Yang,Y. (2010). Mammalian Mst1 and Mst2 kinases play essential roles in organ size control and tumor suppression. Proc. Natl. Acad. Sci. U. S. A *107*, 1431-1436.

Sudol,M. (1994). Yes-associated protein (YAP65) is a proline-rich phosphoprotein that binds to the SH3 domain of the Yes proto-oncogene product. Oncogene *9*, 2145-2152.

Sun,J.S., Hong,R.C., Chang,W.H., Chen,L.T., Lin,F.H., and Liu,H.C. (2001). In vitro effects of low-intensity ultrasound stimulation on the bone cells. J. Biomed. Mater. Res. *57*, 449-456.

Sun,S., Liu,Y., Lipsky,S., and Cho,M. (2007). Physical manipulation of calcium oscillations facilitates osteodifferentiation of human mesenchymal stem cells. FASEB J. *21*, 1472-1480.

Suzuki,A., Takayama,T., Suzuki,N., Kojima,T., Ota,N., Asano,S., and Ito,K. (2009a). Daily low-intensity pulsed ultrasound stimulates production of bone morphogenetic protein in ROS 17/2.8 cells. J. Oral Sci. *51*, 29-36.

Suzuki,A., Takayama,T., Suzuki,N., Sato,M., Fukuda,T., and Ito,K. (2009b). Daily low-intensity pulsed ultrasound-mediated osteogenic differentiation in rat osteoblasts. Acta Biochim. Biophys. Sin. (Shanghai) *41*, 108-115.

Takahashi,I., Nuckolls,G.H., Takahashi,K., Tanaka,O., Semba,I., Dashner,R., Shum,L., and Slavkin,H.C. (1998). Compressive force promotes sox9, type II collagen and aggrecan and inhibits IL-1beta expression resulting in chondrogenesis in mouse embryonic limb bud mesenchymal cells. J. Cell Sci. *111 (Pt 14)*, 2067-2076.

Takeuchi,R., Ryo,A., Komitsu,N., Mikuni-Takagaki,Y., Fukui,A., Takagi,Y., Shiraishi,T., Morishita,S., Yamazaki,Y., Kumagai,K., Aoki,I., and Saito,T. (2008). Low-intensity pulsed

ultrasound activates the phosphatidylinositol 3 kinase/Akt pathway and stimulates the growth of chondrocytes in three-dimensional cultures: a basic science study. Arthritis Res. Ther. *10*, R77.

Tang,C.H., Yang,R.S., Huang,T.H., Lu,D.Y., Chuang,W.J., Huang,T.F., and Fu,W.M. (2006). Ultrasound stimulates cyclooxygenase-2 expression and increases bone formation through integrin, focal adhesion kinase, phosphatidylinositol 3-kinase, and Akt pathway in osteoblasts. Mol. Pharmacol. *69*, 2047-2057.

Thiel,G. and Cibelli,G. (2002). Regulation of life and death by the zinc finger transcription factor Egr-1. J. Cell Physiol *193*, 287-292.

Torkelson,J., Lipsky,S., and Tirrell,M. (1981). Polystyrene fluorescence: effects of molecular weight in various solvents. Macromolecules *14*, 1603-1605.

Tsai,C.L., Chang,W.H., and Liu,T.K. (1992). Preliminary studies of duration and intensity of ultrasonic treatments on fracture repair. Chin J. Physiol *35*, 21-26.

Unsworth,J., Kaneez,S., Harris,S., Ridgway,J., Fenwick,S., Chenery,D., and Harrison,A. (2007). Pulsed low intensity ultrasound enhances mineralisation in preosteoblast cells. Ultrasound Med. Biol. *33*, 1468-1474.

Valhmu,W.B. and Raia,F.J. (2002). myo-Inositol 1,4,5-trisphosphate and Ca(2+)/calmodulin-dependent factors mediate transduction of compression-induced signals in bovine articular chondrocytes. Biochem. J. *361*, 689-696.

Varelas,X. (2014). The Hippo pathway effectors TAZ and YAP in development, homeostasis and disease. Development *141*, 1614-1626.

Varelas,X., Samavarchi-Tehrani,P., Narimatsu,M., Weiss,A., Cockburn,K., Larsen,B.G., Rossant,J., and Wrana,J.L. (2010). The Crumbs complex couples cell density sensing to Hippo-dependent control of the TGF-beta-SMAD pathway. Dev. Cell *19*, 831-844.

Varkey,M., Gittens,S.A., and Uludag,H. (2004). Growth factor delivery for bone tissue repair: an update. Expert. Opin. Drug Deliv. *1*, 19-36.

Vassilev,A., Kaneko,K.J., Shu,H., Zhao,Y., and DePamphilis,M.L. (2001). TEAD/TEF transcription factors utilize the activation domain of YAP65, a Src/Yes-associated protein localized in the cytoplasm. Genes Dev. *15*, 1229-1241.

Volkmer,E., Drosse,I., Otto,S., Stangelmayer,A., Stengele,M., Kallukalam,B.C., Mutschler,W., and Schieker,M. (2008). Hypoxia in static and dynamic 3D culture systems for tissue engineering of bone. Tissue Eng Part A *14*, 1331-1340.

Wada,K., Itoga,K., Okano,T., Yonemura,S., and Sasaki,H. (2011). Hippo pathway regulation by cell morphology and stress fibers. Development *138*, 3907-3914.

Wan,Q., Cho,E., Yokota,H., and Na,S. (2013). Rac1 and Cdc42 GTPases regulate shear stress-driven beta-catenin signaling in osteoblasts. Biochem. Biophys. Res. Commun. *433*, 502-507.

Wang,F.S., Kuo,Y.R., Wang,C.J., Yang,K.D., Chang,P.R., Huang,Y.T., Huang,H.C., Sun,Y.C., Yang,Y.J., and Chen,Y.J. (2004). Nitric oxide mediates ultrasound-induced hypoxia-inducible

factor-1alpha activation and vascular endothelial growth factor-A expression in human osteoblasts. Bone *35*, 114-123.

Warden,S.J., Favaloro,J.M., Bennell,K.L., McMeeken,J.M., Ng,K.W., Zajac,J.D., and Wark,J.D. (2001). Low-intensity pulsed ultrasound stimulates a bone-forming response in UMR-106 cells. Biochem. Biophys. Res. Commun. *286*, 443-450.

Watanabe,Y., Matsushita,T., Bhandari,M., Zdero,R., and Schemitsch,E.H. (2010). Ultrasound for fracture healing: current evidence. J. Orthop. Trauma *24 Suppl 1*, S56-S61.

Welgus,H.G., Jeffrey,J.J., and Eisen,A.Z. (1981). Human skin fibroblast collagenase. Assessment of activation energy and deuterium isotope effect with collagenous substrates. J. Biol. Chem. *256*, 9516-9521.

Wells,R.G. (2008). The role of matrix stiffness in regulating cell behavior. Hepatology *47*, 1394-1400.

Whitney,N.P., Lamb,A.C., Louw,T.M., and Subramanian,A. (2012). Integrin-mediated mechanotransduction pathway of low-intensity continuous ultrasound in human chondrocytes. Ultrasound Med. Biol. *38*, 1734-1743.

Wijdicks,C.A., Virdi,A.S., Sena,K., Sumner,D.R., and Leven,R.M. (2009). Ultrasound enhances recombinant human BMP-2 induced ectopic bone formation in a rat model. Ultrasound Med. Biol. *35*, 1629-1637.

Wiklund,M., Radel,S., and Hawkes,J.J. (2013). Acoustofluidics 21: ultrasound-enhanced immunoassays and particle sensors. Lab Chip. *13*, 25-39.

Yagi,R., Chen,L.F., Shigesada,K., Murakami,Y., and Ito,Y. (1999). A WW domain-containing yes-associated protein (YAP) is a novel transcriptional co-activator. EMBO J. *18*, 2551-2562.

Yang,R.S., Lin,W.L., Chen,Y.Z., Tang,C.H., Huang,T.H., Lu,B.Y., and Fu,W.M. (2005). Regulation by ultrasound treatment on the integrin expression and differentiation of osteoblasts. Bone *36*, 276-283.

Yang,S.H., Sharrocks,A.D., and Whitmarsh,A.J. (2003). Transcriptional regulation by the MAP kinase signaling cascades. Gene *320*, 3-21.

Yano,S., Komine,M., Fujimoto,M., Okochi,H., and Tamaki,K. (2006). Activation of Akt by mechanical stretching in human epidermal keratinocytes. Exp. Dermatol. *15*, 356-361.

Ye,F. and Zhang,M. (2013). Structures and target recognition modes of PDZ domains: recurring themes and emerging pictures. Biochem. J. *455*, 1-14.

Yeatts,A.B. and Fisher,J.P. (2011). Bone tissue engineering bioreactors: dynamic culture and the influence of shear stress. Bone *48*, 171-181.

Zauhar,G., Duck,F.A., and Starritt,H.C. (2006). Comparison of the acoustic streaming in amniotic fluid and water in medical ultrasonic beams. Ultraschall Med. *27*, 152-158.

Zhao,B., Li,L., Wang,L., Wang,C.Y., Yu,J., and Guan,K.L. (2012). Cell detachment activates the Hippo pathway via cytoskeleton reorganization to induce anoikis. Genes Dev. *26*, 54-68.

Zhao,B., Tumaneng,K., and Guan,K.L. (2011). The Hippo pathway in organ size control, tissue regeneration and stem cell self-renewal. Nat. Cell Biol. *13*, 877-883.

Zhou,S., Schmelz,A., Seufferlein,T., Li,Y., Zhao,J., and Bachem,M.G. (2004). Molecular mechanisms of low intensity pulsed ultrasound in human skin fibroblasts. J. Biol. Chem. *279*, 54463-54469.

Zou,Y., Akazawa,H., Qin,Y., Sano,M., Takano,H., Minamino,T., Makita,N., Iwanaga,K., Zhu,W., Kudoh,S., Toko,H., Tamura,K., Kihara,M., Nagai,T., Fukamizu,A., Umemura,S., Iiri,T., Fujita,T., and Komuro,I. (2004). Mechanical stress activates angiotensin II type 1 receptor without the involvement of angiotensin II. Nat. Cell Biol. *6*, 499-506.